A preliminary study of the relations between solar flares and solar magnetic fields

Greatrix, G. R.

A preliminary study of the relations between solar flares and solar magnetic fields.

G.R.Greatrix.

Summary.

A survey of known characteristics of solar flares and related phenomena is given. This survey is supplemented by further characteristics obtained from a statistical analysis of data relating to more than 2,000 solar flares for the period 1947 Jan.1 to 1949 May 1. This analysis yielded the following principal results:

(a). The intensity of a solar flare is independent of its position on the solar disk, the quantity of magnetic flux associated with the spot group, and the rate of change of that flux. There is some indication that the intensity may be governed by the geometry of the associated sunspot magnetic field.

(b). The frequency of solar flares occurring in a given spot group is dependent on the spot magnetic classification, the magnetic flux going through the spot, and the rate of change of that magnetic flux.

(c). In certain cases, the latitude distribution over the solar disk of flares associated with spot groups of a given magnetic classification is skewed relative to the associated spot distribution. The direction of skewness is dependent on the spot magnetic classification.

This last effect can be explained on the

assumption that the sun has a 'general' magnetic field. The explanation is compatible with C.W.Allen's sunspot cycle model which incorporates a mechanism to reverse the magnetic polarity of the sun's general field at every sunspot maximum. The results are discussed briefly in relation to the various electromagnetic theories of solar flares and it is concluded that only F.Hoyle and T.Gold's theory is in accord with them.

Similar statistical analyses carried out for different periods of sunspot activity should yield more information on the behaviour of the general field, and show how the relations between flares, spots, and the general field change with time. Accordingly, the analysis has been arranged so that detailed statistical comparisons may be made whenever any future, similar, work is done.

Introduction.

Of the phenomena that occur in the solar atmosphere, flares are perhaps the most complex. They are connected with the greatest amounts of energy and with the greatest range of associated observable effects. There is great controversy regarding the theoretical interpretation of this phenomenon, and many theories have been suggested.

The purpose of the following work is twofold. Firstly, it is a collection of the known characteristics of solar flares, and secondly it is an attempt to supplement this by deducing further characteristics which will be of use in deciding which of the many theories of the origin of solar flares is the most acceptable. These extra characteristics are derived from observational data and are found to have considerable bearing on the structure and movement of the sun's general magnetic field.

A. The Definition of a Solar Flare.

A solar flare is a localised, short-lived, large and sudden increase in certain monochromatic radiations, which occur within a radius of 10^5 km. of an active sunspot group.

B. The Classification of Solar Flares.

Solar flares are roughly graded according to their areas, brightness, and Hα width, all these being estimated at the flare's maximum intensity. However, classification using these parameters is very difficult since the geometry of a flare is highly complex and is set against a complex chromospheric background. The flare itself varies rapidly in brightness, producing rapid variations in line profile, and different parts of the flare behave differently. As a result of these difficulties accompanied by differing conditions and individual discrepancies of observation, there is a great diversity in classification among observatories. The present system of classification is outlined below, although, considering the above factors, it may be concluded that this system is unreliable and a quantitative method of grading is urgently required.

(a). Class 1-.

This consists of the smallest flares, which have areas less than 100 millionths of the sun's hemisphere. These flares are only observed under good seeing conditions, and when the instrument has a high resolving power. Many observatories

neglect flares of this class altogether.

(b). Class 1.

This consists of flares which have areas ranging from 100 to 300 millionths of the sun's hemisphere. Their average duration is about 17 minutes.

(c). Class 2.

This consists of flares which have areas ranging from >300 to $\leqslant 750$ millionths of the sun's hemisphere. Their average duration is about 29 minutes.

(d). Class 3.

This consists of flares which have areas >750 millionths of the sun's hemisphere. Their average duration is about 62 minutes.

(e). Class 3+.

This consists of flares which are not very different from those of class 3 in their solar quality, but are accompanied by a much greater intensity of geophysical activity than the flares of the other classes. The average duration of these flares is about 3 hours.

C. The Development of a Solar Flare and the Sequence of its Associated Events.

A flare rises to its maximum intensity in less than 2 minutes, and sometimes this sudden intensification may be described as a 'flash' of radiation. The flare maintains its maximum intensity for a period of less than about 5 minutes, and this is followed by a decay which is usually comparatively

slow, although in extreme cases it may be as rapid as the rise to the maximum intensity. Ellison (1) finds, from an analysis of 23 photometric curves, that the mean ratio of the period of initial rise to maximum intensity to the period of decay is 0.29 with extreme values of 0.08 to 1.0.

The brightening of the flare takes place initially in plage areas around active sunspots, and may extend to quite distant parts of those plage regions and follow their geometry. For most flares, different parts of the plage areas brighten simultaneously although these parts may differ in their respective maximum intensities. Sometimes a region brightens, some even brighten and then fade, before the onset of brightening of the main flare region. Dodson (2) finds that there are three 'preferred' rates of rise to maximum intensity, all of these being roughly exponential in form. These three rates of rise are approximately in the ratio 6 : 2 : 1. There is some suggestion that intense flares favour the second rate of rise. No intense flare has been observed to adopt the slowest rate of rise. (See Fig.1.).

The rate of decline from maximum intensity seems to be independent of the rate of rise, but this decline is slower than the rise with very few exceptions.

The development outlined above can be followed by a photometric technique, or by measuring at intervals of about one minute, the effective line width of the $H\alpha$ emission line, or its central intensity. The term 'effective width' can be

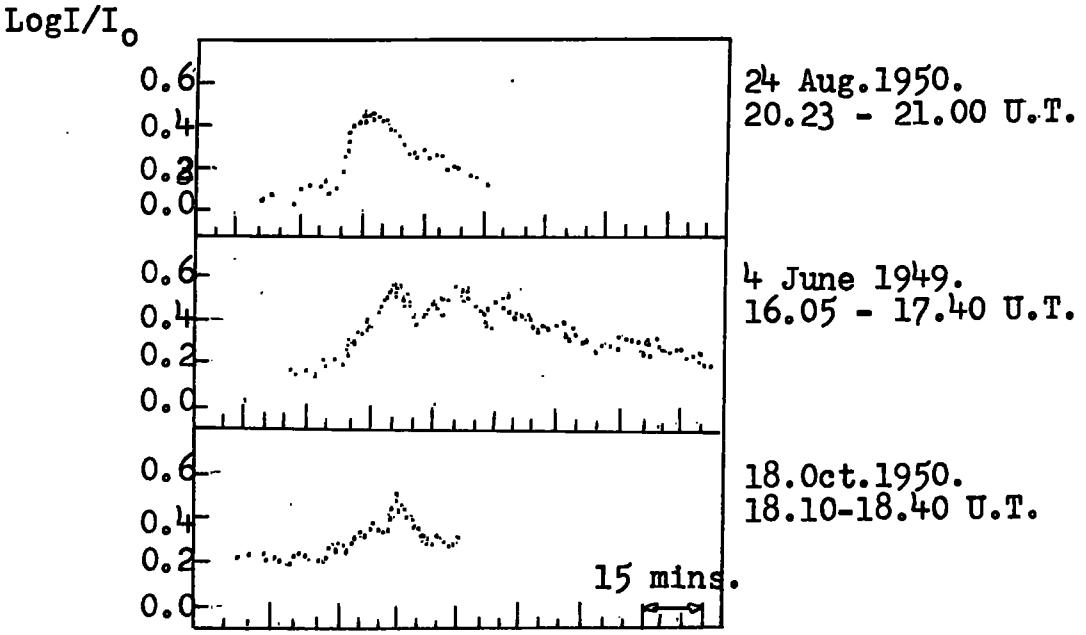

Figure 1. Light curves illustrating the three rates of rise to maximum. (2).

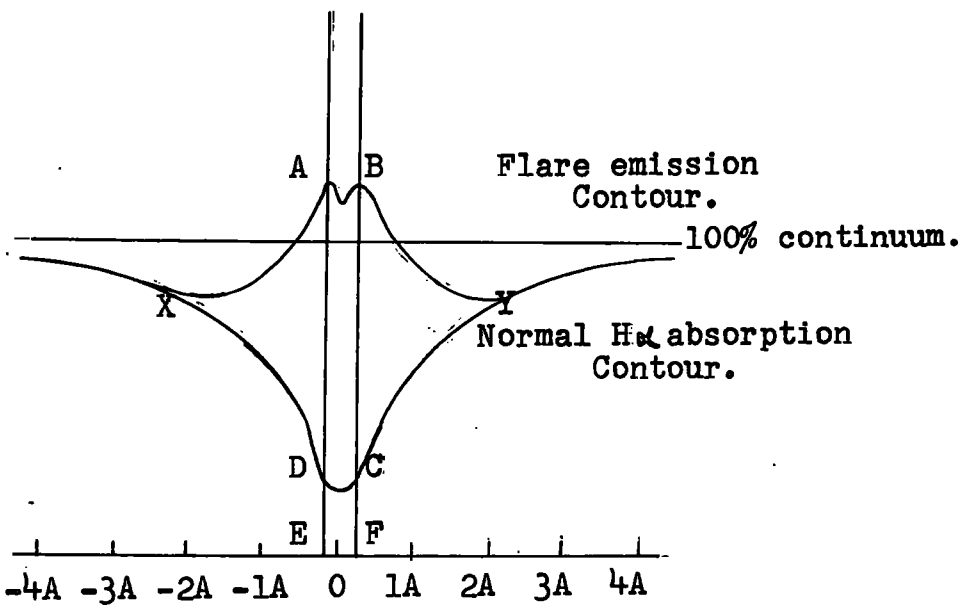

Figure 2.

understood by making reference to Fig.2. The contour XDCY represents the normal contour of the Hα absorption line of the chromosphere, while the contour XABY is that of the flare emission Hα line superimposed upon the normal Hα contour. At the points X and Y the spectral intensities of the flare and its chromospheric background are the same. The wavelength distance, XY, between these two points of equal intensity is known as the effective width of the flare emission line. The development obtained by two different methods would in each case be different. (See Fig.3.).

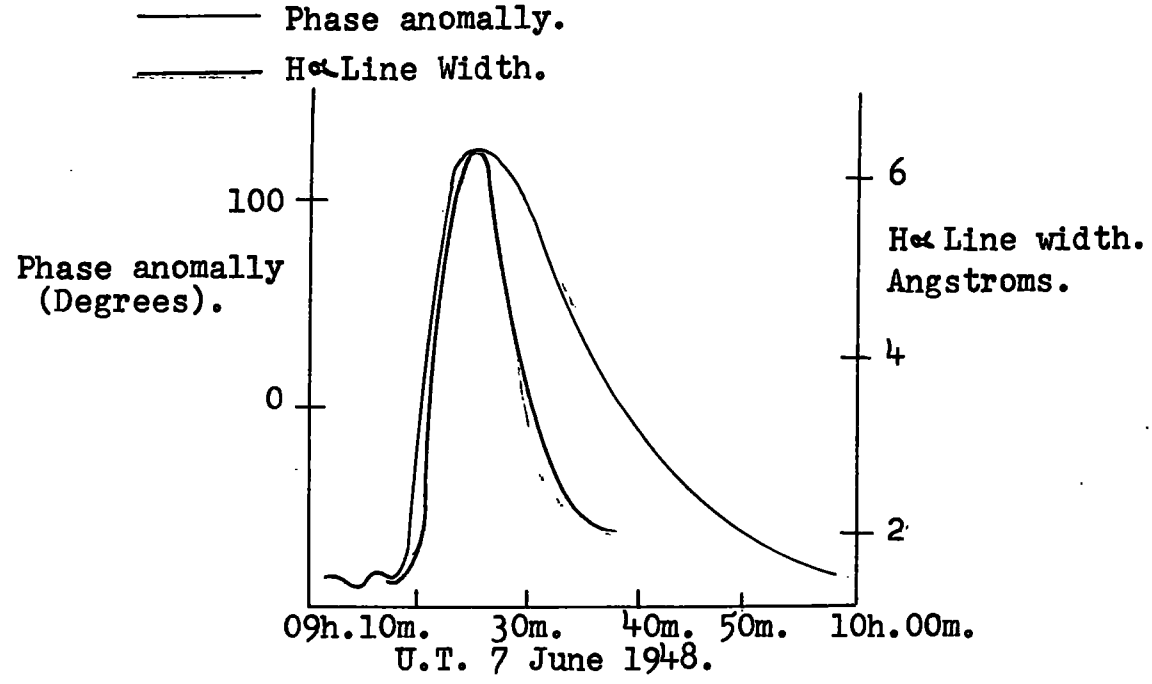

Figure 3. Simultaneous development curves obtained by two different methods. The vertical scales have been adjusted to give equal maxima.

Solar flares are also accompanied by the ejection of large quantities of matter, known as flare surges, from the sun. Giovanelli and McCabe (3) find that the initial direction of these surges is almost invariably radially away from the nearest large sunspot, and that they appear to have a wide variety of appearances at different stages of their lives. The surge usually makes its first appearance during the period when the flare is rising to its maximum intensity. It is seen as a dark, absorption marking with an average velocity of about 50 km./sec. The surge accelerates rapidly and reaches a maximum velocity of more than 100 km./sec. at about the same time as the flare reaches its maximum intensity. During the next few minutes the velocity of the surge falls toward zero, it becomes less dense in appearance, and fades from view at about 30 km./sec. About 2 minutes before this disappearance a second dark marking becomes visible which has a radial velocity of about 35 km./sec. <u>towards</u> the sun's surface. The marking becomes more dense as its velocity increases at a rate slightly less than that due to solar gravity (2.74×10^4 cm./sec.^{2}). This acceleration continues for about 10 minutes and then the marking begins to fade and is lost to view at about 50 km./sec. If the maximum outward velocity of the first absorption marking is large, this inward maximum velocity of the second absorption marking

also tends to be large.

These two absorption markings appear to represent a filament of dense chromospheric material suddenly ejected from the neighbourhood of a flare region and then returning along its original path. The markings are dark in comparison to their photospheric background because, due to the Doppler effect, their absorption leaves the normal Hα line. During the outward journey of the surge its absorption line is displaced to the short wavelength side of Hα, and during its inward journey to the long wavelength side of Hα. At the highest point of the surge's trajectory the velocity becomes zero and there will be no Doppler displacement. This accounts for the apparent fading of the surge as its velocity becomes zero. Fig.4 shows a typical velocity-time graph for these absorption markings.

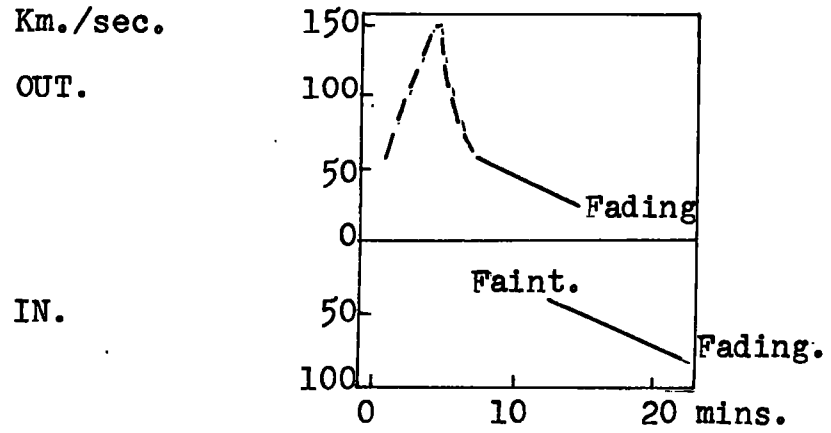

Figure 4. Average radial velocity of 12 out of 19 observed flare surges versus time in minutes. The flares themselves are bright from about 0 to 18 mins., and are at their maximum brightness at 5 mins. The dashed curve is different for different flares. (4).

The electromagnetic radiations emitted by solar flares extend from the far ultra-violet to the radio wavelengths. These radiations reach the Earth in approximately 8.3 minutes. The ultra-violet radiations cause disturbances in the D-layer of the ionosphere in the form of an increase in the electron density and consequently an increase in the conductivity and in the current density. These currents affect the geomagnetic field, producing variations $\sim 10^{-3}$ gauss in H and V. Such variations are called magnetic crochets.

The extra ionisation in the D-layer increases the absorption of short radio waves which are normally reflected from the higher F-layer, causing a temporary, short-wave radio fade out. If the path of the radio waves passes near the point where the sun is directly overhead, the amplitude of the waves is reduced to $\sim 1/50$ of the original value. Very soon after the flare emission has been observed to cease the radio fade out disappears. The effect is apparent only in the sunlit hemisphere of the Earth. However, the D-layer is the reflecting zonerfor very long radio waves of more than 10 km. in wavelength. The reflecting power of the D-layer is dependent on the electron density existing in this layer, and any increase in the electron density would improve the reflecting power causing a temporary improvement in the reception of very long radio waves. This situation is

accompanied by an enhancement of atmospherics, which are long radio waves generated by lightning flashes. This enhancement of atmospherics occurs quite suddenly and can be used as a means of detecting flares.

The sudden increase in the electron density not only improves the reflecting power of the D-layer for very long radio waves but also lowers the height at which the reflection takes place because the conditions for reflection are present at a lower level in the ionosphere. This situation causes a 'sudden phase anomaly' to occur in the reception of very long radio waves from a transmitter situated within a few hundred kilometres of the receiver. The path length of the reflected radio waves has been reduced due to the lowering in height of the effective reflecting region of the D-layer. A receiver will normally be able to receive two series of signals from a transmitter, one series reflected from the D-layer and the other coming by the shortest route along the surface of the Earth. The direct path length from the receiver to the transmitter remains constant, but that of the reflected wave is dependent on the electron density existing in the D-layer, therefore a change in the relative phase between the ground wave and the reflected wave is produced by any variation in this electron density. Bracewell and Straker (5) find that this phase difference provides a very sensitive means of following the development of a flare. This means is independent of observing conditions and gives

a measure of the maximum disturbance produced in the ionosphere by the flare radiation. The measures so obtained are free from personal errors. There is no thoroughly reliable criterion for deciding whether or not a patch of bright hydrogen shall be termed a flare. The occurrence of a sudden phase anomaly associated with a bright hydrogen patch may be used for such a criterion.

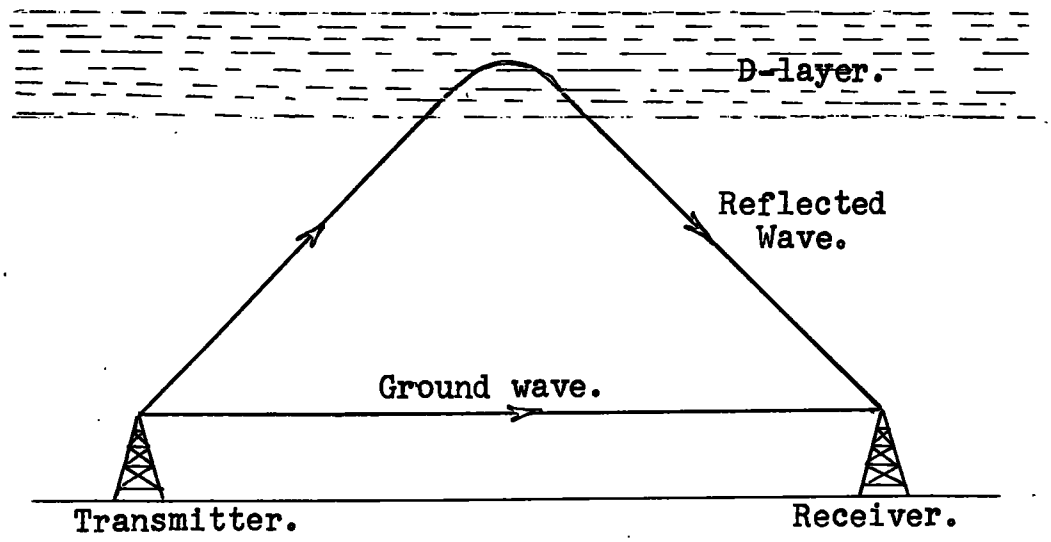

Figure 5. A receiver receiving two series of waves from a transmitter.

The emitted radiations extend to X-ray wavelengths of 1 A, as demonstrated by Chubb et al, and other rocket observations (6) made during the International Geophysical Year. The rocket observations made by Chubb, et al (6) showed that although the flare of June 20, 1956, was still

visible in Hα and the X-ray flux was high, the Lα was not very different from normal. Rocket observations made by the U.S.A. during the total eclipse of 12 October 1958, showed the presence of an intense flare of X-rays in the waveband 1 - 8 A. As totality was reached the ultra-violet intensity diminished to zero whereas the X-ray intensity remained at about the same level. These observations indicate that the ultra-violet radiation emanates from the chromosphere whereas the X-rays emanate from the corona.

The corpuscular emission from flares falls into two main classes and is usually associated with intense flares occurring in latitudes of less than 45°. This indicates that the corpuscular stream leaves the sun in a cone of semivertical angle $\sim 45^{\circ}$. One class consists of slow moving particles which have average speeds $\sim$2,500 km./sec. and reach the Earth in about 20 hours. after the wave radiations. This time of travel, however, varies a great deal and the distribution of travel times for intense solar flares of class 3+, are given in Fig.6.

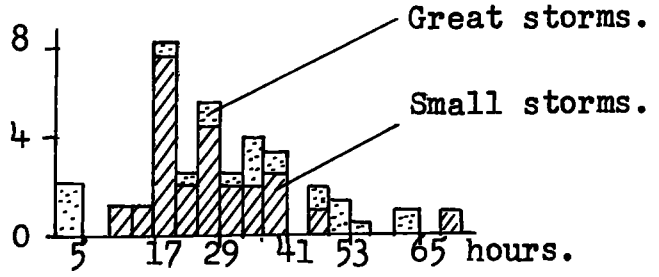

Figure 6. The distribution of time intervals in hours, between intense solar flares (3+) and geomagnetic storms.

The time of travel consists of the time needed to accelerate the particles, the time taken for the particles to travel from the accelerating zone to the Earth, and the time needed to generate the conditions necessary for the occurrence of a magnetic storm. A magnetic storm is characterised by a sudden disturbance of $\gtrsim 10^{-3}$ gauss in H, and the effect is simultaneously apparent at all places with a geomagnetic latitude of less than about 60°, on the night hemisphere as well as the day hemisphere. Such a storm is caused by the Earth's magnetic field encountering a stream or cloud of charged particles that have been ejected from the sun at the time of the solar flare. The resulting variations in the terrestrial magnetic field induces electrical currents beneath the surface of the Earth. The solar particles, on entering the Earth's magnetic field, are guided preferentially along the lines of force, eventually producing Auroral displays in fairly well defined zones near the polar regions. The luminosity of the aurora is caused by the interaction of the solar particles and the terrestrial particles present in the rarefied upper atmosphere. Aurora appear in a variety of forms of which the most common are 'quiet arcs' and 'rays'. A quiet arc has a sharply defined lower border but no clear upper border; the maximum luminous intensity occurs a few kilometres above the lower border and then decreases rapidly just above the ma maximum. The height of aurorae are determined by triangulation

and the greatest auroral frequency occurs at a height of 100 km. Observations made on the aurorae during the International Geophysical Year indicate that quiet arcs lie very nearly along lines of constant magnetic inclination. (8). Aurorae showing a ray structure are aligned parallel to the Earth's magnetic field. They usually show a greater extension in height than the quiet arcs and vary little in luminous intensity. Auroral spectra taken by Gartlein (9) and Meinel (10) show the presence of the first three lines of the Balmer Series. These lines are greatly broadened and displaced. If the displacement is interpreted as a Doppler effect the mean velocity of the incoming solar particles is 450 km./sec. parallel to the geomagnetic field. The maximum velocity is more than 3,000 km./sec. No Doppler displacement could be detected when the observations were made perpendicular to the geomagnetic field.

The second class of corpuscular emission from flares consists of high speed particles, or cosmic rays, which arrive about a quarter of an hour after the visible radiation has reached the Earth. After the occurrence of a flare of medium or high intensity, there is usually a slight increase in the intensity of cosmic radiation. These slight increases are only observable in certain zones on the Earth as the particles are strongly affected by the geomagnetic field. Slight increases are attributed to geomagnetic disturbances

and therefore are probably secondary flare phenomena. However, in five cases, very large, sudden increases in the cosmic ray flux have been observed. These increases are called 'great bursts of cosmic rays', and were associated with the very intense flares of 28 Feb.1942; 7 March 1942; 25 July 1946; 19 Nov.1949; and 23 Feb.1956. The magnitude of the effect was greatly dependent on the latitude, longitude and altitude of the recording station, and in no case was an increase of cosmic ray intensity observed at Huancayo Station on the equator. This indicates that the primary charged solar particles have an energy of less than 15 BeV. It is interesting to note that the flare of Nov. 19, 1949, occurred in association with a spot group whose co-ordinates were 70°W and 2°S, while the flares of 28 Feb. and 7 March, 1942, were associated with a large group of sunspots of which the two principal umbrae had opposite magnetic polarities and a field of some 4,800 gauss. The variations of cosmic ray intensity, recorded at various stations, associated with the flares of 1942 and 1946 are shown in Fig.7. The great decrease in cosmic ray intensity which occurs about 20 hours after the onset of the flare is caused by a geomagnetic storm produced by the slower moving particles of the first class. The subsequent recovery to normal intensity takes several days.

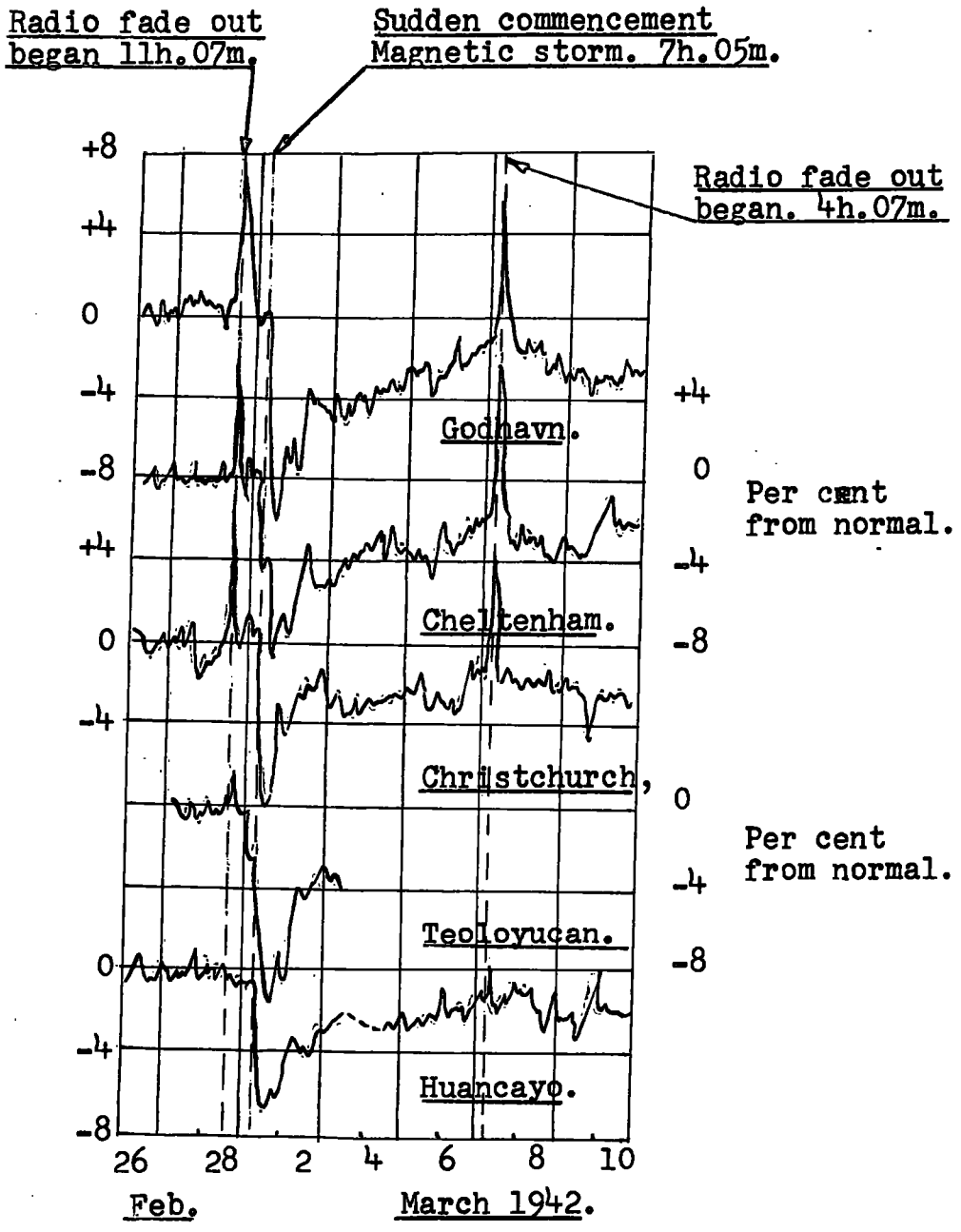

Figure 7. Variations of cosmic ray intensity associated with the flares of 28 Feb. and March 7, 1942. (11).

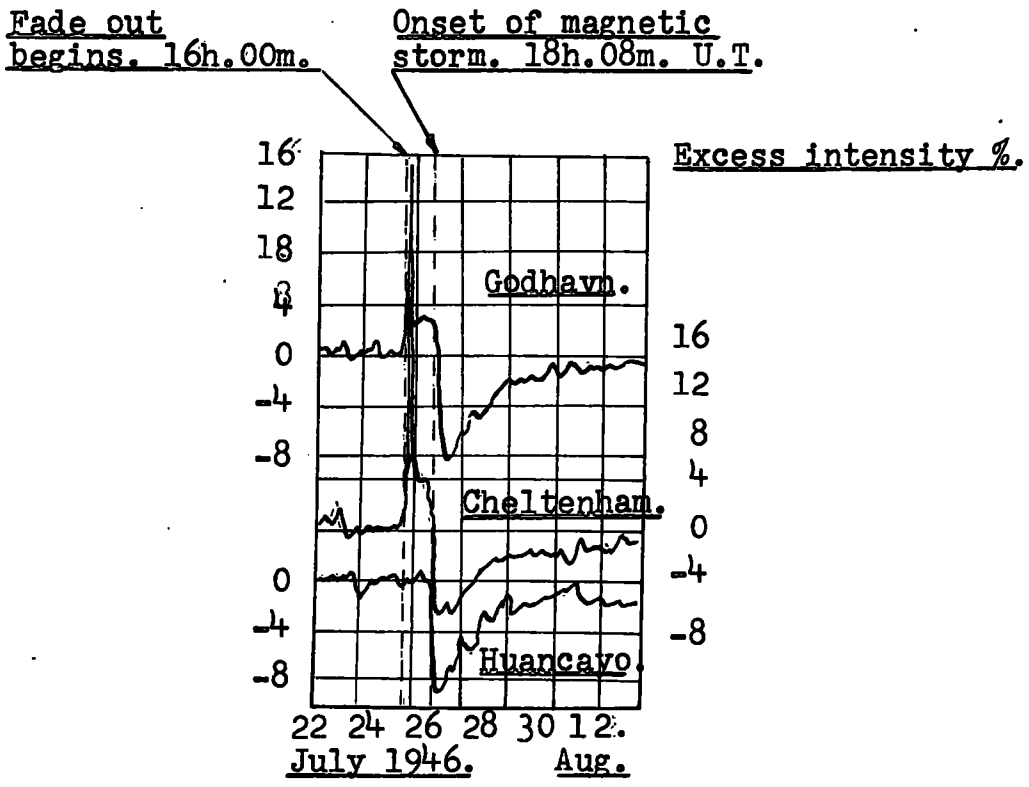

Figure 7. Variations in the intensity of cosmic rays associated with the flare of 25 July 1946. (11).

Increases in intensity, probably associated with flares, have been observed during balloon flights and from aircraft.(12).

Flares are sometimes accompanied by very large increases of solar radio emission. Such increases of radio noise are called 'Outbursts'. The observations of Payne-Scott, Yabsley, and Bolton (13), using frequencies of 200, 100 and 60 Mc/s. suggest that the onset of the flare as shown on a low frequency occurs some time after the onset as shown on a higher frequency. (See Fig.8).

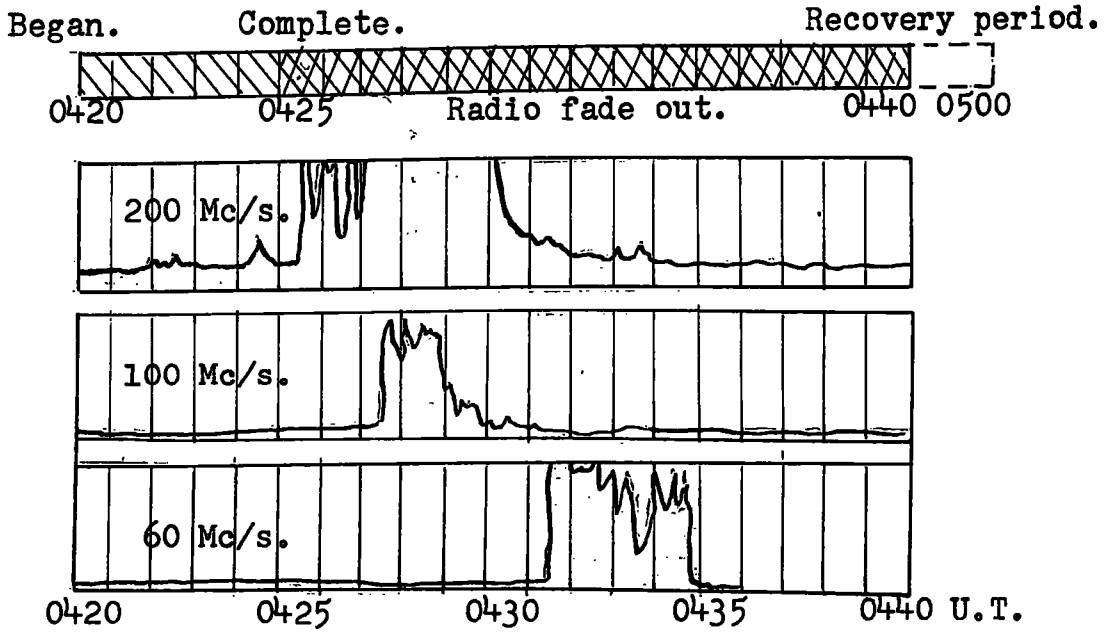

Figure 8. A large outburst on March 8, 1947. (13).

In the same way as the ionosphere is opaque to certain frequency ranges of radiation due to the degree of ionisation of the ionosphere, the ionised atmosphere of the sun is also opaque to certain frequency ranges. Theoretically, electromagnetic radiation can be propagated through a uniformly ionised medium only at frequencies above the critical frequency which is proportional to the square root of the electron density of the medium. Since the electron density of the medium of the solar atmosphere decreases with height, a source of electromagnetic radiation travelling upwards through the chromosphere and corona would exhibit just such a series of delays with the high frequencies preceding the low. The derived velocities of the passage of the source through the solar atmosphere, assuming the Baumbach-Allen electron distribution, is ~ 500 km./sec. The polarisation of an outburst is random during the initial, intense phase, when the source appears to be moving outwards through the chromosphere and corona. The source then seems to drift back towards the solar surface emitting circularly or elliptically polarised radiation, much lower in intensity than that of the initial phase.

The dynamic spectrum of an outburst obtained by Wild, Murray, and Rowe, (14) shows that there is a fairly uniform drift in frequency as time passes, and quite a sharp cut-off at the lower frequencies. (See Fig.10). The outburst also

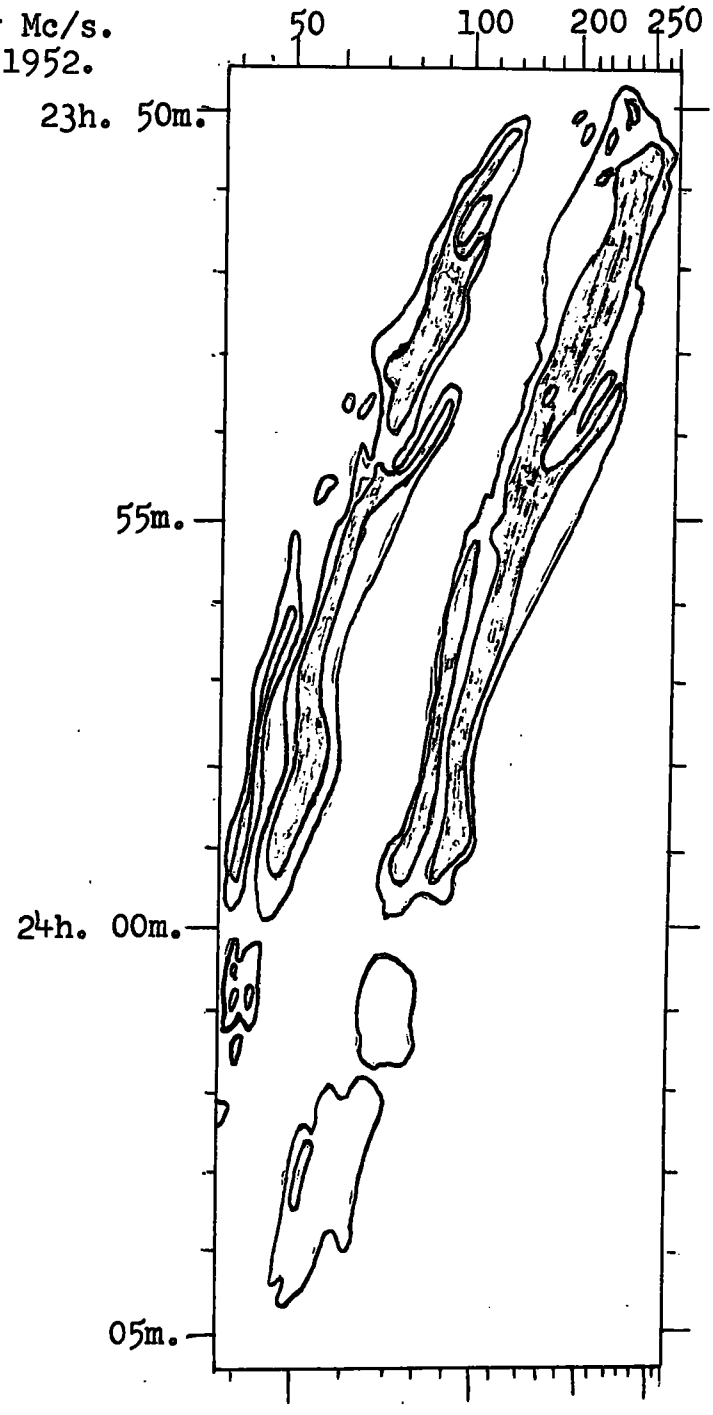

Figure 10. The dynamic spectrum of the outburst of Nov.21, 1952. The two contours represent intensities of 5 and 20 x 10^{-21} watt/sq.metre/cycle/sec. (14).

appears to show the presence of a fundamental and its second harmonic. The multiple peaks of each band of the spectrum could be interpreted as a Zeeman effect caused by a magnetic field of 10 to 30 gauss, but the random polarisation of the outburst is a difficulty here. However, magnetic fields of this order are to be expected in these regions of activity. The slight circular or elliptical polarisation of the later stages of an outburst has been attributed by Payne-Scott and Little to the development of coronal magnetic fields during the outburst while Wild (15) suggests that it may be due to a state of turbulence in the corona produced by the corpuscular emission from flares. The postulated outward velocity of the source suggests an association with the velocity of ejection of the aurora generating particles from the sun. The above results were obtained using a frequency range of only 40 to 240 Mc/s. Later work by Davies (16) with equipment possessing a range from 60 to 10,000 Mc./s. showed that the flare onset is often revealed on 3,000 Mc./s. before any other frequencies. These observations suggest that there is a simultaneous up and down movement of ionised material. It has been already suggested that flare surges appear to exhibit a simultaneous up and down movement near the top of their trajectories. (See page 7).

The development of phenomena associated with a solar flare is shown diagramatically in Fig.11.

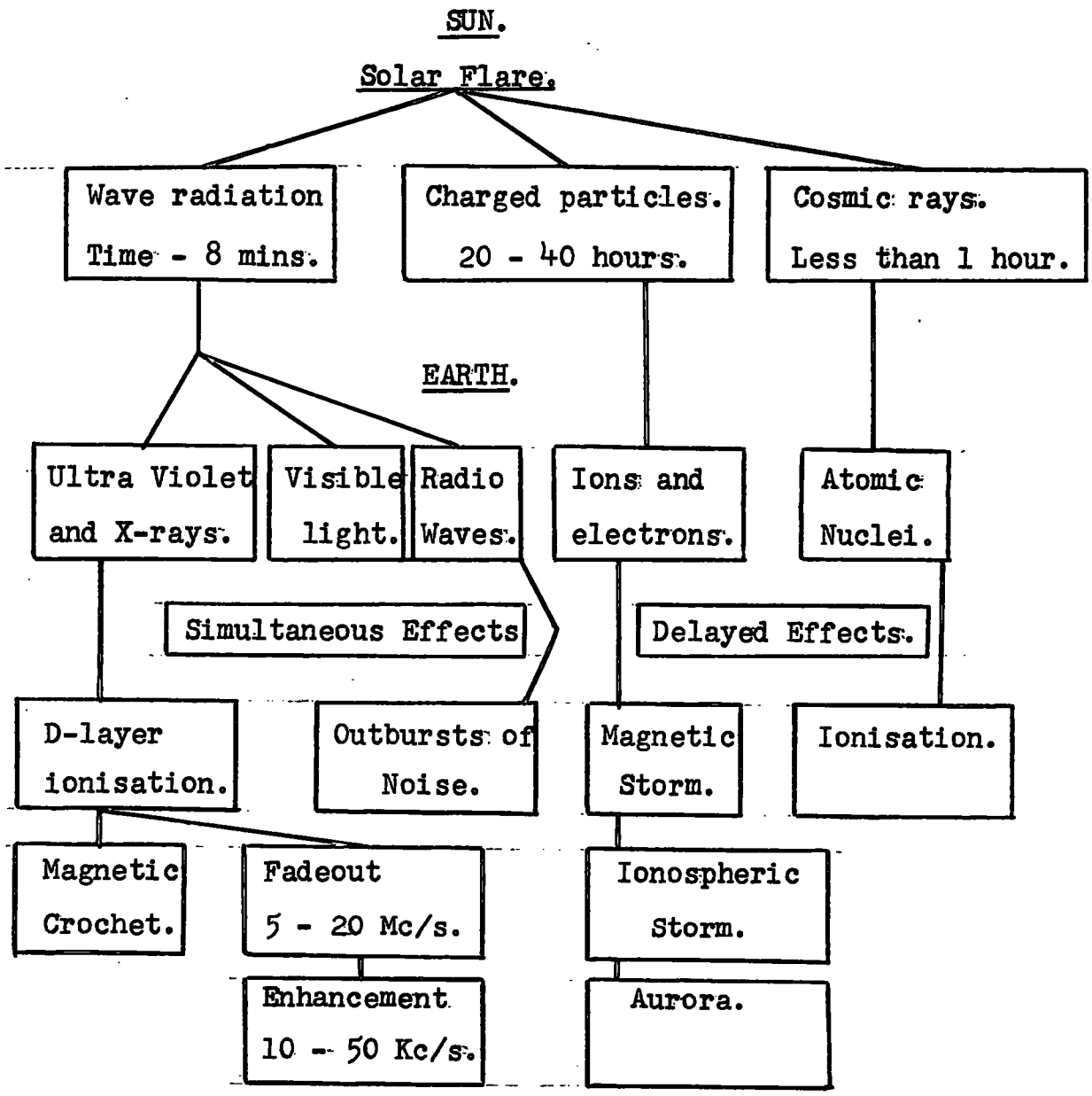

Figure 11. The development of phenomena associated with a Solar Flare.

D.The Characteristics of Solar Flares.

The characteristics of solar flares have been summarised by Ellison (17), Hunter (18), Giovanelli (19), and by Kiepemheuer (20). The following list of features characterising flare emission patches and associated secondary phenomena include those given in the above papers together with some not previously listed.

(i) Visual Characteristics.

1. The areas of flares range from 0 to well over 1,000 millionths of the sun's hemisphere.
2. They develop out of pre-existent normal bright hydrogen flocculi.
3. Their rise to peak intensity is usually very rapid and is nearly always followed by a relatively slow decay.
4. The duration of peak intensity is very short, being less than 5 minutes, although their total life may be many hours.
5. They appear to have no lateral or vertical movement independent of other adjacent chromospheric markings.
6. They are encountered at various levels in height ranging from ~10,000 to ~30,000 km. from the photosphere, i.e. in the chromosphere and lower corona.
7. All available evidence indicates that flares appear suddenly, and there is no detectable emission of masses of gas from deeper layers of the sun's atmosphere.

8. About 80% of flares of intensity 3 and 3+ eject surge type prominences of class 3d. These prominences appear as narrow spikes moving in almost vertical trajectories to a height of~ 30,000 km. (See page 6).
9. The probability of a flare occurring, according to Giovanelli (21), varies with the area, the rate of increase of the area, and the complexity of the associated sun-spot group. No attempt has been made to determine the probability of any particular class of flare occurring.
10. Small flares seem to favour the stages of rapid sunspot growth or decay, while the most intense flares appear to favour the more mature stages of sunspot development.
11. Flares of intensity 3 and 3+ are often characterised by long ribbon-like emission filaments passing over, and often obscuring many of the largest umbrae. The majority of flares of lower intensity are not of this filamentary nature but often appear as oval or irregular patches of light, showing a noticeable avoidance of the main umbrae, and a preference for the smaller spots and pores in the vicinity of the larger ones.
12. Flares of class 3+ are very rare occurring on the average once or twice a year, while flares of class 1 occur every few hours during periods of marked solar activity.
13. If a flare has a filamentary nature, a neighbouring

filam. bur

filament of chromospheric material lying on the geometrical extension of the flare filament is often affected. The perturbation is propagated with a velocity of ~100 km./sec.

14. Some parts of a flare appear to follow the vortex pattern around the associated sunspot group.

(ii). Spectral Characteristics.

15. Although flares are mainly confined to the chromosphere great variations in height have been recorded. Allen (22) has shown that there is a detectable change in the relative intensities of Fraunhofer lines in the lower regions below the flare.

16. The true central intensities in units of the intensity of the surrounding continuous spectrum close to Hα is about 0.6 for class 1; 1.5 for class 2; and 2.3 for class 3.

17. The contour of the bright emission line is nearly symmetrical about the normal position of Hα, and is independent of the position of the flare on the sun's disk. Doppler displacements of the contour have not been observed in excess of ~ 10 km./sec.

18. There is a greater extension in the red wing of the bright Hα emission than in the blue wing. This extension increases with the importance of the flare, reaching about 0.7A for flares of class 3.

19. Flare spectra show bright reversals in the Balmer

absorption lines of Hydrogen, neutral helium, ionised calcium, iron, silicon and a few other metallic elements, but there is much variation in detail between different flares. There is no evidence that black body radiation, sufficient to account for the observed geophysical effects is associatedcwith solar flares.

20. In a few cases very intense flares have been visible in integrated white light.

21. The effective line width of the Hα emission at the peak intensity of the flare usually varies from 1.75A to about 16A, but Ellison and Conway (23) reported a width as great as 22A for the flare of November 19th.1949.

22. Bruck and Ruttlant (24) report that there is some indication of a small depression in the violet wings of the H and K lines in the solar spectrum during a magnetic storm. This depression, if interpreted as a Doppler effect would represent a velocity of a cloud of particles of about 750 km./sec.

23. Richardson and Minkowski (25) find that there appears to be no essential difference in the spectral characteristics of solar flares of different classes. Spectroscopically the distinction between one class and another is merely one of intensity.

24. Variation between the two helium lines $D_3(3^3D - 2^3P)$ and $\lambda 6678$ $(3^1D - 2^1P)$ is very marked. D_3 appears sometimes in

emission, sometimes in absorption, and often not at all. λ6678 appears only in emission from a few intense flares.

25. Allen (22) finds that the Fe^+ lines are enhanced in solar flares.

(iii). Radio Emission Characteristics.

26. An outburst of emission associated with a solar flare usually lasts several minutes and is observable in frequency range of 38,000 Mc./s. to 20 Mc./s.

27. The polarisation of such an outburst is random, although Akabane and Atanaka (26) find that changes in polarisation on 9,000 Mc./s. took place during the three large flares on 3 July 1957. They suggest that these changes in polarisation were due to a shift in the flare activity centre relative to the sunspot magnetic field.

28. The emitting material often appears to be moving simultaneously up and down with velocities of the order of 1,000 km./sec.

29. The outburst of 21 Nov.1952, observed by Wilde, Murray and Rowe (14) showed the presence of a fundamental and its second harmonic.

(iv). Magnetic Characteristics.

30. Detailed studies of magnetic fields in active sunspot regions made during the I.G.Y. show that the lines of force are suddenly redistributed during a solar flare.

31. There is no close correlation between sunspot magnetic

fields and the shape of solar flares, but the flares of 18 Feb.1942 and 25 July 1946, followed the line of demarcation between the regions of opposite magnetic polarity.

32. Flares are most frequent during the initial and final stages of the life of the associated sunspots, indicating that changes in magnetic flux are more important than actual field strength.

(v). Cosmic Ray Characteristics.

Increases in cosmic ray intensity are associated with a very intense flares and these increases have the following characteristics:-

33. They are extremely rare. The information available so far shows that they usually occur every few years.

34. The maximum intensity occurs about one hour after the beginning of a solar flare.

35. No appreciable increase in cosmic ray intensity has been recorded at the equator (Huancayo), indicating that the particles were charged and had energies $\lesssim 15$ BeV.

36. The magnitude of the effect at the American stations was several times as great as at the European stations.

37. The magnitude of the effect of the ionising component rapidly increases with elevation above sea level and at mountain levels is about four times as great as at sea level.

38. The magnitude of the neutron component effect is many times as great as the ionising component.

39. The increase in intensity proceeds very rapidly in a few minutes; the return to normal level is much slower and takes several hours.

40. There are differences in the variations of intensity at the middle and high latitude stations.

41. A flare, irrespective of its location on the solar disk, may emit cosmic rays detectable on the Earth.

(vi). Auroral and other Characteristics.

42. Observation made on aurorae during the International Geophysical Year show that the zones of equal frequency of occurrence of aurorae in the two hemispheres appear to be nearly along lines of constant magnetic inclination and not along lines of equal geomagnetic latitude.

43. Magnetic storms and aurorae take place only if the flare occurs near the centre of the disk as seen from the Earth.

44. The first 3 lines of the Balmer series have been observed in certain auroral spectra (27). These lines are greatly broadened indicating that the aurorae-generating particles consist of hydrogen atoms travelling with speeds of $\gtrsim 450$ km./sec. However, Meinel and Fan (28) find evidence of some helium nuclei in the aurorae-generating particles.

45. The height at which aurorae most frequently occur is about 100 km. (29). This height would necessitate energies of $\sim$1 MeV if the particles are protons and 4 KeV

if they are electrons. However, the velocities corresponding to 1 MeV are ~ 15,000 km./sec. and no Doppler shift has been observed corresponding to velocities much greater than 3,000 km./sec.

46. The maximum auroral frequency occurs at latitudes of 67°.

47. The occurrence of aurorae depends on local time and has a maximum frequency at about 23.00 hrs.

48. Aurorae with a ray structure occur more frequently before 23.00 hrs. than after.

49. Rapidly fading radar echoes are obtained from Aurorae on frequencies of more than 20 Mc./s. These echoes are probably produced as a result of scattering by the fine raylets of ionisation.

50. There is some evidence that aurorae are caused by particles leaking from the Van Allen radiation belts and that the rate of leakage is associated with the intensity of flare activity.

51. Flares cause increased conductivity in the D-layer of the ionosphere, which causes abnormal attenuation in short radio waves, and produces small characteristic disturbances in the Earth's magnetic elements. These disturbances are in the same sence as the normal diurnal variation and last only as long as the visible flare.

52. Bracewell and Straker (5) have found that the phase of very long radio waves is highly sensitive to the occurrence of of solar flares. Many so called flares of class 1- produce

no phase anomaly.

53. Warwick (30) finds from a statistical analysis of flare data obtained at the Sacremento Peak Station, New Mexico, that there is no certain evidence of a Sudden Ionospheric Disturbance associated with a flare having a height of less than 15,000 km. above the Hα limb.

54. Nonweiler (31) discovered that there is an apparent correlation between the fluctuations in the rate of decrease of the period of an Earth Satellite and contempor--ary fluctuations in total flare intensity. This indicates that flares are associated with a temporary decrease in air density and/or temperature within the lower ionosphere.

E. A brief survey of the characteristics of Sunspots, the Chromosphere and the lower Corona.

Since flares occur in the chromosphere and the lower corona, and always in the vicinity of active susnpot groups, any adequate theory of solar flares must explain how the conditions in these regions reach the stage where a flare occurs. The principal features of these regions may be summarised as follows:-

Sunspot Groups.

(1). They are formed by the coalescence of a number of pores.

(2). Their effective surface temperatures are of the order of 4,500°K.

(3). Their lives range from a few hours up to about two months.

(4). When fully developed they are roughly circular in shape with a dark inner region, or umbra, surrounded by a less dark annulus or penumbra. The line of demarcation between umbra and penumbra is remarkably clear. The umbra occupies about a fifth of the total area.

(5). Large spots are usually distorted in shape.

(6). There is some suggestion that the surface of the spot has the form of a depression.

(7). The average radius of a spot is of the order of 10,000 km.

(8). 90% of spots tend to occur in pairs, lying approximately in the same latitude, and having different polarities.

(9). The distance between the two spots of a pair increases during the initial stages of spot development and then decreases during the later stages of development. (See Fig.12).

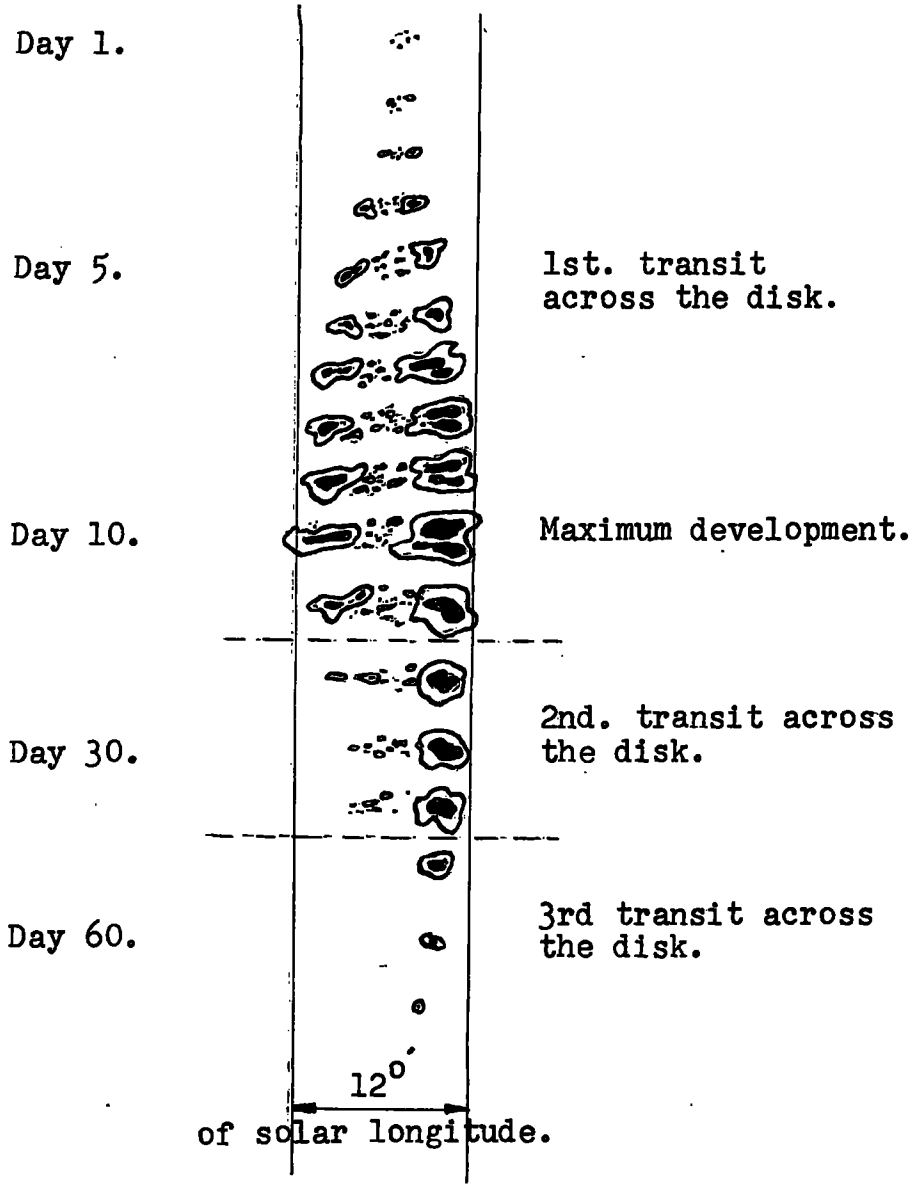

Figure 12. The development of a typical spot group.

(10). Their magnetic fields are about 3,000 gauss.

(11). The magnetic field of the leading component of a bipolar spot group tends to be stronger than that of the following component.

(12). 90% of spot groups are bipolar, 10% unipolar, and about 1% are multipolar.

(13). The material at the surface of a spot is observed to be flowing out of the spot at about 2 km./sec. This phenomenon is known as the Evershed effect.

(14). The frequency of sunspot occurrence varies over a period of about 11.1 years, having an interval of 4.5 years from minimum to maximum and 6.6 years from maximum to minimum.

(15). There is an asymmetry in the distribution of spots in the two hemispheres.

(16). They show a periodic variation in latitude. New cycle spots break out in belts approximately in latitudes 30^{o}N and 30^{o}S. and these belts gradually drift towards the equator as the sunspot activity increases until latitudes 16^{o}N and 16^{o}S are reached. The drift towards the equator continues with decreasing activity until the spots finally die out at 8^{o}N and 8^{o}S. Two or three years before this disappearance new spots begin to appear in latitudes 30^{o}N and 30^{o}S, and the cycle repeats itself.

(17). During any one cycle the magnetic polarities of bipolar spot groups are systematically orientated in each hemispheres. The leader spots are North seeking in one hemisphere and South seeking in the other hemisphere. During the succeeding cycle this orientation is reversed. Thus the sunspot cycle may be said to be 22.2 years.

The Chromosphere and Lower Corona.

The emission spectrum of the lower chromosphere resembles a reversal of the Fraunhofer absorption spectrum of the solar disk. However, there are more lines of ionised metals and high excitation lines of neutral atoms in the spectrum of the lower chromosphere than in the spectrum of the disk. The first members of the Balmer and Paschen series of hydrogen, the H and K lines of Ca^+, some He lines and one He^+ line are visible to heights of more than 10,000 km. The Hα line extends to the greatest height in the chromosphere and cannot be detected at heights of more than 12,000 km. This height is regarded as the upper limit of the chromosphere and the base of the corona. The base of the chromosphere is at a height of 1,500 km. Above this conditions become non-thermodynamic. From the photosphere to a height of 1,500 km. conditions are approximately thermodynamic and this region of the solar atmosphere is known as the reversing layer.

The temperature of the lower chromosphere as given by Van de Hulst (32) after analysing the available observational evidence, is $\sim 10^4$ ^oK. The temperature of the upper chromosphere above 6,000 km. has a steep gradient and reaches a temperature of $\sim 3 \times 10^4$ ^oK near the base of the corona. This temperature gradient is maintained in the corona where the temperature reaches values of $\sim 10^6$ ^oK. Above disturbed regions of the solar surface parts of the chromosphere may extend themselves into the corona. These extensions are called prominences.

Electrodynamics of the Chromosphere and the Lower Corona overlying Sunspots.

It is now generally accepted that electromagnetic phenomena play an essential role in nearly all solar events. However, the subject is still in an early stage of development and in consequence no detailed correlations can be expected between theory and observation. It is obviously desirable to have an experimental check on the theory but the difficulties involved in any attempt to construct laboratory models of solar phenomena are very great. It is necessary to have solid bounding walls which often have complicated effects exceedingly difficult to interpret. It is difficult to obtain a high enough degree of ionisation in a discharge tube and the characteristic dimension of the laboratory model is necessarily very small compared to that of the solar system. Furthermore, no liquid has a high enough conductivity to make a good scale model, and this combined with the small characteristic dimension, makes it very difficult to investigate the required phenomena owing to the rapidity of their decay. However, certain experiments have provided confirmation of the theory. In particular, the inhibition of turbulence and convection by a magnetic field, and the presence of magnetohydrodynamic waves in mercury.

In general the theoretical method of attack is easier than the experimental method and this chapter is intended to give an outline of the accepted fundamental

theory relevant to solar flares and related phenomena. Any theoretical model should be at least consistent with the following ideas.

The fundamental equations used in solar electrodynamics are those of electromagnetism and hydrodynamics, with appropriate modifications. In any work of this kind it is usually necessary to make rough calculations of orders of magnitude using a characteristic length 'a' and a characteristic time 't' to obtain the orders of magnitude of derivatives. In the solar atmosphere overlying sunspots 'a' may be taken as $\sim 10^9$ cm.

Faraday's law states that the rate of change of flux through a closed loop is equal to the e.m.f. round that loop. If the loop consists of a perfectly conducting fluid, as is the case with the solar atmosphere to a high degree of approximation, the e.m.f. must be zero and hence the flux cannot change. If the fluid is in motion this result can be extended to apply to a loop, every point of which moves with the velocity u of the fluid at that point. The condition of perfect conductivity requires that at each point the electric field in the frame moving with the velocity u should be zero, or, in Gaussian units,

$$E = -u \times H/c \quad . \quad . \quad . \quad . \quad . \quad . \quad . \quad . \quad (1).$$

where E and H are the electric and magnetic field respectively and c is the velocity of light. The departures from unity of both the dielectric constant and the magnetic permeability are negligible in the case of the solar atmosphere. It will

be shown later that (1) is a good approximation in solar conditions, and may be regarded as valid for the purposes of this chapter.

If we consider next the Maxwell equation

$$4\pi j = c.\mathrm{curl}\ H - \partial E/\partial t \quad . \quad . \quad . \quad . \quad . (2).$$

we have, using orders of magnitude,

$$|\mathrm{curl}\ H| \sim H/a$$

and from (1), $E \sim uH/c$ giving $\partial E/\partial t \sim uH/ct$ and thus

$|\partial E/\partial t| \ll c.\mathrm{curl}\ H.$

and $$4\pi j \approx c.\mathrm{curl}\ H \quad . \quad . \quad . \quad . \quad . \quad . \quad . (3).$$

Consistent with (3) is the equation

$$\mathrm{div}\ j = 0 \quad . \quad . \quad . \quad . \quad . \quad . \quad . (4).$$

which expresses the fact that the flow of currents leads to no piling up of charge.

The equation of electromagnetic induction is

$$c.\mathrm{curl}\ H = -\partial H/\partial t \quad . \quad . \quad . \quad . \quad . \quad . (5).$$

showing that the induced currents flow in such a way as to oppose the motions and changes of field causing them.

From (1) equation (5) can be written

$$\mathrm{curl}(u \times H) = \partial H/\partial t \quad . \quad . \quad . \quad . \quad . \quad . (6).$$

which is the equation obtained by supposing that the lines of force are dragged about with the velocity u of the material. The lines of force may be said to be 'frozen' into the material. The effect may also be interpreted as electromagnetic shielding in large masses of gas.

For small masses of gas the induced currents will not appreciably affect the magnetic field and we may adopt the following treatment. The force P on a charge e moving with velocity u is

$$P = e(E + u \times H/c) \quad . \quad . \quad . \quad . \quad . \quad (7).$$

Because of the term u x H/c in this a current density j leads to a body force j x H/c per unit volume. Thus if v is the material velocity, and p and ρ are the pressure and mass density respectively, the equation of hydrodynamic flow is

$$\rho\, dv/dt = -\text{grad.}p + \rho g + j \times H/c \quad . \quad . \quad . \quad (8).$$

where g is the vector acceleration of gravity. The body force j x H/c can be expressed in terms of H alone using (3). It is equivalent to an electromagnetic tension $H^2/8\pi$ along the lines of force, and a pressure $H^2/8\pi$ per unit area perpendicular to the lines of force. In the solar atmosphere $\rho g \approx \text{grad.}p$ and (8) reduces to

$$\rho\, dv/dt = j \times H/c.$$

$$= \sigma E \times H/c = \sigma(v \times H/c^2) \times H$$

$$\therefore \rho\, dv/dt = -\sigma v H^2/c^2$$

where σ is the conductivity.

Thus for any motion across the lines of force, v will decay like $\exp.(-t\sigma H^2/\rho c^2)$. The decay time τ is therefore given by $\tau = \rho c^2/\sigma H^2 \quad . \quad . \quad . \quad . \quad (9).$

In the chromosphere, where flares usually occur we may take $\rho \sim 2 \times 10^{-13}$, and $\sigma/c^2 \sim 3 \times 10^{-8}$ e.m.u., giving

$\tau \simeq 10$

$\tau \sim 6 \times 10^{-6}/H^2$. Thus for any appreciable magnetic field H the velocity across the lines of force is likely to disappear in a very small fraction of a second. Thus, small scale motion in a magnetic field is likely to be along lines of force.

It is clear that in solar conditions inductive drags are very important, and may be more important than the conductivity in determining the currents which flow.

Conductivity in the Solar Atmosphere.

The relation between the current j and the electric field E in the presence of a magnetic field H can be considered as a combination of two particular cases. (33).

(1) E parallel to H.

The current j is given by

$$j = \sigma E \quad . \quad . \quad . \quad . \quad . \quad . \quad . \quad (10).$$

where σ is the conductivity given by $\sigma = c^2 n_e e^2/\nu m_e$, where n_e is the electron density, and the electron-proton collision frequency $\nu = 15 n_e T^{-3/2}$ for fully ionised hydrogen.

$$\therefore \sigma/c^2 = e^2 T^{3/2}/15 m_e$$

$$= T^{3/2}/5.35 \times 10^{13} \quad . \quad . \quad . \quad . \quad (11).$$

Equation (10) is also valid in the absence of a magnetic field.

(2) E perpendicular to H.

In this case the current is given by

$$j = \sigma^{I}E + (\sigma^{II}E \times H)/H \quad . \quad . \quad . \quad . \quad (12).$$

and $\sigma^{I} + i\sigma^{II} = c^2(5.35 \times 10^{13}T^{3/2} - i.8.6 \times 10^{3}HT/P_e)^{-1}$

where σ^{I} and σ^{II} are the conductivities parallel to E and perpendicular to both E and H respectively; $i = \sqrt{-1}$, and P_e is the electron pressure in dynes/cm^2. From these equations the following relations can be obtained:

$$\sigma^{I}/\sigma^{II} = 6.2 \times 10^{9}P_e/HT^{5/2} \quad . \quad . \quad . \quad . \quad (13).$$

$$\sigma/\sigma^{I} = 1 + (\sigma^{II}/\sigma^{I})^2 \quad . \quad . \quad . \quad . \quad (14).$$

$$\sigma/\sigma^{II} = \sigma^{I}/\sigma^{II} + \sigma^{II}/\sigma^{I} \quad . \quad . \quad . \quad . \quad (15).$$

In the chromosphere overlying sunspots we may take $P_e \sim 10^{-2}$ dynes/cm^2 and $T \sim 2 \times 10^{4}$ ^{o}K. These values give $\sigma^{I}/\sigma^{II} \sim 1.1 \times 10^{-3}/H$ and since H is usually ~ 100 gauss it is clear that

$$\sigma \gg \sigma^{II} \gg \sigma^{I}.$$

However, well beneath the photosphere P_e probably reaches $\sim 10^{7}$ dynes/cm^2 and $T \sim 3 \times 10^{4}$ ^{o}K. These values now give $\sigma^{I}/\sigma^{II} \sim 4 \times 10^{5}/H$. Thus, deep in the solar interior, provided $H < 4 \times 10^{5}$ gauss, we have

$$\sigma^{I} > \sigma^{II} \quad \text{and} \quad \sigma \approx \sigma^{I}.$$

Therefore, in the chromosphere and lower corona overlying sunspots the conductivity perpendicular to H is negligible, while deep in the solar interior and in the main body of a spot it is comparable to the conductivity parallel to H.

<u>The Decay of Magnetic Fields</u>.

Consider the equation $4\pi j$ = c.curl H; this can be written as c.curl H = 4

written as c.curl H = $4\pi\sigma$E. Taking the curl of both sides of this equation we obtain c.curl(curl H) = $4\pi\sigma$curl E which, using (5), reduces to

$$c^2.\text{curl}(\text{curl H}) = 4\pi\sigma.\partial H/\partial t \quad . \quad . \quad . \quad (16).$$

This is a diffusion equation indicating that the field decays by leaking to regions where the field is in the opposite direction and so being neutralised. Using orders of magnitude (16) becomes

$$c^2H/a^2 = 4\pi\sigma H/t.$$

where t is a decay time during which H changes by an appreciable fraction of itself, and a is the characteristic dimension $\sim 10^9$cm. Taking $\sigma/c^2 \sim 3 \times 10^{-8}$ e.m.u., then $t \sim 4 \times 10^{11}$secs $\sim 10^4$ years.

Even if 'a' is reduced by a factor of 10 the decay time is still about 100 years. From the above considerations it is obvious that a sunspot magnetic field cannot grow or decay while the spot is a visible surface feature which is ~10 to 100 days. The observed decay must be due to material motions carrying the lines of force beneath the solar surface. There seems to be little chance of a line of force shrinking to a point and so disappearing.

<u>The validity of E = -u x H/c.</u>

Strictly speaking equation (1) should be written as E = -u x H/c + E_r. The extra term E_r is due to electric fields produced by any relative motion between the magnetic

field and the material other than the velocity u. The following causes of such relative motion are:

(a) Hall effect.

(b) Electrical Resistance.

(c) Enhancement of resistance by turbulence.

(d) Thermoelectric effects.

(e) Viscous effects.

(f) Radiation pressure.

(g) Relative motion of neutral particles.

(h) Recombination and ionisation.

Equation (1) will be valid provided the electric fields produced by these effects are negligible compared to the induction field $-u \times H/c$.

The Hall Effect.

The Hall effect results from the difference between the masses of electrons and protons, m_e and m_p respectively, and can be represanted in (1) by the addition of an extra term

$$(m_p - m_e).j \times H/ec^2(n_p m_p + n_e m_e) \quad . \quad . \quad . \quad (17).$$

where n_p is the proton density. In ionised hydrogen $n_e \approx n_p$ and omitting the factor $(m_p - m_e)/(m_p + m_e)$ which is $\approx$ unity, (17) may be written as

$$j \times H/n_e ec^2 \quad . \quad . \quad . \quad . \quad . \quad (18).$$

which is very small compared to the induction field in all solar applications. (See table 1 for orders of magnitude).

The electrical resistance.

The ohmic field can be represented by the term j/σ. The rationof the ohmic field to the induction field is $\sim c^2/4\pi au\sigma$ and is seen to be very small.

Turbulence.

The Reynolds stresses, due to the transfer of momentum can be represented approximately by ρu^2 where ρ is the mass density of the material. The total magnetic stress is comparable with $H^2/4\pi$. Thus the magnetic field will inhibit turbulence if $H^2 > 4\pi\rho u^2$. This is always true in the chromosphere overlying sunspots and therefore turbulence is unlikely to occur and will give no contribution to the induction field.

Thermoelectric effects.

J.W.Dungey (34) has shown that the resulting field due to thermoelectric effects is kT/eac where k is Boltzmann's constant. By making reference to table 1 it will be seen that the thermoelectric field is quite negligible.

Viscous effects.

Viscosity, like all transport phenomena, is affected by a magnetic field. The rate of transport of charged particles across the maghetic field is reduced by a factor $\sim \nu_{pp}/(\Omega^2 + \nu_{pp}^2)^{\frac{1}{2}}$, the rate of transport parallel to the field remaining unchanged. Here, ν_{pp} is the proton-proton collision frequency and Ω is the proton angular gyrofrequency given by $\Omega = eH/m_p$. In the chromosphere and lower corona

overlying sunspots the gyrofrequency is large compared to the collision frequency and in consequence the rate of transport of charged particles perpendicular to H is considerably impeded. Thus, viscous effects may be neglected when considering their contribution to the electric field.

Radiation pressure.

The movement of charged particles perpendicular to the magnetic field due to radiation pressure can be regarded as a transport phenomenon. This effect can be treated in the same way as viscous effects and may be neglected in the solar atmosphere overlying sunspots.

Relative motion of neutral particles.

If the velocity of the neutral particles differs from the bulk velocity an electric field will be produced in the following manner. Because of their smaller masses, the electrons will be affected more than protons by collisions with neu-tral particles, and the consequent contribution to the electric field will be in the opposite direction to the induction field. However, such relative motion is opposed by collisions between the neutral and charged particles and the effect can only be of importance where the neutral particlesdensity exceeds, or is at least comparable with, the charged particle density. This condition is only satisfied at photospheric level. The effect has been discussed by Hoyle (35) and found to be small.

Recombination and ionisations.

Charged particles may be effectively transported

across the magnetic field if the ions recombine, move across the field, and then become reionised. However, in the chromosphere and lower corona the hydrogen is nearly fully ionised and any electric field produced in this way would be negligible compared to the induction field. Even at photospheric level, where neutral hydrogen is the dominant constituent, the process is far too slow to warrant consideration.

Table 1. Various orders of magnitude for the chromosphere and lower corona overlying sunspots.

Quantity.		Order of magnitude.
a	cm.	10^9
u	cm./sec.	10^6
H	gauss.	5×10^2.
T	^oK.	2×10^4.
σ/c^2.	e.m.u.	10^{-8}
$H^2/8\pi$	dynes/cm^2.	10^4
uH/c		2×10^{-2}
$j \times H/n_e ec^2$.		3×10^{-5}
$c^2/4\pi au\sigma$		10^{-8}
kT/eac		10^{-11}

A Statistical Preliminary.

Measures of Central Tendency.

The mean or arithmetical average of a set of observations is given by the sum of those observations divided by the number of observations. The mean is denoted by placing a bar over the appropriate variable. i.e. $\bar{x} = \Sigma x/n$.

The median is the central value of a set of observations. The median will coincide with the mean only if the observations are distributed symmetrically about the mean. The deviation of the median from the mean is therefore indicative of an asymmetry, or skewness, in the distribution.

The mode is the value of the measurement occurring with the greatest frequency.

Measures of spread.

The variance is the sum of the squares of the deviations from the mean divided by the number of degrees of freedom. The number of degrees of freedom is usually one less than the number of observations. The variance is denoted by σ^2. Thus, $\sigma^2 = \Sigma(x - \bar{x})^2/(n - 1)$.

The standard deviation is taken as the square root of the variance and is denoted by σ.

The standard error is a measure of the accuracy of an estimated parameter. For example the standard error of the mean can be arrived at in the following way. The

variance of the sum, or difference of a set of observations is equal to the sum of the variances of the individual observations. Thus, if each of n observations has a variance σ^2, the variance of their distribution will be $n\sigma^2$ and the standard deviation $\sigma\sqrt{n}$. Thus, the standard deviation of the mean will be $\sigma\sqrt{n}/n$ or $\sigma/\sqrt{n}$. This quantity is termed the standard error of the mean to avoid confusion with the standard deviation of a distribution.

The difference between two means, $\bar{x}_1$ and $\bar{x}_2$ estimated from n_1 and n_2 observations respectively, will be subject to variability, and this variability will be made up of the individual variabilities of the two means. Thus the variance of the difference between $\bar{x}_1$ and $\bar{x}_2$ will be $\sigma_1^2/n_1 + \sigma_2^2/n_2$, and the standard error of the difference will be

$$\sqrt{\left[\sigma_1^2/n_1 + \sigma_2^2/n_2\right]}$$

Regression Analysis.

Measurements of two independent variables, x and y, may show some association. If the form of this association can be determined then any change in one variable can be accounted for by a change in the other variable. The measurements of x and y can be represented by means of a scatter diagram and the approximate form of the relationship deduced visually. To take a simple example, let us suppose that the association appears to be linear. Its form will be

$y = bx + c$. When the constants b and c have been determined the resulting equation is termed the regression equation of y on x. The best value of x corresponding to $\bar{y}$ will obviously be the mean $\bar{x}$, and therefore the regression equation can be written as $(y - \bar{y}) = b(x - \bar{x})$. However, there will be a certain proportion of y which cannot be accounted for by variations in x, and this can be represented by an extra term, e. The resulting equation becomes $(y - \bar{y}) = b(x - \bar{x}) + e$. The term, e, is known as the residual variation about the regression line. The value of b is now chosen so that Σe^2 is a minimum. Σe^2 is obviously given by

$$\Sigma e^2 = \Sigma[(y - \bar{y}) - b(x - \bar{x})]^2 \quad . \quad . \quad . \quad (1).$$

and we require $\frac{\partial}{\partial b}(\Sigma e^2)$ to be zero. This gives $b = \Sigma(x - \bar{x})(y - \bar{y})/\Sigma(x - x)^2$. The best straight line through the scatter is therefore given by:

$$(y - \bar{y}) = \frac{\Sigma(x - \bar{x})(y - \bar{y})}{\Sigma(x - \bar{x})^2}(x - \bar{x}) \quad . \quad . \quad (2).$$

Using the above value for b and substituting in (1) we find that Σe^2 is given by

$$\Sigma e^2 = \Sigma(y - \bar{y})^2 - \frac{\Sigma(x - \bar{x})(y - \bar{y})^2}{\Sigma(x - \bar{x})^2}$$

and this quantity is known as the residual sum of squares about the regression line.

The sum of squares which is ascribable to x will be

$$\Sigma(y - \bar{y})^2 - \Sigma e^2 = \Sigma[(x - \bar{x})(y - \bar{y})]^2 / \Sigma(x - \bar{x})^2.$$

Corresponding to any sum of squares there will be a variance, or mean sum of squares, obtained by dividing the sum of squares by the number of degrees of freedom. In the case of a regression line these variances may be set out in a variance table. Such a table is shown overleaf.

If the observations are well fitted by the regression line, the variation, or variance, which can be ascribed to x will be large compared to the residual variation. These two variances will be subject to variability in the same way as any other estimated parameter, and so their ratio will be subject to variability. The extent of the variability in the ratio can be predicted from a knowledge of the normal distribution combined with the number of degrees of freedom on which the two variances are based. The resulting distribution is known as the F-distribution and can be used to test the significance of the variance ratio.

To take an example, suppose a regression equation had been calculated from 12 observations, and the sum of squares is 50. The variance which can be ascribed to x is 48/1 = 48 on one degree of freedom, while the residual variance is 50/(12 - 2) = 5 on 10 degrees of freedom. The ratio of these variances is 48/5 = 9.6 on 1 and 10 degrees of freedom. Tables of the F-distribution have been drawn up showing the value of the variance ratio, or F, which will be exceeded

Source.	Degrees of Freedom.	Sum of Squares.	Mean Sum of Squares
Variation due to x	1	$\frac{[\Sigma(x-\bar{x})(y-\bar{y})]^2}{\Sigma(x-\bar{x})^2}$	$\frac{[\Sigma(x-\bar{x})(y-\bar{y})]^2}{\Sigma(x-\bar{x})^2}$
Residual variation	n - 2	$\Sigma(y-\bar{y})^2 - \frac{[\Sigma(x-\bar{x})(y-\bar{y})]^2}{\Sigma(x-\bar{x})^2}$	$\frac{\left\{\Sigma(y-\bar{y})^2 - \frac{[\Sigma(x-\bar{x})(y-\bar{y})]^2}{\Sigma(x-\bar{x})^2}\right\}}{(n-2)}$
Total.	n - 1	$\Sigma(y-\bar{y})^2$	$\Sigma(y-\bar{y})^2/(n-1)$.

The formal layout of an analysis of variance table. The ratio of the mean sum of squares ascribable to x to the residual mean sum of squares can be used to test the significance of the regression line.

with a given degree of probability for various combinations of degrees of freedom. From these tables we have that a value of 6.94 for F on 1 and 10 degrees of freedom, would arise by pure chance in 2½% of all cases and a value as high as 10.04 in 1% of all cases. Our value of F is 9.6, a value which could only have arisen by pure chance once in slightly less than a hundred cases.

We now have two alternative conclusions:

(1) The calculated regression line is a good representation of the observations.

(2) An unlikely event has occurred and the line is not a good representation of the observations.

In the case of the example quoted above, the value of F could only arise by pure chance in about 1% of all cases and since this is therefore, a fairly rare event, we prefer to accept the hypothesis that the line is a good representation of the observations rather than think that an unlikely event has happened.

The t-test.

If we wish to test the hypothesis that an estimated mean $\bar{x}_1$ could have come from a population whose mean is $\bar{x}_2$ and whose standard deviation is σ_2, we calculate the ratio

$$t = \frac{|\bar{x}_2 - \bar{x}_1|}{\text{Standard error of } \bar{x}_2} = \frac{|\bar{x}_2 - \bar{x}_1|}{(\sigma_2/\sqrt{n})}$$

If the mean $\bar{x}_1$ comes from the same population as the mean $\bar{x}_2$ we shall expect no significant difference between the variance associated with $\bar{x}_1$, σ_1^2, and the variance of $\bar{x}_2$, σ_2^2. The ratio of these two variances can be tested by means of the F-test, and if they are not significant a better estimate of the population variance may be made by pooling the two sets of observations from which $\bar{x}_1$ and $\bar{x}_2$ have been determined. The resulting estimate of the population variance will be

$$\frac{\Sigma(x_1 - \bar{x}_1)^2 + \Sigma(x_2 - \bar{x}_2)^2}{(n_1 - 1) + (n_2 - 1)}$$

and the value of t is given by

$$t = \frac{|\bar{x}_1 - \bar{x}_2|\sqrt{(n_1 + n_2 - 2)}}{\Sigma(x_1 - \bar{x}_1)^2 + \Sigma(x_2 - \bar{x}_2)^2}$$

Now t will have its own probability distribution, also based on the normal distribution and the number of degrees of freedom, $(n_1 + n_2 - 2)$. Obviously, when $(n_1 + n_2 - 2) \rightarrow \infty$ the distribution of t reduces to the normal distribution.

The t-distribution can therefore be used for testing the significance of the difference between two estimated means in the same way as the F-distribution is used to test the significance of the ratio of two estimated variances.

The χ^2-test.

The χ^2-test is used in the comparison of proportions. It can be shown that the estimates of a proportion p, based on n observations, will be distributed about the mean, p, with variance $p(1 - p)/n$. The variance of a single observation is $p(1 - p)$, which is a residual mean square based on $(n - 1)$ degrees of freedom. The proportion p, is only an estimate of the true proportion, π, but the difference between p and π is usually negligible provided a sufficient number of observations have been taken. The population variance can therefore be taken as $p(1 - p)$ based on an infinite number of degrees of freedom.

If we have r groups of observations and the proportions in each group with a certain attribute are observed, then we may wish to test whether these proportions differ significantly. This may be done in exactly the same way as for ordinary observations, by means of the variance ratio test. In this case, the mean sum of squares between the groups, based on $(r - 1)$ degrees of freedom, is compared to the population variance $p(1 - p)$ based on an infinite number of degrees of freedom. The χ^2-test is, in fact, a variance ratio test on $(r - 1)$ and an infinite number of degrees of freedom.

Special computational techniques have been formulated to facilitate the calculation of χ^2-testing. The

two most generally applicable procedures are outlined as follows:-

(1). If it is desired to test whether the observed frequencies in a distribution differ significantly from the frequencies which might be expected according to some assumed hypothesis, we have that

$$\chi^2 = \sum \frac{(O - E)^2}{E}$$

where O represents the observed frequency and E the expected frequency.

(2). If it is desired to compare the significance of the difference of proportions in two samples on the null hypothesis that they could have come from the same population, the observed frequencies are first tabulated in a 2 x 2-table as follows

	First classification.		Total.
Second	a	b	(a + b)
Classification.	c	d	(c + d)
Total.	(a + c)	(b + d)	N.

Then $\chi_1^2 = \dfrac{N(ad - cb)^2}{(a + c)(b + d)(c + d)(a + b)}$

The number of degrees of freedom is equal to the number of frequencies which could be arbitrarily entered in the 2 x 2-table without disturbing the totals. Thus, in a 2 x 2-table the number of degrees of freedom will always be 1.

A mathematical difficulty arises because of the discrete changes in the differences between the observed and

expected frequencies. The χ^2-distribution is a continuous distribution, and consequently a significant value of χ^2 may arise from these discrete changes. This difficulty is partially overcome by adjusting the observed frequency by $\frac{1}{2}$ to make the difference less extreme. This procedure is called Yates's correction for continuity.

The relation between the normal distribution, the F-distribution the t-distribution and the χ^2-distribution.

The F, t, and χ^2 distributions are all modifications of the normal distribution, and they are related in the following manner. The χ^2-distribution based on ν degrees of freedom is an F-distribution based on ν and an infinite number of degrees of freedom. The t-distribution on ν degrees of freedom is the square root of the F-distribution based on 1 and ν degrees of freedom. The t-distribution on an infinite number of degrees of freedom is a normal distribution. Therefore,

$\chi^2_\nu = F_{\nu,\infty}$; $t_\nu = \sqrt{F_{1,\nu}}$; and t_∞ = Normal Distribution.

(A more detailed account of the statistical techniques used in the following chapters can be found in 'Introductory Statistics', M.H.Quenouille, Pergamon Press, 1950.)

The Statistical Relations between Solar Flares and Sunspots.

(1). Introduction.

The relations between solar flares and sunspots were first examined by Giovanelli (21) using data for the years 1935 to 1937 when sunspot activity reached a maximum. The material used by Giovanelli consisted of:-

(a) The lists of flares published in the 'Bulletin for Character Figures of Solar Phenomena'. Data involving 1,400 flares were used.

(b) The areas of spots published in the 'Monthly Weather Review'.

(c) The types and maximum magnetic fields of spot groups published in the 'Publications of the Astronomical Society of the Pacific'.

No attempt was made in Giovanelli's work to find out how the relations varied with flare importance and rigorous statistical methods do not appear to have been used to test the significance of the relationships obtained. At the time the Greenwich values for spot areas were not available and those used in the investigation were taken from different observatories. In order to reduce these observations to standard Greenwich values, mean factors had to be applied to the values obtained by different observatories. During the early part of the period comparatively few observatories were contributing flare data to the 'Bulletin

for Character Figures of Solar Phenomena', so most flares passed unreported. However, since spots are much longer lived than flares, their presence on the solar disk is almost always noticed, and this will render the material used slightly inconsistent. Giovanelli arrived at the following conclusions:-

The frequency F, of a solar flare occurring in the neighbourhood of a spot group is

(a). A linear function of the area A of the spot group. The relation can be represented by the equation

$$F = 8.25 \times 10^{-4} A + 0.20.$$

(b). The gradient of the relation given above is for all flares, irrespective of class, and for all spot groups irrespective of magnetic classification. If the spot groups are grouped according to their magnetic type it is found that the gradient differs from type to type. The gradients obtained by Giovanelli for the various types are given in the table below:

Type.	No.of Groups.	No.of flares.	Gradient.
αf	11	1	. .
α	68	6	. .
αp	508	130	8.1×10^{-4}
βf	246	110	9.6×10^{-4}
β	589	255	9.6×10^{-4}
βp	1124	416	9.6×10^{-4}
βγ	286	314	12.0×10^{-4}
γ	73	117	20.5×10^{-4}

(c). The frequency of flare occurrence per unit area is also dependent on the rate of increase of spot area. The figure below shows the empirical relation of F against dA/dt.

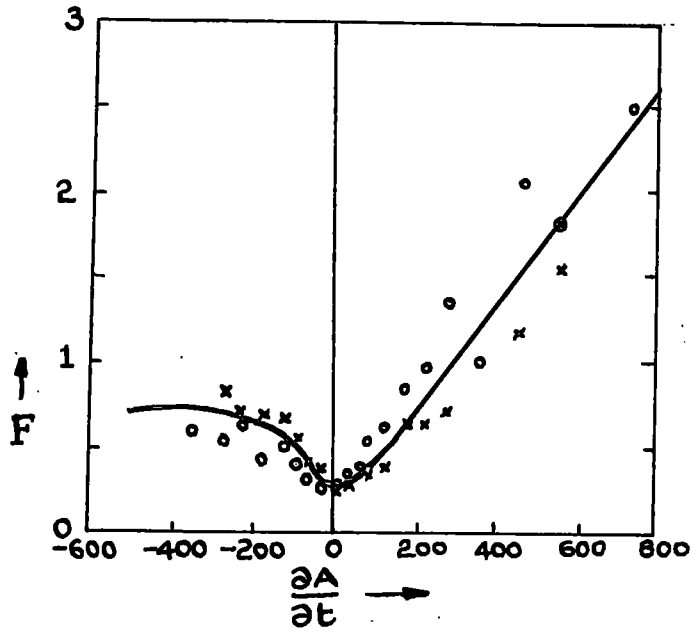

(d). The flare frequency is not influenced by the <u>maximum</u> magnetic field of the spot group.

(e). There is no definite influence of the age of the spot group on flare activity, except a possible increase in the final stages of spot decay.

Behr and Siedentopf (36) found that the reduced number of flares per solar rotation, N_F, and the corresponding mean spot numbers, $\overline{R}$, are related. If the relationship is

represented in the form $N_F = a(\overline{R} - 10)$ the mean values for 'a' are as follows:

$a = 1.98 \pm 0.02$ (17th. cycle, maximum in 1937).

$a = 1.47 \pm 0.02$ (18th, cycle, maximum in 1948).

The 18th. cycle had more spots than the 17th. cycle, but 'a' is smaller and the flares about the same in number. Thus flares may in general fluctuate less in number than spots do. Behr and Siedentopf also found that the distribution of flares over the solar disk closely follows the spot distribution, even to the extent of an East-West asymmetry.

No other work appears to have been done on this subject.

In this work, the statistical relations between solar flares and sunspots for the 18th. cycle will be examined. The results obtained will be compared with those of Giovanelli's for the 17th. cycle to see if there are any significant differences. Such differences could arise as a result of a varying component of the solar general magnetic field.

Since a large sample of flares has been used, it has been possible to investigate the relations between sunspots and solar flares of different class or importance. Rigorous statistical methods are used throughout and the conclusions obtained from the analysis are applied to the various theories of the origin of solar flares.

2. Material.

Information regarding more than 2,000 solar flares was obtained from the 'I.A.U.Quarterly Bulletin of Solar Activity' for the years 1947, 1948, and 1949.

The corrected areas of sunspots were obtained from the 'Greenwich Photo-Heliographic Results' while the magnetic classification of these spots were taken from the 'Publications of the Astronomical Society of the Pacific'.

A flare can be associated with a particular spot group by comparing the co-ordinates of the flare with those of the spot group. In the same way a particular spot group can be identified in the different sets of data. From the material available the following information was tabulated:

(a). The date and time of the flare.

(b). The importance of the flare.

(c). The latitude of the flare.

(d). The magnetic classification of the spot group according to the Mt.Wilson Observatories.

(f). The area of the spot group on the day preceding the flare, on the day of the flare, and on the day following the flare.

The 'area' given by the Greenwich Photo-Heliographic Results' is corrected for foreshortening and is expressed in millionths of the visible solar disk.

The following analysis does not include those

sunspots which were not accompanied by a solar flare. During 1947, 544 spot groups were recorded in the 'Greenwich Photo-Heliographic Results' and the 'I.A.U. Querterly Bulletin of Solar Activity' recorded 190 spot groups as having been flare active. Thus, 0.35 of all spot groups were observed to be accompanied by at least one solar flare. The sun was under observation for 2,670 hours giving an average observing time of 7.3 hours per day. The majority of spots have a life of less than one day and so many small spot groups may be missed. To account for these small, short lived groups, the observed proportion of flare active groups should be reduced slightly to give the true observed proportion. It is quite likely that this true observed proportion merely reflects the average observing time of 7.3 hours per day. If this is the case, the number of observing hours per day should be less than 0.35 x 24 or, less than 8.4 hours per day. This suggests that, in actual fact, nearly all spot groups are associated with flare activity.

3. Results of the Analysis.

(1). The relation between flare frequency and the areas of sunspots.

The daily corrected areas were grouped into convenient area ranges and the frequency of the solar flares occurring in each area range was obtained. In the first instance all flares were assumed to be of equal importance

and the values obtained from the data for the flare frequencies were plotted against the mean areas of the spot groups. A linear association seemed indicated and the regression line of the flare frequencies on the corresponding mean areas of spot groups was calculated. The flares were then grouped according to their class or importance and the same procedure adopted. In each case the coefficient of correlation was calculated and an analysis of variance was carried out to test whether or not such a linear correlation could easily have arisen by chance. The standard error of the estimate of the flare frequency was determined for each regression line.

Let F, $\bar{F}$, A and $\bar{A}$ be the flare frequency, the mean of the observed flare frequencies, the area of the spot group, and the mean of the areas of the observed spot groups respectively, then the regression line of F on A is given by:

$$F - \bar{F} = \frac{\Sigma (F - \bar{F})(A - \bar{A})}{\Sigma (A - \bar{A})^2}(A - \bar{A}).$$

the correlation coefficient, r, is given by

$$r = \frac{\Sigma (F - \bar{F})(A - \bar{A})}{\sqrt{\left[\Sigma (F - \bar{F})^2\right]\left[\Sigma (A - \bar{A})^2\right]}}$$

the standard error, S_F, of the estimate of F is given by

$$S_F = \sigma_F \sqrt{1 - r^2}$$

where $F = \left[\frac{\Sigma(F - \bar{F})^2}{n - 1}\right]^{\frac{1}{2}}$ where n is the number of the observed estimates of F calculated from the data. If we use the regression line to predict a value of F for a given A, the errors in this prediction will have an approximately normal distribution with mean F and standard deviation S_F.

Table 2 shows the values obtained for n, $\bar{F}$, $\bar{A}$, $\Sigma(F - \bar{F})^2$, $\Sigma(A - \bar{A})^2$, $\Sigma(F - \bar{F})(A - \bar{A})$, the correlation coefficient r, and the standard error of the estimate of F, S_F. The appropriate regression lines are given by the equations:

For all flares:

$$F = 6.36 \times 10^{-4}A + 0.36 \quad . \quad . \quad . \quad . \quad (1).$$

For class 1 flares:

$$F = 4.64 \times 10^{-4}A + 0.25 \quad . \quad . \quad . \quad . \quad (2).$$

For class 2 flares:

$$F = 1.46 \times 10^{-4}A + 0.07 \quad . \quad . \quad . \quad . \quad (3)$$

For class 3 flares:

$$F = 0.217 \times 10^{-4}A + 0.01 \quad . \quad . \quad . \quad . \quad (4)$$

Figures 1, 2, 3, and 4 show the values of F plotted against A for each regression together with the calculated regression lines. Control limits have been placed at one standard error of estimate, S_F on either side of each regression line. To test the significance of these regression lines the null hypothesis was set up that the variation in F due to A is not significantly different from

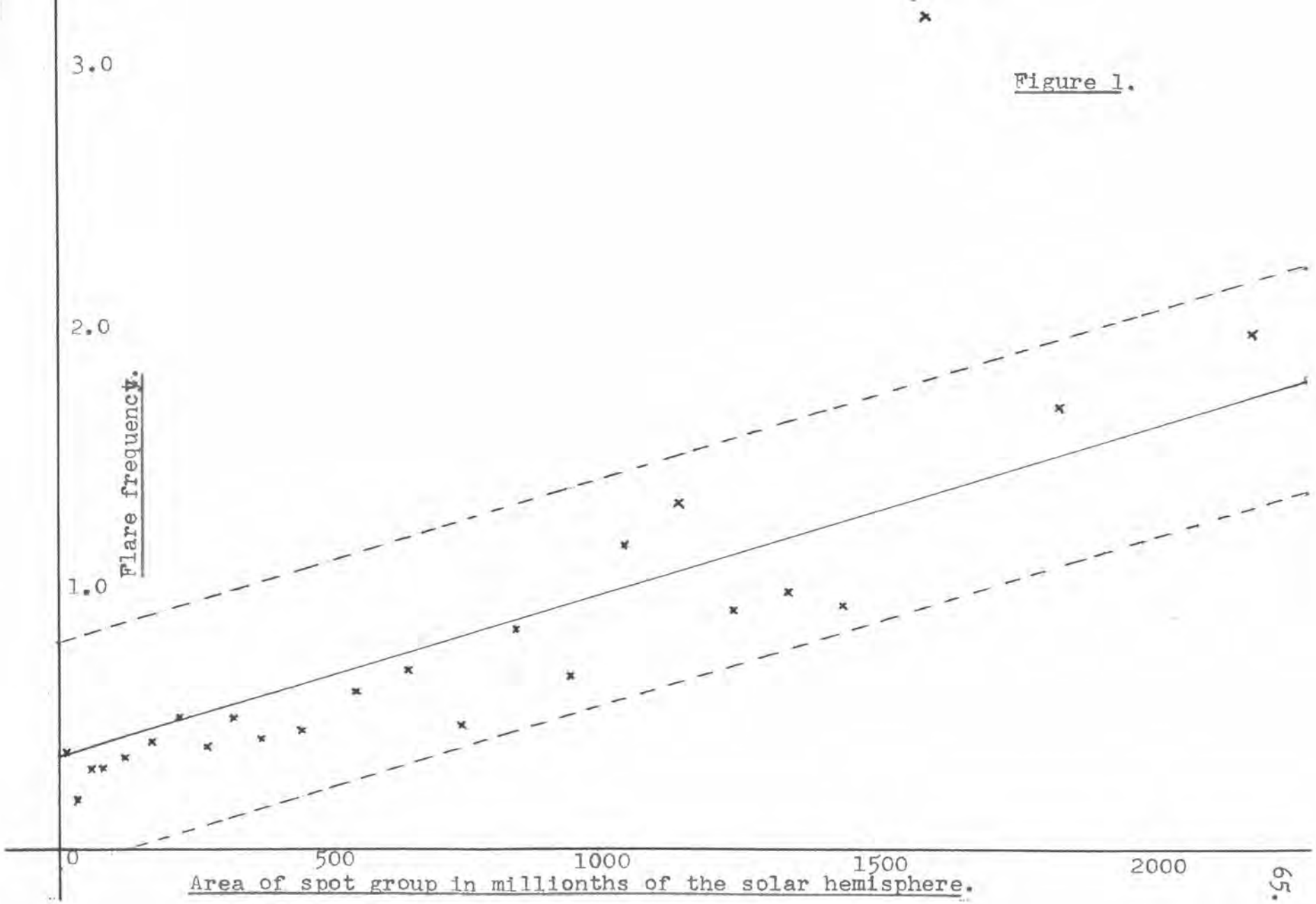
3.0
2.0
1.0
Flare frequency.
0
500
1000
1500
2000
Area of spot group in millionths of the solar hemisphere.

Figure 1.

Figure 2.

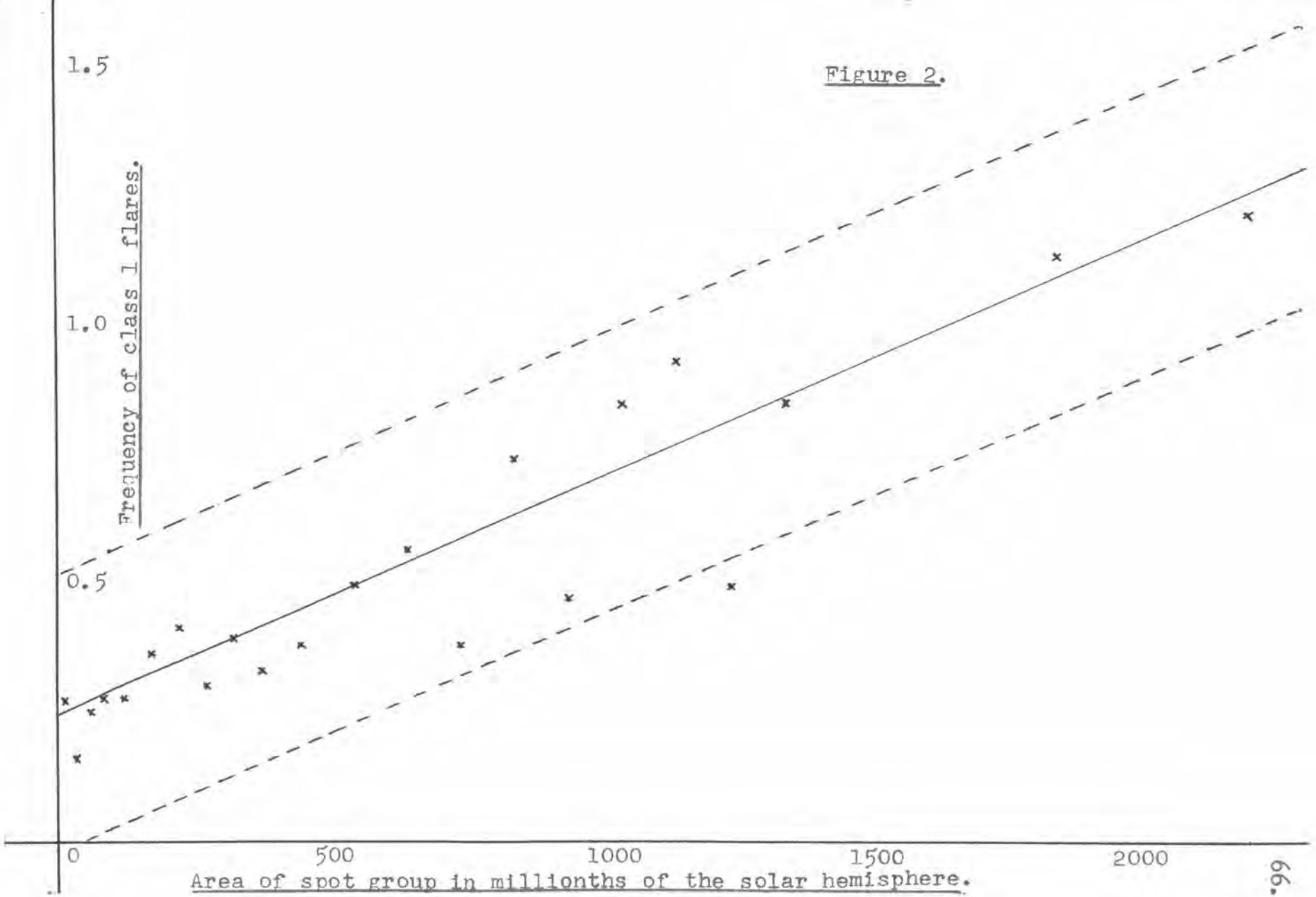
1.5
1.0
0.5
Frequency of class 1 flares.
0
500
1000
1500
2000
Area of spot group in millionths of the solar hemisphere.

Figure 3.

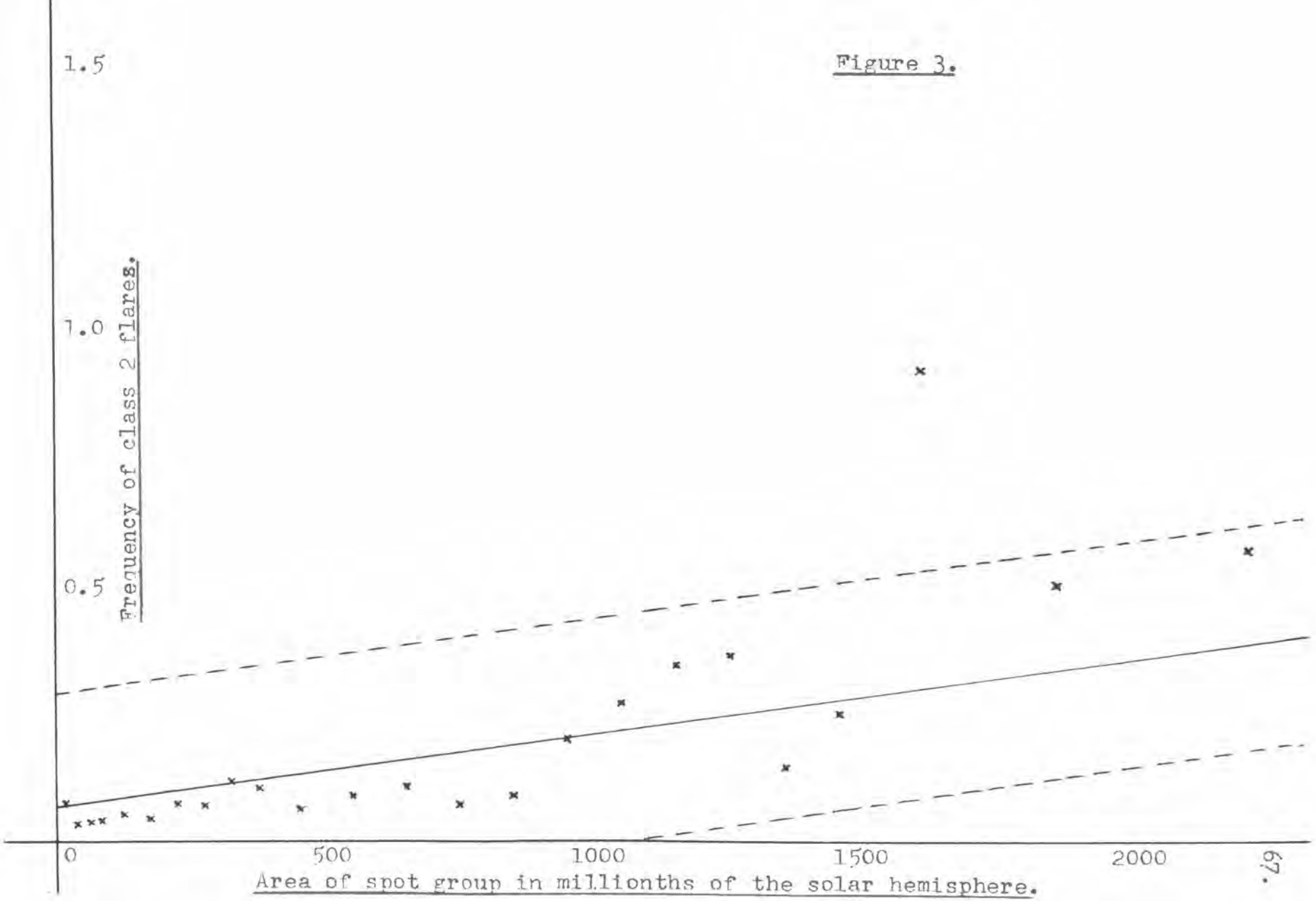
1.5
1.0
0.5
Frequency of class 2 flares.
0
500
1000
1500
2000
Area of spot group in millionths of the solar hemisphere.

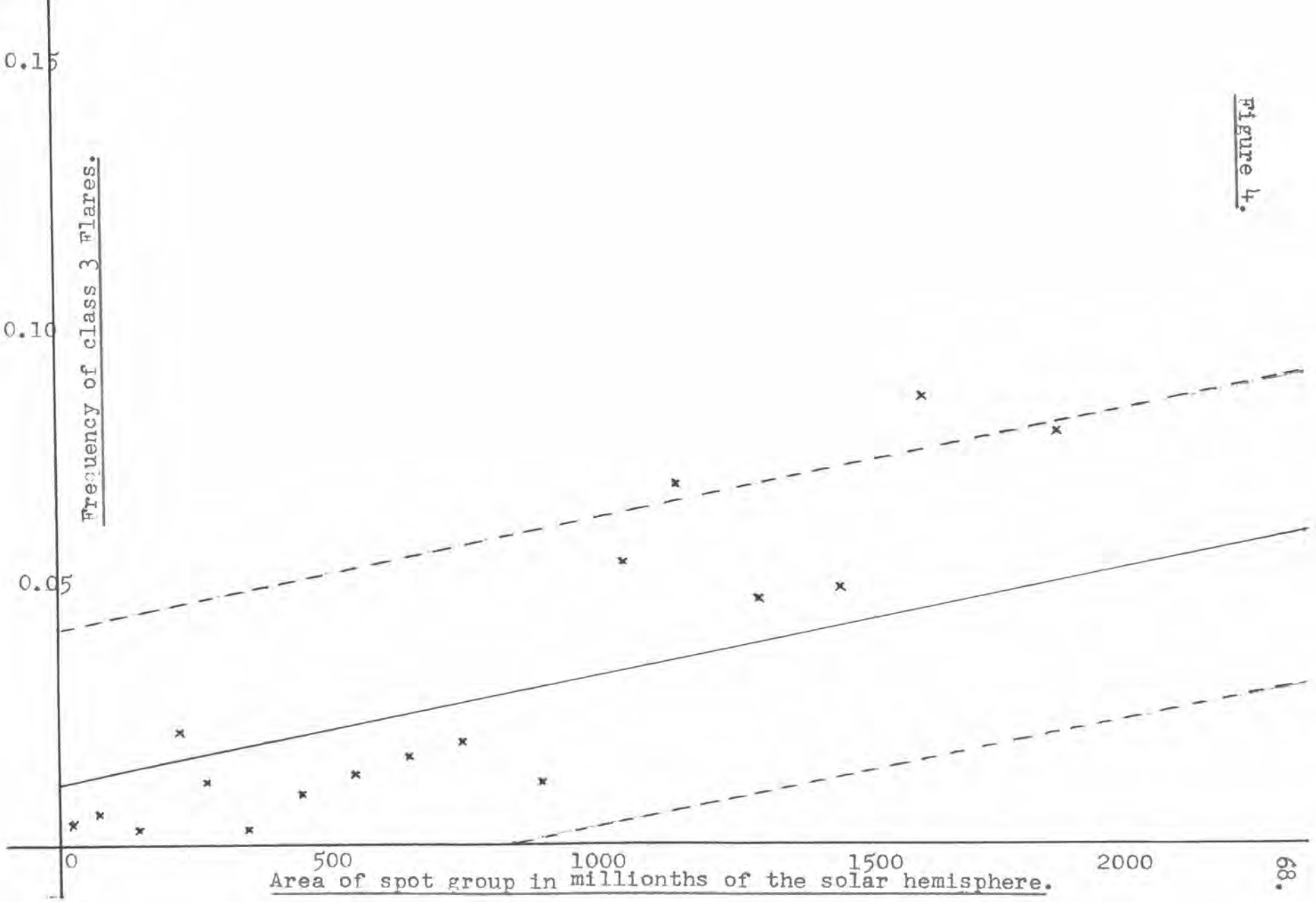
0.15
0.10
0.05
Frequency of class 3 Flares.
0
500
1000
1500
2000
Area of spot group in millionths of the solar hemisphere.

Figure 4.

residual variation. This null hypothesis was tested by the following analysis of variance tests:

For all flares:

	Degrees of freedom.	Sums of Squares	Mean of Squares	Variance Ratio.
Variation dur to A	1	10.20	10.200	52
Residual variation	24	4.69	0.195	***
Total.	25	14.89		

For flares of class 1:

	D.f.	S.s.	M.s.	V.R.
Variation due to A	1	5.420	5.420	67
Residual variation	24	1.944	0.081	***
Total.	25	7.364		

For flares of class 2:

	D.f.	S.s.	M.s.	V.R.
Variation due to A	1	0.542	0.542	7.42
Residual variation	24	1.738	0.073	* 2½%
Total.	25	2.280		

For flares of class 3:

	D.f.	S.s.	M.s.	V.R.
Variation due to A	1	0.0057	0.0057	6.40
Residual variation	16	0.0138	0.0009	* 2½%
Total.	17	0.0195		

When Snedecor's Variance Ratio, or F-test, is applied to the above variance ratios we arrive at the following conclusions: The regression lines for all flares, irrespective of class, and for flares of class 1 taken by themselves, are

both significant at the 0.1% level. This means that such a linear correlation could only have arisen by pure chance once in a thousand cases. The regression lines for flares of class 2 and class 3 are significant at the 2½% level, indicating that such a linear correlation could only arise by chance in about one in forty cases. We therefore reject our null hypothesis and conclude that the regression lines are significant.

Several points of interest arise from these regression lines. It will be noticed that the observed value of F for daily groups in the range 1,501 to 1,700 millionths of the solar hemisphere is well off the regression line in all four cases. An explanation of this irregularity will be given later. At first sight it appears that flares are liable to occur in a spot free zone, but observations show that this is an exceedingly rare event. The intercepts of the regression lines can probably be accounted for in the following manner. Only those spot groups which were accompanied by at least one solar flare are included in the analysis. However, since a flare is such a transient phenomenon it is quite likely to escape observation, and because of this, spot groups with a low flare frequency association may well be classed as 'non-flare active'. Thus, as the spot groups become smaller in area the greater will be the probability that they are not included in the analysis, and this will introduce a systematic error in the observed flare frequencies used in

the calculation of the regression lines..This effect will account for the intercepts of the regression lines.

Table 1.

Case	n	$\bar{F}$	$\bar{A}$	$\Sigma(F-\bar{F})^2$	$\Sigma(A-\bar{A})^2$	$\Sigma(F-\bar{F})(A-\bar{A})$
All flares	26	0.968	954	14.890	25.12×10^6	15.97×10^3
Class 1	26	0.693	954	7.364	25.12×10^6	11.68×10^3
Class 2	26	0.208	954	2.280	25.12×10^6	3.68×10^3
Class 3	18	0.030	900	0.0195	12.02×10^6	0.261×10^3

Case.	r	S_F
All flares	0.828	0.43
Class 1	0.865	0.27
Class 2	0.382	0.22
Class 3	0.540	0.030

Note: A spot is counted once for each day it appears on the Solar Disk.

Figure 5 shows the regression lines of F on A for the different classes of flares. The regression lines have been extrapolated until they meet. It appears that these three lines converge to the same point and that this point lies on the A axis. Although there is no physical significance in the extrapolated parts of the regression lines, it is clear that these lines could not meet in the same point unless the vast majority of flares came from the same population. That is to say, the only physical difference between flares of different classes is one of intensity

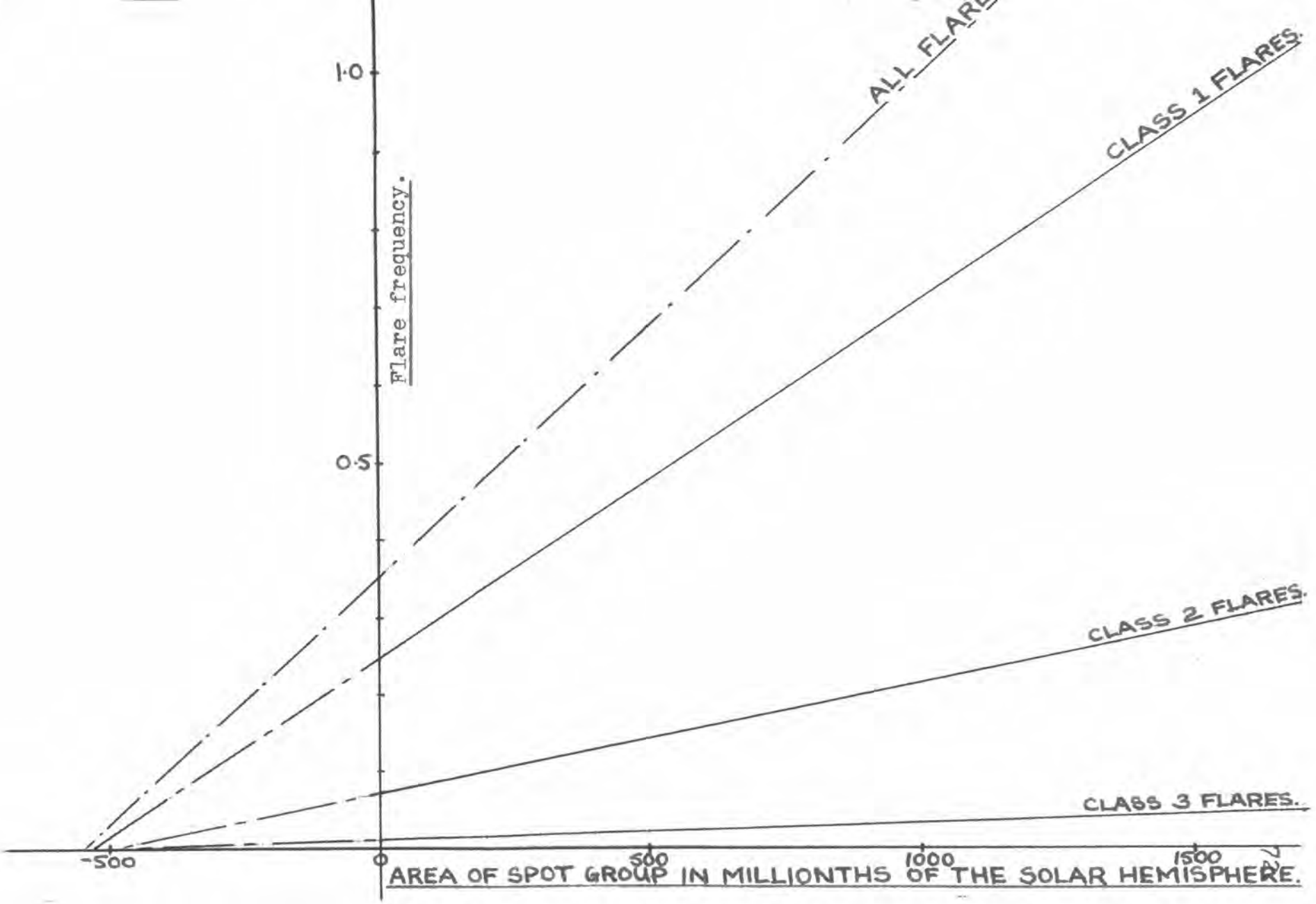
1·0
0·5
Flare frequency.
ALL FLARES.
CLASS 1 FLARES.
CLASS 2 FLARES.
CLASS 3 FLARES.
-500
0
500
1000
1500
AREA OF SPOT GROUP IN MILLIONTHS OF THE SOLAR HEMISPHERE.

and the same flare mechanism is operative in these different classes. Although other mechanisms of flare generation may be responsible for some of the flares, the data indicate that a very large proportion of the flares are caused by the same mechanism. If the above reasoning is correct the gradients of the regression lines should merely reflect the proportions of flares falling in the different classes.

The gradients of the four regression lines are:

$$\left.\begin{array}{ll} \text{For all flares:} & 6.36 \times 10^{-4}. \\ \text{For flares of class 1:} & 4.64 \times 10^{-4}. \\ \text{For flares of class 2:} & 1.46 \times 10^{-4}. \\ \text{For flares of class 3:} & 0.217 \times 10^{-4}. \end{array}\right\} \quad . \quad . \quad . \quad (5).$$

Of the 2,000 flares which occurred during this period 1,585 were of class 1, 375 were of class 2, and 40 were of class 3. Thus, the hypothesis is set up, that the gradients of the four regression lines are in the ratios

$$2{,}000 : 1{,}585 : 375 : 40.$$

The sum of the four gradients is 12.68×10^{-4} and the total number of flares used in the calculation of each regression line must be multiplied by a factor of $(12.68 \times 10^{-4})/4{,}000 = 3.17 \times 10^{-7}$ to obtain the appropriate gradients on this hypothesis. This gives:

For all flares: 6.34×10^{-4}.
For flares of class 1: 5.20×10^{-4}.
For flares of class 2: 1.19×10^{-4}.
For flares of class 3: 0.13×10^{-4}. } . . . (6).

In order to test this hypothesis we determine control limits set at one standard error from the regression coefficients. These limits are calculated according to the expression $\beta \pm \sqrt{\frac{s^2}{\Sigma(A - \bar{A})}}$ where β is the regression coefficient or gradient and

$$s^2 = \Sigma(F - \bar{F})^2 - \frac{[\Sigma(F - \bar{F})(A - \bar{A})]^2}{\Sigma(A - \bar{A})^2}$$

The limits so determined are:

For all flares: 5.48×10^{-4} to 7.24×10^{-4}
For flares of class 1: 4.07×10^{-4} to 5.21×10^{-4}
For flares of class 2: 0.92×10^{-4} to 2.00×10^{-4}
For flares of class 3: 0.13×10^{-4} to 0.30×10^{-4} } . . (7).

If these results are compared with those given in (6) it will be seen that the gradients expected on our hypothesis all lie within one standard error of the gradients of the regression lines shown in (5). We therefore have good reason to believe that the gradients of the regression lines shown in Figure 5 merely reflect the proportions of flares falling in the different classes.

We conclude that spot area has no significant influence on flare intensity. The frequency of solar flares occurring in a given interval of time and associated with a

particular spot group is a linear function of the area of the spot group.

(2). The relation between flare frequency and magnetic classification according to Mt.Wilson.

The Mt.Wilson magnetic classification of spot groups can be summarised as follows:-

β. Bipolar groups in which the preceding and following members, whether single ormultiple are about equal in area.

βp. Bipolar groups in which the preceding member is the principal component.

βf. Bipolar groups in which the following component is the principal member.

βγ. Groups with bipolar characteristics but no marked North-South dividing line.

α. Unipolar groups in which the East - West distribution of calcium flocculi is approximately symmetrical.

αp. Unipolar groups which were the preceding members of a bipolar group.

αf. Unipolar groups which were the following members of a bipolar group.

γ. Those groups which are so complex as to prevent classification.

In this section of the analysis regression lines of F on A were again determined. However, because of the results of section (1), all flares may be taken as of equal importance and the spot groups are subdivided according to their magnetic classification. Table 2 shows the values of

Table 2.

Case.	n.	$\bar{F}$	$\bar{A}$	$\Sigma(F-\bar{F})^2$	$\Sigma(A-\bar{A})^2$	$\Sigma(F-\bar{F})(A-\bar{A})$
β	21	0.841	712	4.825	10.7×10^6	2.85×10^3
$\beta\rho$	25	0.820	816	7.604	12.4×10^6	9.26×10^3
βf	22	0.652	728	5.574	9.02×10^6	3.20×10^3
$\beta\gamma$	24	1.260	1030	49.255	23.01×10^6	16.87×10^3
$\alpha\rho$	22	0.612	609	8.388	5.54×10^6	3.26×10^3
γ	17	2.510	916	56.000	19.83×10^6	15.19×10^3

Case	r	S_F.
β	0.400	0.45
$\beta\rho$	0.945	0.18
βf	0.455	0.29
$\beta\gamma$	0.502	1.10
$\alpha\rho$	0.480	0.55
γ	0.456	1.65

obtained for n, $\bar{F}$, $\bar{A}$, $\Sigma(F - \bar{F})^2$, $\Sigma(A - \bar{A})^2$, $\Sigma(F - \bar{F})(A - \bar{A})$, the correlation coefficient r, and the standard error of the estimate of F, F_S. A linear correlation was found to exist for all cases except types α and αf for which there was insufficient data. The regression lines are:

$$\left.\begin{array}{ll}
\beta \text{ groups:} & F = 2.67 \times 10^{-4}A + 0.651. \\
\beta p \text{ groups:} & F = 7.42 \times 10^{-4}A + 0.214. \\
\beta f \text{ groups:} & F = 3.55 \times 10^{-4}A + 0.394. \\
\beta \gamma \text{ groups:} & F = 7.32 \times 10^{-4}A + 0.510. \\
\alpha p \text{ groups:} & F = 5.78 \times 10^{-4}A + 0.260. \\
\gamma \text{ groups:} & F = 7.60 \times 10^{-4}A + 1.820.
\end{array}\right\} \quad . \quad . \quad . \quad (8).$$

These lines are shown in figure 6. To test the significance of these lines the following analysis of variance tests were carried out:

β groups:

	D.f.	S.s.	M.s.	V.R.
Variation due to A	1	0.761	0.761	3.6
Residual Variation	19	4.064	0.214	10%
Total.	20	4.825		

βp groups:

	D.f.	S.s.	M.s.	V.R.
Variation due to A	1	6.920	6.920	228
Residual variation	23	0.684	0.030	***
Total.	24	7.604		

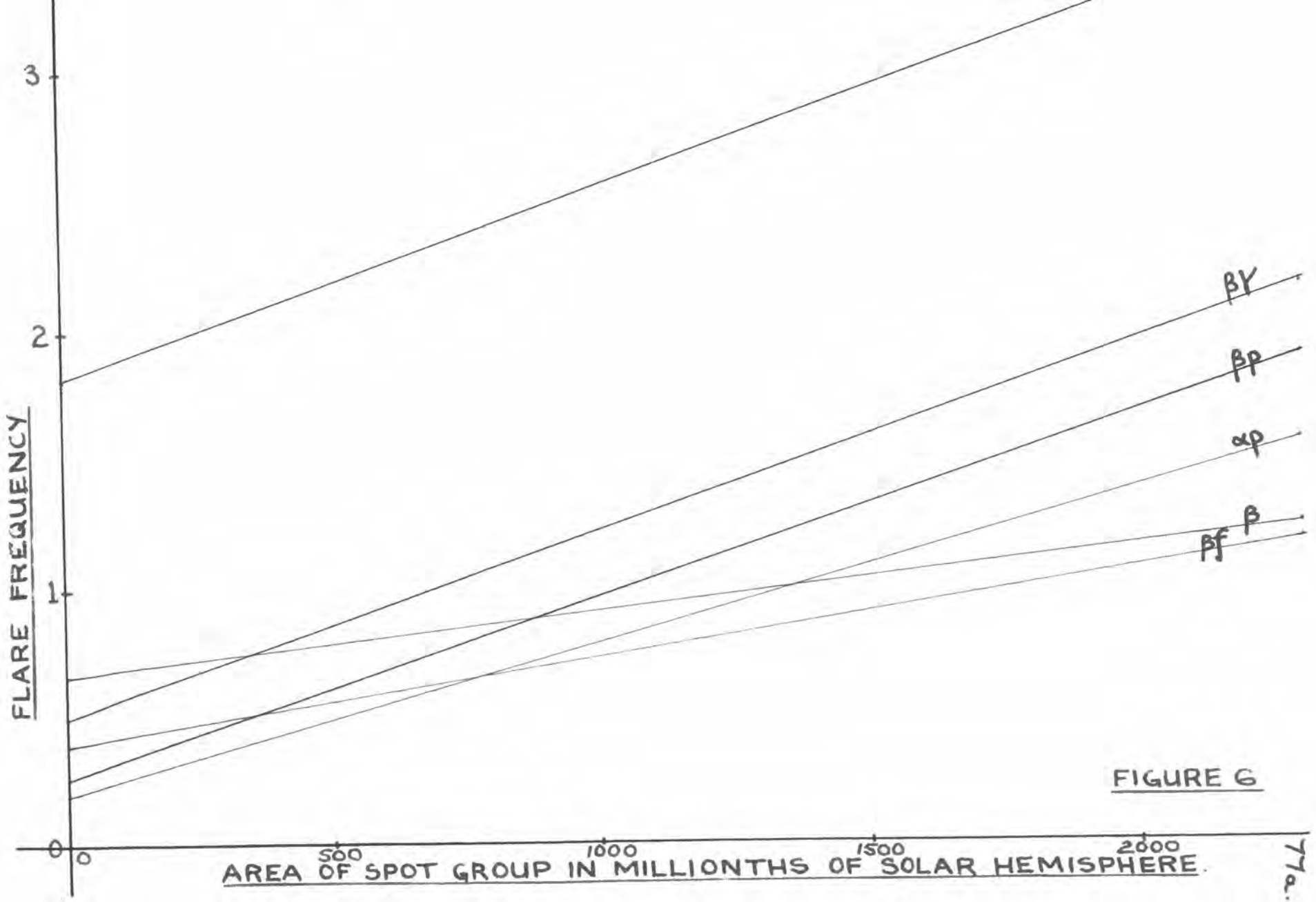
FLARE FREQUENCY
0
1
2
3
βγ
βp
αp
β
βf
0
500
1000
1500
2000
AREA OF SPOT GROUP IN MILLIONTHS OF SOLAR HEMISPHERE.

FIGURE 6

β groups:

	D.f.	S.s.	M.s.	V.R.
Variation due to A	1	1.140	1.140	5.3
Residual Variation	20	4.334	0.216	* 5%
Total.	21	5.574		

$\beta\gamma$ groups:

	D.f.	S.s.	M.s.	V.R.
Variation due to A	1	12.40	12.40	7.4
Residual Variation	22	36.86	1.67	* 2½%
Total.	23	49.26		

$\alpha\rho$ groups:

	D.f.	S.s.	M.s.	V.R.
Variation due to A	1	1.93	1.93	6.0
Residual Variation	20	6.46	0.32	* 2½%
Total.	21	8.39		

γ groups:

	D.f.	S.s.	M.s.	V.R.
Variation due to A	1	11.6	11.6	3.9
Residual Variation	15	44.4	3.0	10%
Total.	16	56.0		

From these tests it appears that all the lines are significant except those for types β and γ. However, the variance ratios for these two cases reach the 10% level, which means that such a linear correlation could only arise by chance once in ten cases. We may therefore regard the

regression lines for β and γ groups as having some physical significance. From Figure 6 it will be seen that there is not a great deal of difference between the flare activity of the various types with the exception of the βγ and γ groups, where the flare frequencies are greater than the rest. This will account for the irregularity pointed out in the previous section where the observed value of F for daily groups lying in the range 1,501 to 1,700 millionths of the solar hemisphere was much higher than expected. This large value of F was mainly due to group number 15089 which came into view on the 29th. July 1947 and had the magnetic classification of βγ. During the period 1st. August to 3rd. August when the area of the group lay in the range 1,501 to 1,700 millionths of the solar hemisphere, it was accompanied by 16 solar flares.

The hypothesis is now set up that all these regression lines are parallel, and in order to test this hypothesis we examine the ratios of the residual mean squares by means of the F-test, to see if the variations about each pair of lines are comparable. When this is done we find that types β, βδ, and αβ are comparable and also types γ and βγ. To compare the regression coefficients of a pair of lines a pooled estimate of the variance is obtained and from this the standard error of the difference between the regression coefficients is determined.

Pooling the variances for types β and $\beta\phi$: $(4.064 + 4.334)/(19 + 20) = 0.216$. The standard error is now given by

$$\sqrt{\left[\frac{0.216}{1017 \times 10^6} + \frac{0.216}{9.02 \times 10^6}\right]} = \pm 2.10 \times 10^{-4}.$$

The difference between the regression coefficients is 0.88×10^{-4}. The ratio $(0.88 \times 10^{-4})/2.10 \times 10^{-4} = 0.420$ is now tested by the t-variate on 39 degrees of freedom, and it is found that the difference is not significant and we may regard the regression lines for types β and $\beta\phi$ as being parallel. The same procedure is adopted for the other pairs of lines, and it is found that the regression coefficients for types β , $\beta\phi$ and $\alpha\rho$ are not significantly different and neither are the regression coefficients for types γ and $\beta\gamma$.

The hypothesis is now set up that the distance between the regression lines for types β , $\beta\phi$, $\alpha\rho$ are not significantly different from zero. Since the regression coefficients are not significantly different from each other we may calculate a joint regression coefficient by combining the sums of squares and products:

$$\Sigma\left[\Sigma(F - \bar{F})^2\right] = 18.79$$

$$\Sigma\left[\Sigma(A - \bar{A})^2\right] = 25.26 \times 10^6$$

and $$\Sigma\left[\Sigma(A - \bar{A})(F - \bar{F})\right] = 9.32 \times 10^3.$$

This gives a joint regression coefficient of

$9.32 \times 10^3/25.26 \times 10^6 = 3.68 \times 10^{-4}$.

The analysis of variance here is:

	D.f.	S.s.	M.s.	V.R.
Joint regression	1	3.45	3.45	13.7
Residual.	61	15.34	0.25	***
Total.	62	18.79		

and so this joint coefficient is highly significant.

The three fitted lines are now:

$$\left.\begin{aligned} &\text{For } \beta \text{ groups:} && F = 0.841 + 3.68 \times 10^{-4}(A - 712) \\ &\text{For } \beta f \text{ groups:} && F = 0.652 + 3.68 \times 10^{-4}(A - 728) \\ &\text{For } \alpha p \text{ groups:} && F = 0.612 + 3.68 \times 10^{-4}(A - 609) \end{aligned}\right\} \quad . \quad . \quad (9).$$

The distance between the lines for β and βf groups is 0.195 and its standard error is

$$\sqrt{\left\{0.25\left[\frac{1}{21} + \frac{1}{22} + \frac{16^2}{25.3 \times 10^6}\right]\right\}} = \pm 0.152$$ with 61 degrees of freedom. The value of t is thus 1.28, indicating that the observed distance between these two lines would occur by chance about once in four times so that it is doubtful whether there is a significant difference between the regressions.

Testing the difference between the β and αp regression lines we find that this distance is 0.191 and its standard error is $\pm$0.152. The t value on 61 degrees of freedom is 1.37, and so there is again doubt as to whether there is a significant difference between the regressions.

The distance between the βf and αp lines is 0.004 and its standard error $\pm$ 0.151 and so is obviously not significant.

For the γ and $\beta\gamma$ regression lines the joint regression coefficient is 7.47×10^{-4} which is highly significant. The distance between the lines is 1.34 with a standard error of ± 0.284 on 39 degrees of freedom giving a value of t of 4.70 which is significant at the 0.1% level showing that such a distance could only arise by chance in one in a thousand cases. Thus, although the regression lines for types γ and $\beta\gamma$ are parallel the flare activity associated with γ groups is generally higher than $\beta\gamma$ groups.

At this stage it is interesting to see if all types of spot groups produce flares of different classes in the same ratios. The hypothesis is set up that this is so. The observed and predicted frequencies of flares falling in the different classes for all types are shown in table 3. The hypothesis can be tested by means of the χ^2-test on 2 degrees of freedom. If O represents an observed frequency and E represents an expected frequency based on the hypothesis then,

$$\chi^2 = \sum \frac{(O - E)^2}{E}$$

Thus, for the β type we have:

$$\chi^2_{(2)} = \frac{10^2}{309} + \frac{9^2}{73} + \frac{1^2}{8} = \underline{1.56}$$

This value might easily occur by chance and we conclude that the observed frequencies agree with the hypothesis. Since the frequencies for class 3 flares are less than 5 for certain types the χ^2-test becomes invalid but by pooling the observed and predicted frequencies for different pairs of types to

TABLE 3.

The observed and predicted frequencies of flares falling in the different classes for the various spot group types.

	Observed.			Predicted.			
Group	Class1	Class2	Class3	Class1	Class2	Class3	Total.
β	319	64	7	309	73	8	390
βp	626	137	11	613	145	16	774
βf	133	35	1	134	32	3	169
$\beta\gamma$	179	63	13	202	48	5	255
αp	198	38	3	190	45	4	239
γ	86	26	3	91	22	2	115
α	44	12	2	46	11	1	58
Total.	1585	375	40				2000

obtain frequencies greater than 5 this test may still be used. The conclusion so obtained was that all types of spot groups produce flares of different classes in the same ratios, with the exception of type $\beta\gamma$ for which the $\chi^2_{(2)}$ value is 20.46, a value which could only arise by chance one in more than a thousand times. If the flare frequencies for type $\beta\gamma$ are examined it will be found that the observed frequencies for classes 2 and 3 are much higher than the values predicted by the hypothesis. We conclude that the magnetic conditions existing around $\beta\gamma$ groups are more favourable for the generation of intense flares than those of other groups.

The conclusions of this section may be summarised as follows:

(1). Linear relationships between F and A were obtained for all types of spot group with the exception of types α and $\alpha\beta$ for which there was insufficient data.

(2). The regression lines for types β, $\beta\beta$ and $\alpha\beta$ have no significant difference which indicates that the flare activity in these groups is probably the same.

(3). The regression lines for types $\beta\beta$, $\beta\gamma$ and γ have no virtually the same slopes but are separated by significant distances. This indicates that the flare activity in these types increases from type $\beta\beta$, to type $\beta\gamma$, to type γ, although the increase in flare activity for a given increase in spot area is the same for all three types.

(4). It is interesting to note that for a given increase in area, the corresponding increase in activity for types $\beta\beta$, $\beta\gamma$ and γ is apparently just twice the increase in activity associated with types β, $\beta\beta$ and $\alpha\beta$.

(5). All types, with the exception of type $\beta\gamma$, produce flares of different classes in the same ratios. The geometry of the magnetic fields accompanying $\beta\gamma$-types is probably more favourable for the generation of intense flares than that of other types.

(3). The relation between flare frequency and the rate of change in area of the associated spot group.

The rate of change in area of a spot group at the time that a flare occurs is not available. In order to overcome this difficulty the area of the spot group on the day preceding the flare, on the day of the flare, and on the day following the flare was tabulated. Using this material the rate of change in area was estimated for the 24 hours preceding and the 24 hours following the flare. The mean of these two values can then be used as an estimate of the rate of change in area at the time of the flare.

The rates of change of spot areas were grouped into convenient ranges and the frequency of solar flares occurring in each range was obtained. In the first instance all flares were assumed to be of equal importance and the values obtained for the flare frequencies were plotted against the mean rates of change in spot area. An inspection of the plotted points indicated that the flare frequency seemed to increase as the rate of change inspot area increased, and was independent of the direction of the rate of change in spot area. However, the association, overall, did not seem to be quite linear and it was therefore decided to fit and test a quadratic expression of the form

$$F = C + b_1|i| + b_2|i|^2.$$

where F is the flare frequency, C is a constant, i the rate of change in spot area, and b_1 and b_2 are the regression coefficients. The coefficients b_1 and b_2 can be determined from the equations

$$b_1\Sigma(i - \bar{i})^2 + b_2\Sigma(i - \bar{i})(i^2 - \overline{i^2}) = \Sigma(i - \bar{i})(F - \bar{F}).$$

$$b_1\Sigma(i - \bar{i})(i^2 - \overline{i^2}) + b_2\Sigma(i^2 - \overline{i^2})^2 = \Sigma(i^2 - \overline{i^2})(F - \bar{F}).$$

The negative rates of change in spot area were considered first. The following values were obtained:

$n = 15.$ $\quad \Sigma(i - \bar{i})(F - \bar{F}) = 2549.$ $\quad \overline{i^2} = 307 \times 10^3.$

$\bar{F} = 0.87.$ $\quad \Sigma(F - \bar{F})^2 = 3.95.$ $\quad \Sigma(i^2 - \overline{i^2})^2 = 5.81 \times 10^{12}.$

$\bar{i} = 376.$ $\quad \Sigma(i - \bar{i})^2 = 2.47 \times 10^6.$

$\Sigma(i - \bar{i})(i^2 - \overline{i^2}) = 3.56 \times 10^9.$ $\quad \Sigma(i^2 - \overline{i^2})(F - \bar{F}) = 3.26 \times 10^6.$

Using these values the equations to estimate the regression coefficients are:-

$$b_1 . 2.47 \times 10^6 + b_2 . 3.56 \times 10^9 = 2.55 \times 10^3$$

and $$b_1 . 3.56 \times 10^9 + b_2 . 5.81 \times 10^{12} = 3.26 \times 10^6$$

giving:

$$b_1 = 1.89 \times 10^{-3} \text{ and } b_2 = -5.6 \times 10^{-7}.$$

The regression equation can now be written as:

$$F - 0.87 = 1.89 \times 10^{-3}(i - 376) - 5.6 \times 10^{-7}(i^2 - 307 \times 10^3).$$

or $$F = 1.89 \times 10^{-3} i - 5.6 \times 10^{-7} i^2 + 0.33. \quad . \quad . \quad .(1).$$

The analysis of variance is:

	D.f.	S.s.	M.s.	V.R.
Linear term.	1	2.63	2.63	29.9 0.1%
Quadratic term.	1	0.27	0.27	3.1 10%.
Regression.	2	2.90	1.45	16.5 0.1%
Residual.	12	1.05	0.088	* * *
Total.	14	3.95		

For the positive rates of change in spot area we have:

$n = 15.$ $\Sigma(i - \bar{i})(F - \bar{F}) = 1863.$ $\overline{i^2} = 354 \times 10^3$

$\bar{F} = 0.96.$ $\Sigma(F - \bar{F})^2 = 4.21.$ $\Sigma(i^2 - \overline{i^2})^2 = 9.33 \times 10^{12}.$

$\bar{i} = 390\frac{1}{2}$ $\Sigma(i - \bar{i})^2 = 3.09 \times 10^6$

$\Sigma(i - \bar{i})(i^2 - \overline{i^2}) = 5.03 \times 10^9.$ $\Sigma(i^2 - \overline{i^2})(F - \bar{F}) = 2.05 \times 10^6.$

These values give the following simultaneous equations for estimating the regression coefficients b_1 and b_2:

$$b_1 3.09 \times 10^6 + b_2 5.03 \times 10^9 = 1.86 \times 10^3.$$

and $$b_1 5.03 \times 10^9 + b_2 9.33 \times 10^{12} = 2.05 \times 10^6.$$

and so $b_1 = 2.05 \times 10^{-3}$ and $b_2 = -8.9 \times 10^{-7}$,

and the fitted regression equation is

$$F = 2.05 \times 10^{-3} i - 8.9 \times 10^{-7} i^2 + 0.47. \quad . \quad . \quad .(2).$$

The analysis of variance is:

	D.f.	S.s.	M.s.	V.R.
Linear term.	1	1.12	1.12	6.0 <5%
Quadratic term.	1	0.86$\frac{7}{8}$	0.86	4.6 ~5%
Regression.	2	1.98	0.99	5.3 2$\frac{1}{2}$%
Residual.	12	2.23	0.186	
Total.	14	4.21		

We now wish to compare equations (1) and (2) to see if they differ significantly from each other. Before this can be done we must compare the residual mean squares in the regressions by means of the variance ratio test. The appropriate variance ratio here is 2.10 which is not significant, indicating that the regression coefficients b_1 and b_2 are comparable.

The sums of squares and products in the two sets of data are now combined, giving:

$\Sigma[\Sigma(i - \bar{i})(F - \bar{F})] = 4412.$ $\quad \Sigma[\Sigma(i^2 - \bar{i^2})^2] = 15.1 \times 10^{12}.$

$\Sigma[\Sigma(F - \bar{F})^2] = 8.16.$ $\quad \Sigma[\Sigma(i - \bar{i})(i^2 - \bar{i^2})] = 8.59 \times 10^9.$

$\Sigma[\Sigma(i - \bar{i})^2] = 5.57 \times 10^6.$ $\quad \Sigma[\Sigma(i^2 - \bar{i^2})(F - \bar{F})] = 5.31 \times 10^6.$

The equations to estimate the joint regression coefficients will be:

$$b_1 5.57 \times 10^6 + b_2 8.59 \times 10^9 = 4.41 \times 10^3$$

and $$b_2 8.59 \times 10^9 + b_2 15.1 \times 10^{12} = 5.31 \times 10^6$$

giving $b_1 = 2.04 \times 10^{-3}$ and $b_2 = -8.10 \times 10^{-7}$.

The fitted regression equations now become, for negative rates of change in spot area:

$F = 0.87 + 2.04 \times 10^{-3}(i - 376) - 8.1 \times 10^{-7}(i^2 - 307 \times 10^3).$

and for positive rates of change:

$F = 0.96 + 2.04 \times 10^{-3}(i - 390) - 8.1 \times 10^{-7}(i^2 - 354 \times 10^3)$.

The distance between these curves is 0.10 and the standard error of this distance is

$$\sqrt{\left\{0.13\left[\frac{1}{15} + \frac{1}{15} + \frac{(0.09)^2}{4.21 - 3.95}\right]\right\}} = \pm 0.146.$$

on 26 degrees of freedom. The t-value is thus 0.10/0.146 = 0.685 and is clearly not significant. We therefore conclude that the distance between the separate regression curves is not significantly different from zero.

From both sets of data we now obtain the values of $\overline{|i|} = 383$, $\overline{i^2} = 330 \times 10^3$ and $\overline{F} = 0.92$, and the joint regression equation becomes:

$F - 0.92 = 2.04 \times 10^{-3}(|i| - 383) - 8.10 \times 10^{-7}(i^2 - 330 \times 10^3)$.

or $F = 2.04 \times 10^{-3}|i| - 8.10 \times 10^{-7} i^2 + 0.41$ . . .(3).

The analysis of variance becomes:

	D.F.	S.s.	M.s.	V.R.
Linear term.	1	3.52	3.52	12.30 <1%
Quadratic term.	1	1.28	1.28	4.45 ~5%
Regression.	2	4.70	2.35	8.15 <1%
Residual.	12	3.46	0.288	
Total.	14	8.16		

From the above analysis we conclude that for a given increase in the rate of change of spot area there is

a corresponding increase in flare frequency, independent of the direction of that rate of change in spot area. It also appears quite probable that the rate of change in flare frequency with respect to the rate of change in spot area, becomes less as the rate of change in spot area becomes larger.

Although a quadratic expression will adequately fit the observed results it is not conclusive that other forms of curve will not fit the data better. It is therefore very dangerous to extrapolate any fitted expression beyond the range of the observed results.

The flares were now regrouped according to their class and the regression curves of F on i determined. No distinction is made between positive and negative rates of change in spot area. Table 4 shows the values of n, $\overline{F}$, $\overline{i}$, $\overline{i^2}$, $\Sigma(F - \overline{F})^2$, $\Sigma(i - \overline{i})^2$, $\Sigma(F - \overline{F})(i - \overline{i})$, $\Sigma(i^2 - \overline{i^2})$; $\Sigma(i - \overline{i})(i^2 - \overline{i^2})$, and $\Sigma(i^2 - \overline{i^2})(F - \overline{F})$ for the flares of the different classes.

TABLE 4.

Case.	n.	$\overline{F}$.	$\overline{i}$	$\overline{i^2}$	$\Sigma(F-\overline{F})^2$	$\Sigma(i-\overline{i})^2$
All flares.	15	0.920	383	330 x10^3	8.160	5.57 x 10^6
Class 1.	15	0.703	377	331 x10^3	1.875	2.76 x 10^6
Class 2.	15	0.195	377	331 x10^3	0.199	2.76 x 10^6
Class 3.	14	0.0259	347	307 x10^3	0.00585	2.64 x10^6.

TABLE 4 (Continued).

Case.	$\Sigma(F-\bar{F})(i-\bar{i})$.	$\Sigma(i^2-\bar{i^2})^2$.	$\Sigma(i-\bar{i})(i^2-\bar{i^2})$	$\Sigma(i^2-\bar{i^2})(F-\bar{F})$
All flares.	4412.0	15.1×10^{12}	8.59×10^{9}	5.31×10^{6}.
Class 1.	1569.9	7.43×10^{12}	4.27×10^{9}	1.85×10^{6}.
Class 2.	538.8	7.43×10^{12}	4.27×10^{9}	0.711×10^{6}.
Class 3.	103.3	7.29×10^{12}	4.10×10^{9}	0.167×10^{6}.

The appropriate regression equations are:

For all flares:

$$F = 2.04 \times 10^{-3} i - 8.10 \times 10^{-7} i^2 + 0.41$$

For class 1 flares:

$$F = 1.70 \times 10^{-3} i - 7.30 \times 10^{-7} i^2 + 0.31$$

For class 2 flares:

$$F = 0.442 \times 10^{-3} i - 1.59 \times 10^{-7} i^2 + 0.082$$

For class 3 flares:

$$F = 0.039 \times 10^{-3} i + 0.012.$$

. . . . (4).

These curves are shown in figures 7, 8, 9, and 10, together with the observed values of F plotted against i for each of these cases. To test the significance of these regressions the following analysis of variance tests were carried out:

For class 1 flares:

	D.f.	S.s.	Ms.s.	V.R.
Linear term.	1	0.895	0.895	19.5 0.1%
Quadratic term.	1	0.425	0.425	9.2 1%
Regression.	2	1.320	0.660	14.4 0.1%
Residual.	12	0.555	0.046	* * *
Total.	14	1.875		

For class 2 flares:

	D.f.	S.s.	M.s.	V.R.
Linear term.	1	0.105	0.105	17.1 1%
Quadratic term.	1	0.020	0.020	3.25 <10%
Regression.	2	0.1250	0.0625	10.02 1%
Residual.	12	0.0737	0.00615	✲ ✲
Total.	14	0.1987		

For flares of class 3:

	D.f.	S.s.	M.s.	V.R.
Regression.	1	4.03×10^{-3}	4.03×10^{-3}	26.5 0.1%
Residual.	12	1.82×10^{-3}	1.52×10^{-4}	✲ ✲ ✲
Total.	13	5.85×10^{-3}		

For the flares of class 3 the observed data indicated that the inclusion of a quadratic term would not provide any significant improvement in fit. However, more extensive observations on class 3 flares might easily make a quadratic term significant.

Figure 11 shows the regression curves of F on i for the different classes of flares. The regression curves have been extrapolated until they meet. It seems that these curves converge to the same point and that this point lies on the i-axis. Although there is no physical significance in the extrapolated portions, the situation again suggests that all the flares come from the same population. In order to test this suggestion the following procedure was adopted. 1,824 flares were examined in this section of the analysis and of

Figure 7. All flares, irrespective of class.

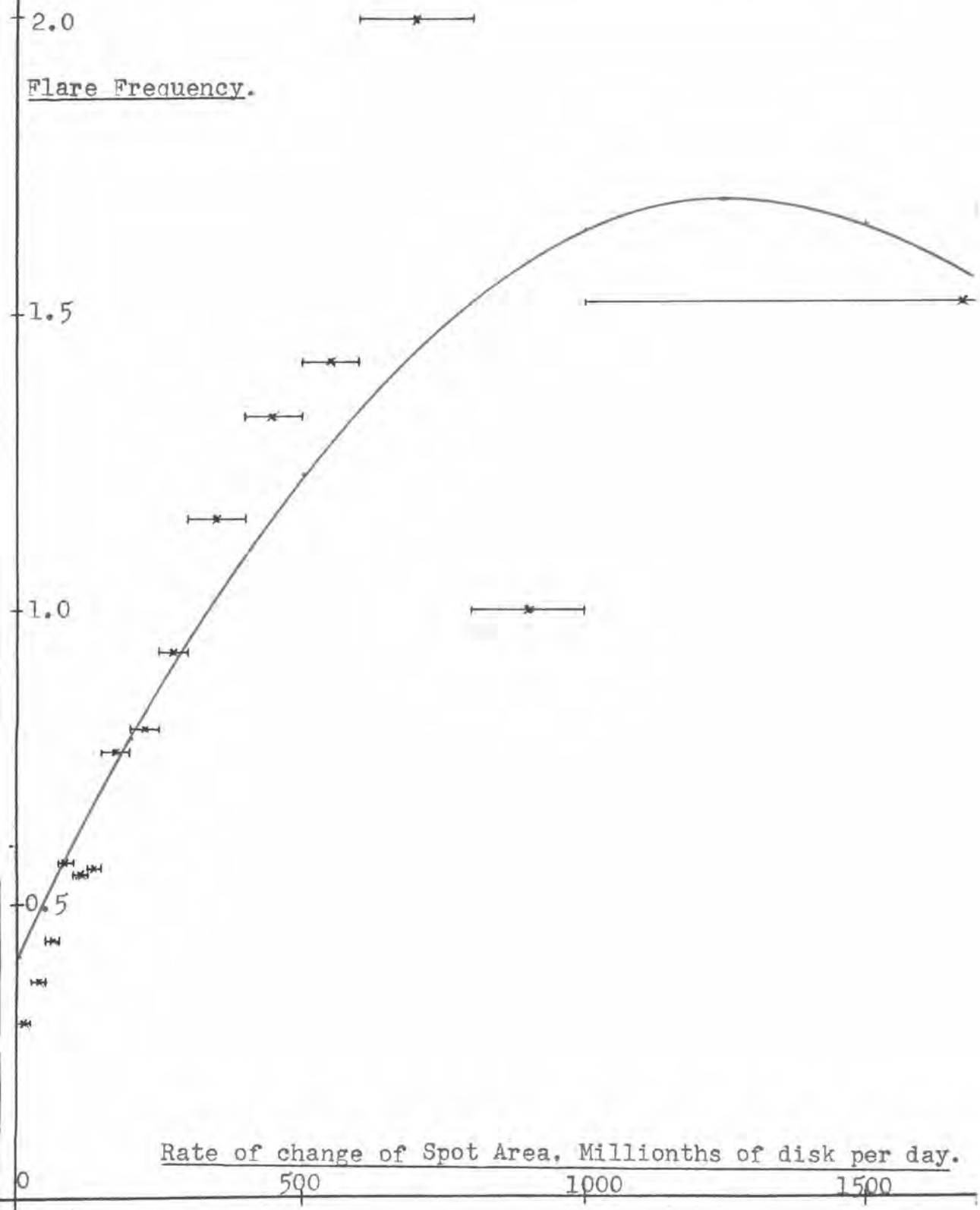

Figure 8. Class 1 flares.

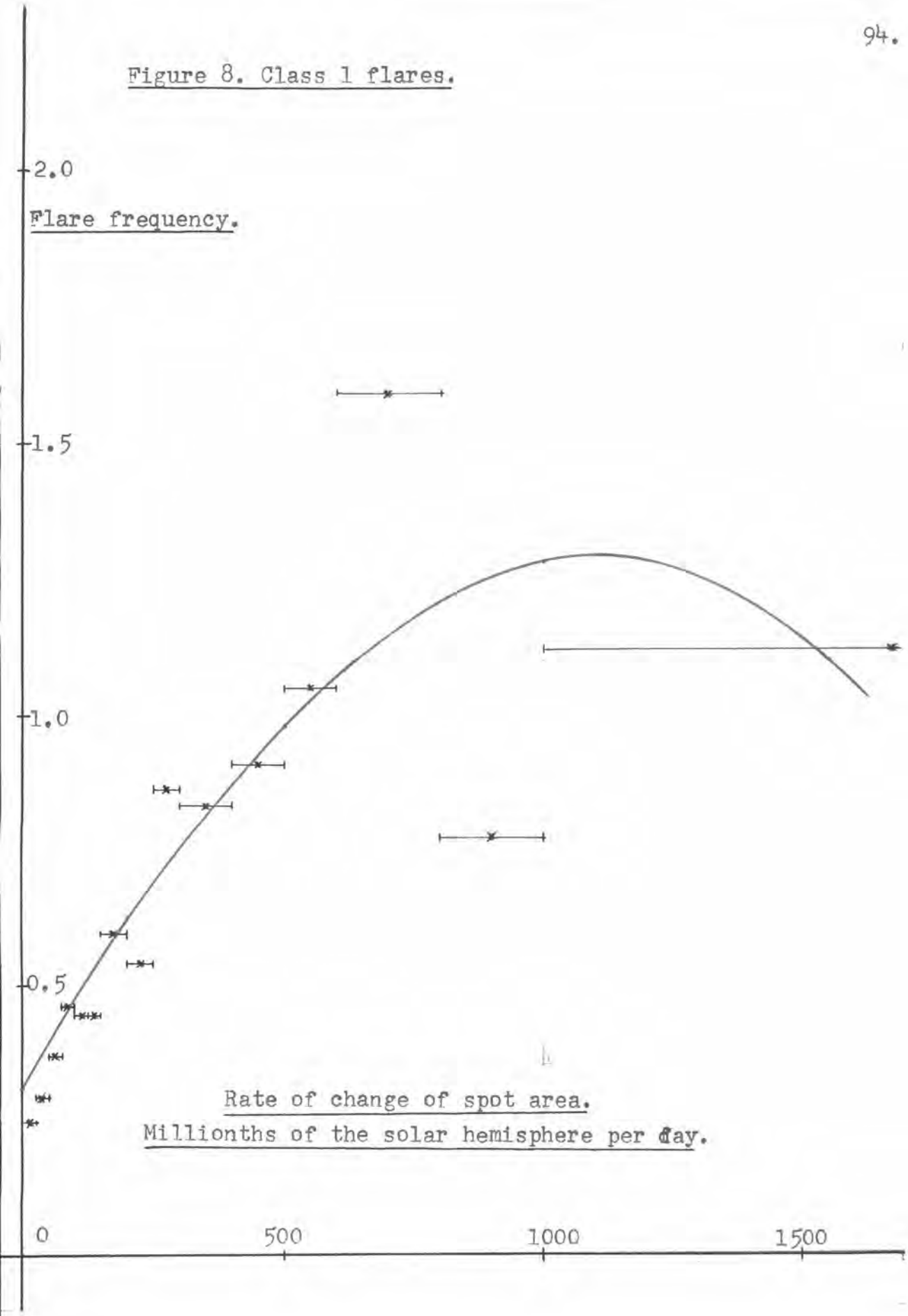

Figure 9. Class 2 flares.

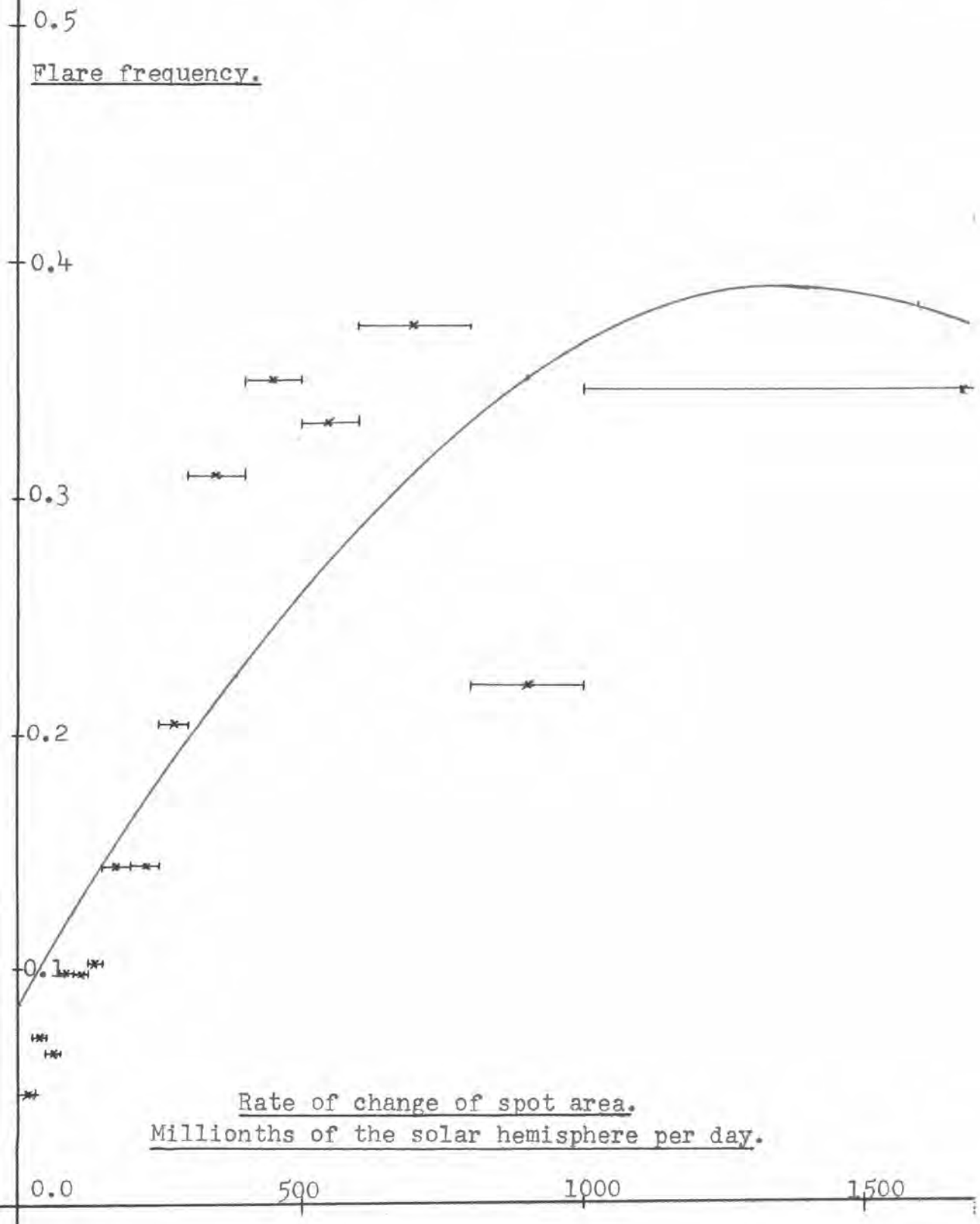

Figure 10. Class 3 flares.

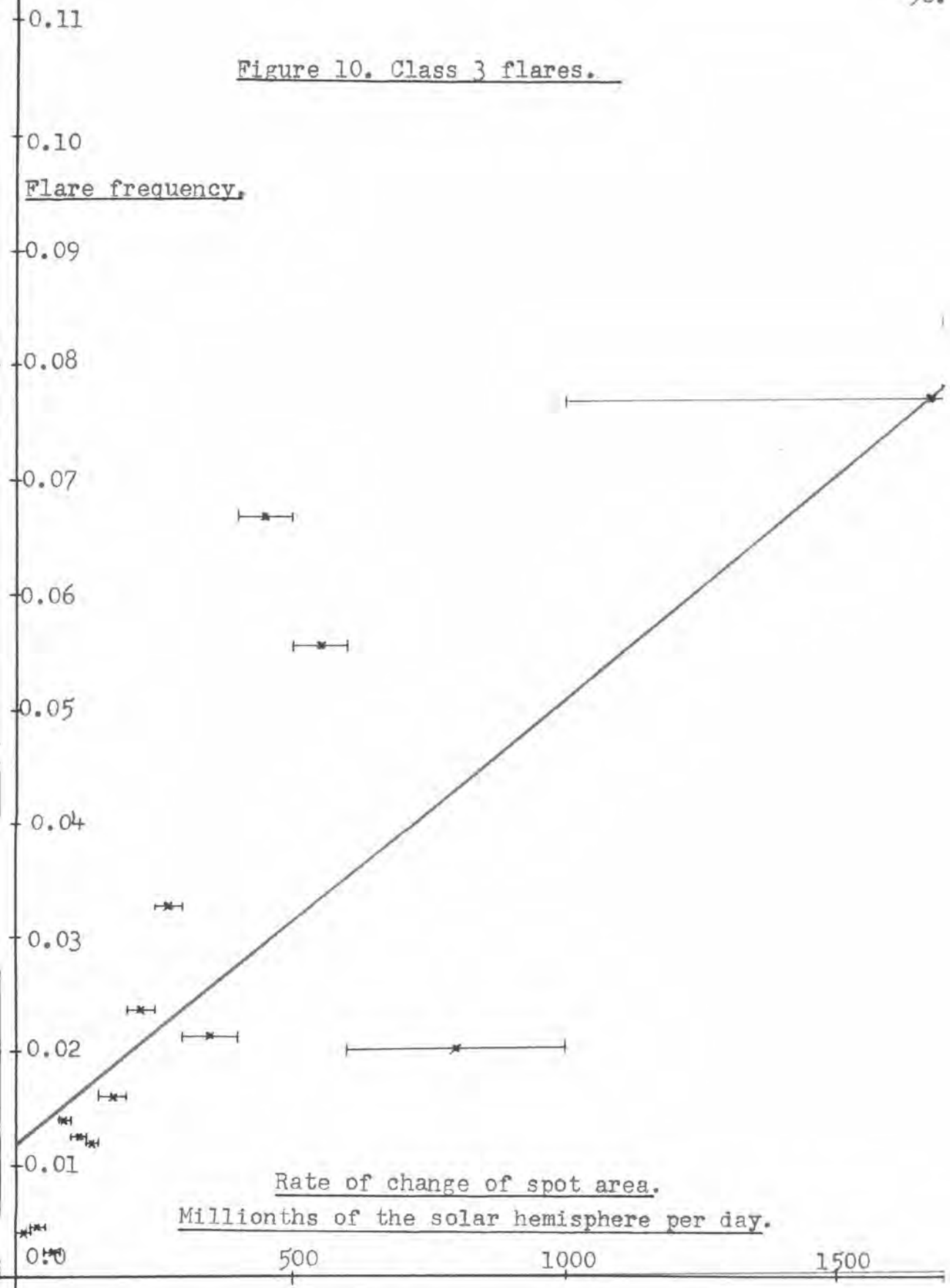

Figure 11.

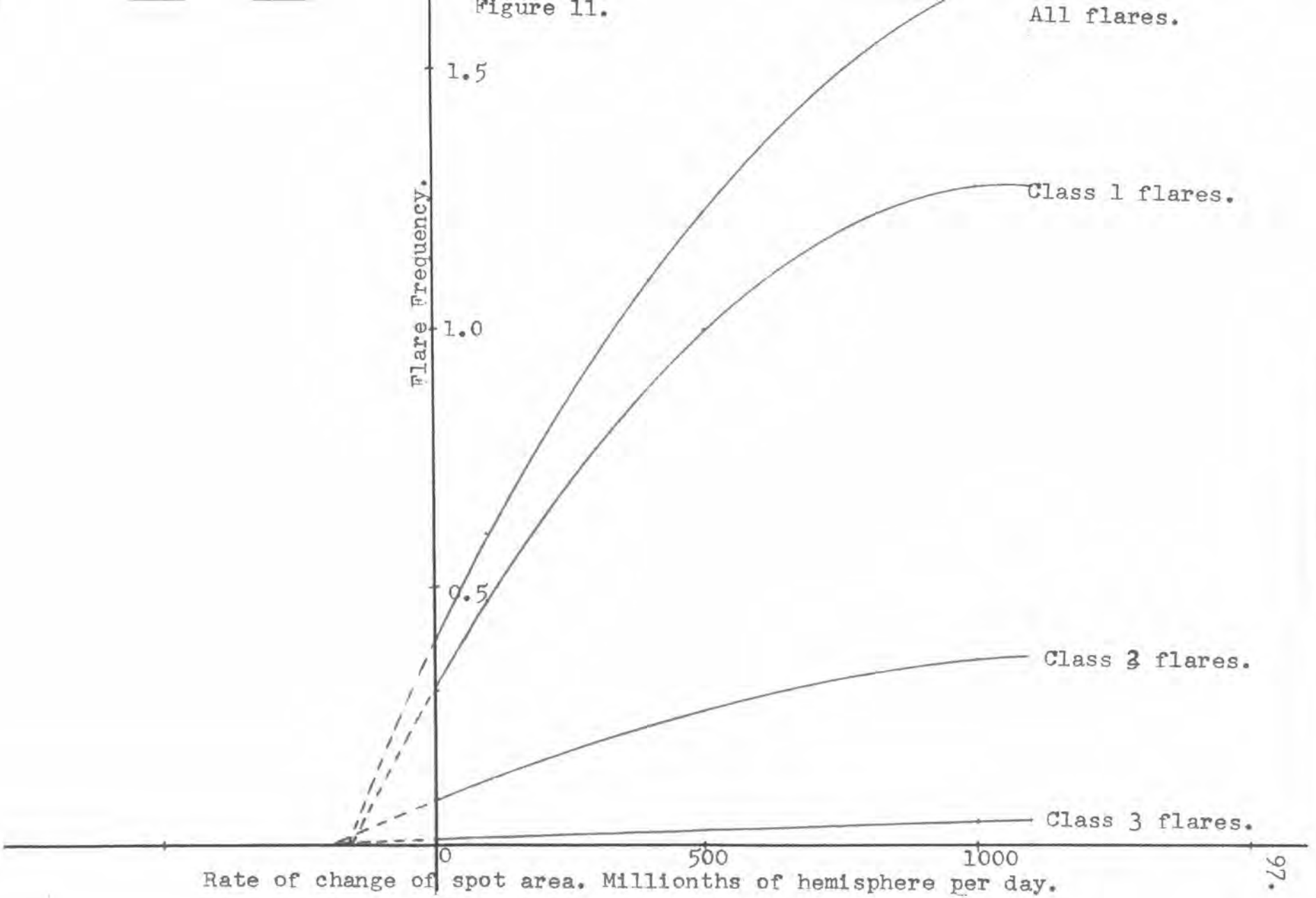
All flares.
1.5
Class 1 flares.
Flare Frequency.
1.0
0.5
Class 2 flares.
Class 3 flares.
0
500
1000
Rate of change of spot area. Millionths of hemisphere per day.

Figure 11a.

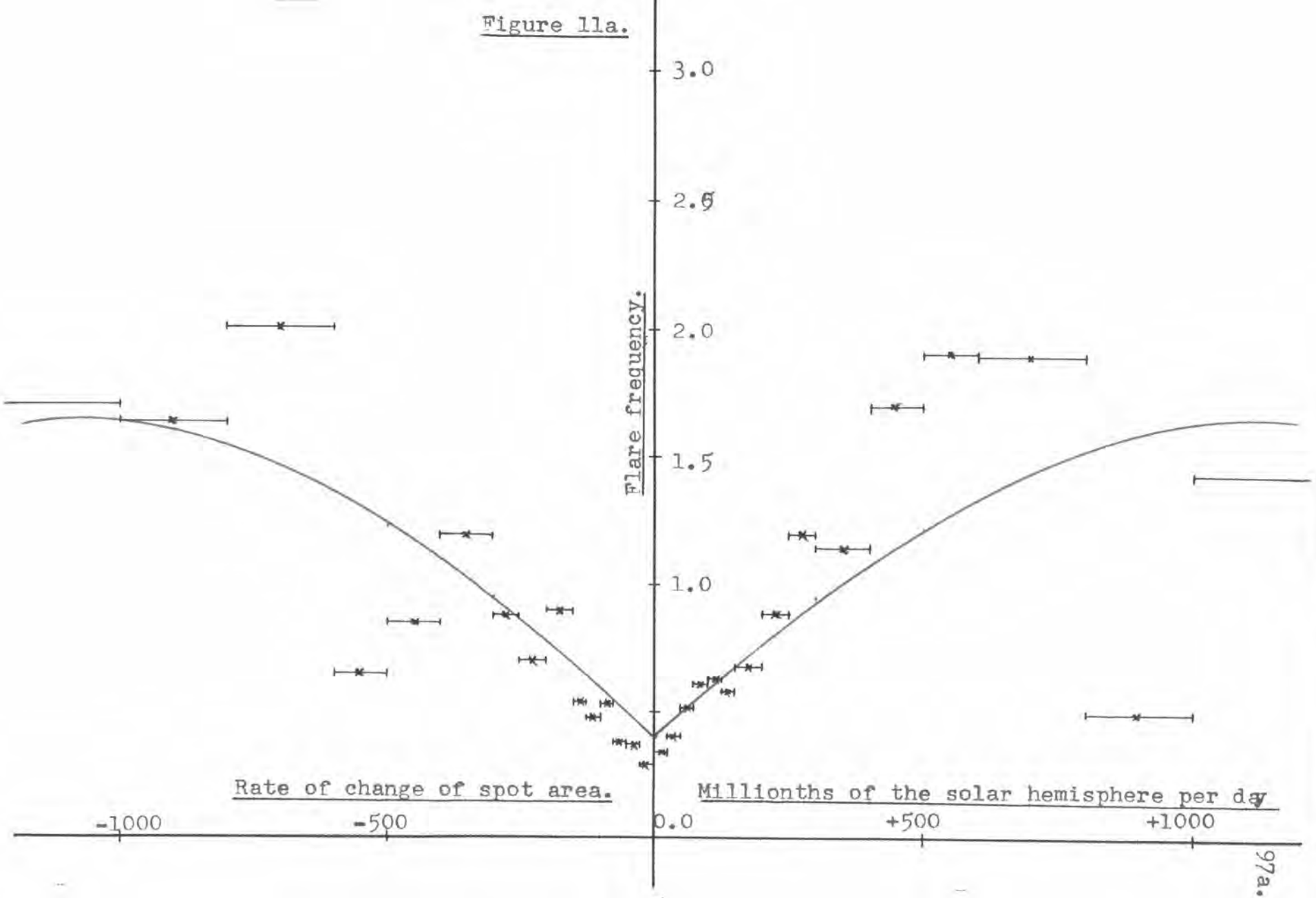
3.0
2.5
2.0
1.5
1.0
Flare frequency.
Rate of change of spot area.
Millionths of the solar hemisphere per day
-1000
-500
0.0
+500
+1000

these 1,459.5 were of class 1, 331.0 of class 2 and 33.5 of class 3. (The half-flares occur here because of the method used in determining the value of i associated with each flare). If the suggestion is correct the constants in the four regression equations should be in the ratio,

1,824.0 : 1,459.5 : 331.0 : 33.5.

Thus, using these ratios in conjunction with any one of the regression equations we should be able to predict any of the other equations.

The regression equation for the flares of class 2 is

$$F = 0.442 \times 10^{-3} |i| - 1.59 \times 10^{-7} i^2 + 0.082 \quad . \quad . \quad (5).$$

and if the right hand side of this equation is multiplied by 1,459.0/331.0 we obtain the predicted equation for the flares of class 1:-

$$F = 1.95 \times 10^{-3} |i| - 7.00 \times 10^{-7} i^2 + 0.36 \quad . \quad . \quad .(6).$$

This predicted equation must now be compared with the actual equation:

$$F = 1.70 \times 10^{-3} |i| - 7.30 \times 10^{-7} i^2 + 0.31 \quad . \quad . \quad .(7).$$

The ratio of the residual mean squares about equations (6) and (7) is tested by means of the variance ratio test. If this ratio is not significant a pooled estimate of the sums and products can then be calculated and a joint regression carried out. The difference between the sum of squares removed by the

joint regression and the sum of squares removed by the separate regressions will then test the difference between equations (6) and (7).

The sums of squares and products for equations (6) can be determined from those for equation (5) by applying the ratio 1,459.5/331.0. This yields:

$n = 15.$ $\bar{F} = 0.859.$ $\bar{i} = 377.$ $\overline{i^2} = 331 \times 10^3.$

$\Sigma(F-\bar{F})^2 = 3.680.$ $\Sigma(i-\bar{i})^2 = 2.764 \times 10^6.$

$\Sigma(F-\bar{F})(i-\bar{i}) = 2.37 \times 10^3.$ $\Sigma(i^2-\overline{i^2})^2 = 7.43 \times 10^{12}.$

$\Sigma(i^2-\overline{i^2})(i-\bar{i}) = 4.27 \times 10^9.$ $\Sigma(i^2-\overline{i^2})(F-\bar{F}) = 3.13 \times 10^6.$

The sum of squares due to this regression will be $1.95 \times 10^{-3} \times 2.370 \times 10^3 - 7.00 \times 10^{-7} \times 3.13 \times 10^6 = 2.44.$ The sum of squares due to the actual regression is 1.320. The residual sum of squares will be (3.86 - 2.44) = 1.42 and (1.875 - 1.320) = 0.555 respectively, both on 12 degrees of freedom. The ratio of these residual mean squares is not significant and so a pooled estimate of the sums and squares and products may be made:

$\Sigma[\Sigma(F-\bar{F})^2] = 5.735.$ $\Sigma[\Sigma(i-\bar{i})^2] = 5.528 \times 10^6.$

$\Sigma[\Sigma(F-\bar{F})(i-\bar{i})] = 3.94 \times 10^3.$ $\Sigma[\Sigma(i^2-\overline{i^2})^2] = 14.9 \times 10^{12}.$

$\Sigma[\Sigma(i-\bar{i})(i^2-\overline{i^2})] = 8.54 \times 10^9.$ $\Sigma[\Sigma(i^2-\overline{i^2})(F-\bar{F})] = 4.98 \times 10^6.$

The joint regression coefficients calculated from these pooled estimates are

$$b_1 = 1.78 \times 10^{-3} \text{ and } b_2 = -6.89 \times 10^{-7}.$$

and the sum of squares is 3.580 compared to (1.320 + 2.440) =

= 3.760 removed by the separate regressions. These two sums of squares can now be tested by means of an analysis of variance:

	D.f.	S.s.	M.s.	V.R.
Joint regression.	2	3.580	1.790	21.80 0.1%
Difference between regressions	2	0.180	0.090	1.09
Sum of separate regressions.	4	3.760	0.940	
Residual.	24	1.975	0.082	
Total.	28	5.735		

Thus, the joint regression is significant but the difference between the regressions is not. This result indicates that the ratio of class 1 to class 2 flares remains constant and is independent of the rate of change of spot area.

The regression equation for flares of class 3 is

$$F = 0.0389 \times 10^{-3} |i| + 0.012 \quad . \quad . \quad . \quad . \quad .(8).$$

and if the right hand side of this equation is multiplied by 331.0/33.5 we obtain the predicted equation for the flares of class 2:

$$F = 0.396 \times 10^{-3} |i| + 0.122 \quad . \quad . \quad . \quad . \quad .(9).$$

The sums of squares and products for equation (9) are estimated as:

$n = 14.$ $\quad \bar{F} = 0.256.$ $\quad \bar{i} = 347.$ $\quad \overline{i^2} = 307 \times 10^3.$

$\Sigma(F-\bar{F})^2 = 0.571.$ $\quad \Sigma(i^2-\overline{i^2})^2 = 7.290 \times 10^{12}.$

$\Sigma(i-\bar{i})^2 = 2.644 \times 10^6.$ $\quad \Sigma(F-\bar{F})(i-\bar{i}) = 1.020 \times 10^3.$

$\Sigma(i^2-\overline{i^2})(i-\bar{i}) = 4.10 \times 10^9.$ $\quad \Sigma(i^2-\overline{i^2})(F-\bar{F}) = 1.64 \times 10^6.$

The sum of squares calculated from this data amounts to 0.398. The sum of squares due to the actual regression is 0.1250. The residual sum of squares will be (0.571 - 0.398) = 0.173, and (0.1987 - 0.1250) = 0.0737, respectively. These give a variance ratio of 2.56 on 11 and 12 degrees of freedom. This ratio does not quite reach significance and so a pooled estimate of the sums of squares and products may be made:

$\Sigma[\Sigma(F-\bar{F})^2] = 0.7697\frac{1}{2}$ $\quad \Sigma[\Sigma(i-\bar{i})^2] = 5.41 \times 10^6.$

$\Sigma[\Sigma(F-\bar{F})(i-\bar{i})] = 1.56 \times 10^3.$ $\Sigma[\Sigma(i^2-\bar{i^2})^2] = 14.72 \times 10^{12}.$

$\Sigma[\Sigma(i-\bar{i})(i^2-\bar{i^2})] = 8.37 \times 10^9.$ $\Sigma[\Sigma(i^2-\bar{i^2})(F-\bar{F})] = 2.35 \times 10^6.$

The joint regression coefficients calculated from these pooled estimates are:

$$b_1 = 0.340 \times 10^{-3} \text{ and } b_2 = -0.326 \times 10^{-7}.$$

and the sum of squares due to the regression is 0.463 compared to (0.398 + 0.1250) = 0.523 removed by the separate regressions. These two sums of squares can now be tested by the following analysis of variance:

	D.f.	S.s.	M.s.	V.R.
Joint regression.	2	0.4630	0.2315	17.8 0.1%
Difference between regressions	2	0.0600	0.0300	2.3
Sum of separate regressions.	4	0.5230	0.1307	
Residual.	19	0.2467	0.0130	
Total.	23	0.7697		

Once again, the joint regression is highly significant and the difference between the separate regressions is not significant. We therefore conclude that all the flares come from the same population and that, in consequence, the proportions of flares occurring in the different classes are independent of the rate of change of spot area.

---oOo---

From a visual inspection of the plotted points in figures 7, 8, 9, and 10 it is obvious that the points representing the rates of change of spot area up to 700 millionths of the solar hemisphere per day, indicate a good linear relationship. For values of $|i| \gtrsim 700$ millionths of the solar hemisphere per day there appears to be a sudden drop in the flare frequency, and the two points which represent these values must carry enormous weight in any regression analysis. If these two points are omitted from the data, and the analysis repeated by fitting straight lines to the remaining points, the validity of the conclusions already derived can be checked.

The fitted regression lines are:-

For all flares:

Negative rates of change: $F = 2.20 \times 10^{-3} i + 0.21.$

Positive rates of change: $F = 2.56 \times 10^{-3} i + 0.33.$

Joint regression, All flares: $F = 2.39 \times 10^{-3} |i| + 0.33.$

For flares of class 1: $F = 1.72 \times 10^{-3} |i| + 0.25.$

For flares of class 2: $F = 0.54 \times 10^{-3}i + 0.05.$

For flares of class 3: $F = 0.111 \times 10^{-3}i - 0.001.$ . . . (10).

All these regression lines are significant at the 0.1% level and are shown in figure 12. Once again, the lines appear to converge to the same point, and the hypothesis is set up that all the flares come from the same population. Of the 1,824 flares which were observed, 1,459.5 were of class 1; 331.0 were of class 2; and 33.5 were of class 3. Therefore, if the hypothesis is correct, the gradients of the four reg regression lines should be in the ratios:

1,824.0 : 1,459.5 : 331.0 : 33.5.

The sum of the gradients of the four regression lines is 4.76×10^{-3} and the total number of flares equivalent to this is 3,648. Thus, the number of flares used in the calculation of each regression line must be multiplied by a factor of $(4.76 \times 10^{-3})/3,648 = 1.30 \times 10^{-6}$ to obtain the predicted gradients. This gives:

For all flares: 2.37×10^{-3}.

For flares of class 1: 1.90×10^{-3}.

For flares of class 2: 0.43×10^{-3}.

For flares of class 3: 0.044×10^{-3}. . . . . (11).

Control limits are now set at one standard error from the regression coefficients and the limits so determined are:

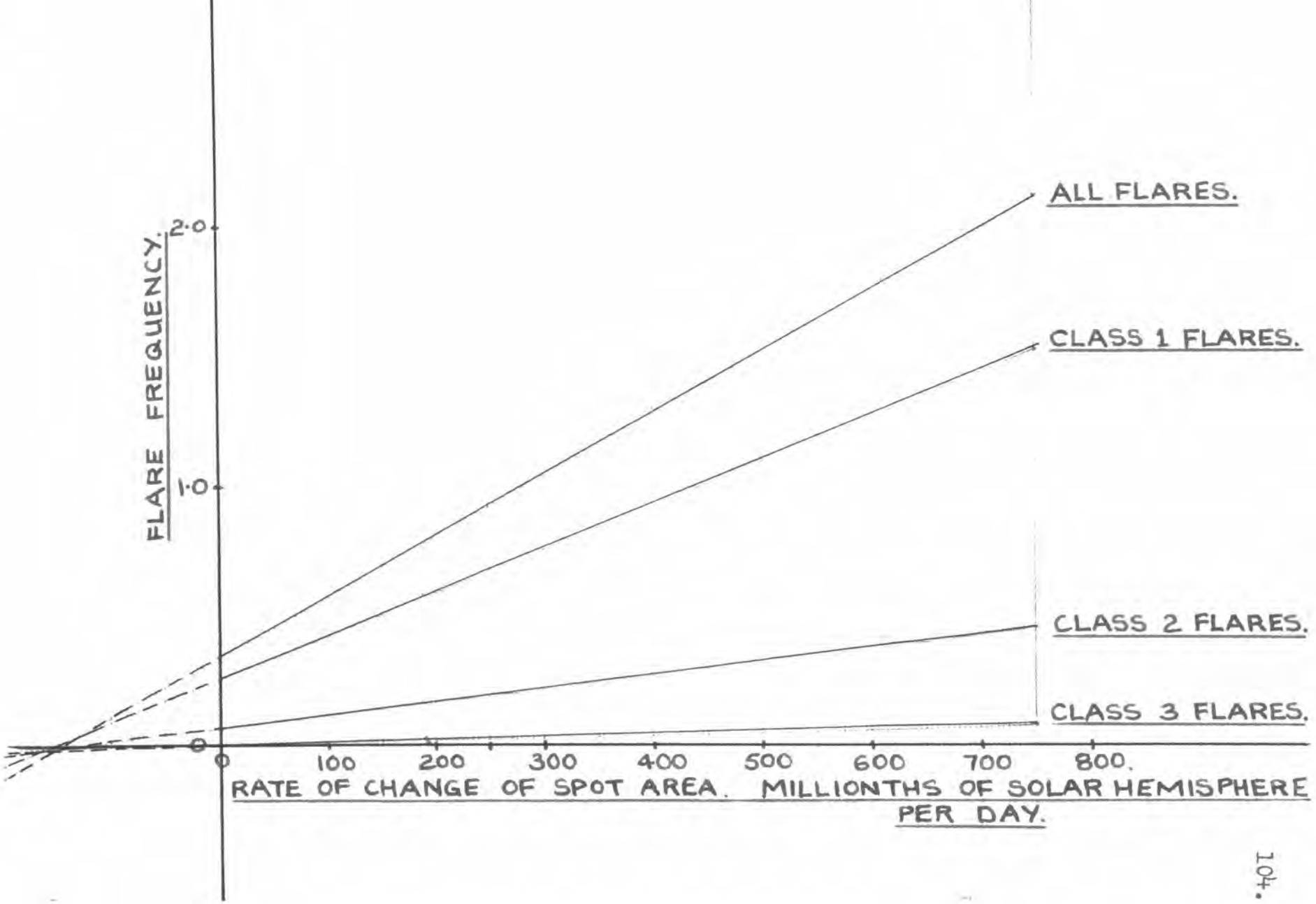
ALL FLARES.
CLASS 1 FLARES.
CLASS 2 FLARES.
CLASS 3 FLARES.
FLARE FREQUENCY.
2·0
1·0
0
0
100
200
300
400
500
600
700
800.
RATE OF CHANGE OF SPOT AREA. MILLIONTHS OF SOLAR HEMISPHERE PER DAY.

$$\left.\begin{array}{ll} \text{For all flares:} & 0.97 \times 10^{-3} \text{ to } 3.81 \times 10^{-3}. \\ \text{For flares of class 1:} & 1.29 \times 10^{-3} \text{ to } 2.15 \times 10^{-3}. \\ \text{For flares of class 2:} & 0.36 \times 10^{-3} \text{ to } 0.72 \times 10^{-3}. \\ \text{For flares of class 3:} & 0.065 \times 10^{-3} \text{ to } 0.157 \times 10^{-3}. \end{array}\right\} \quad (12).$$

If these results are compared to those given in (11) it will be seen that the gradients expected on our hypothesis all lie withim one standard error of the observed gradients, with the exception of the expected gradient for flares of class 3. This case can be determined in more detail as follows. The difference between the observed and predicted gradients is 0.067×10^{-3} and the standard error of this difference can be estimated as $\sqrt{2}$ x (standard error of the regression coefficient) = 0.065×10^{-3}. The ratio $(0.067 \times 10^{-3})/(0.065 \times 10^{-3}) = 1.03$ can now be tested by means of the t-variate and is found not to be significant. We therefore have good reason for believing the hypothesis that all flares come from the same population to be correct.

The results of this section can now be summarised as follows:

(a). The frequency of solar flares occurring in a given spot group increases as the rate of change of spot area increases, and is independent of the direction of that rate of change.

(b). The proportions of flares occurring in the different classes are not influenced by the rate of change of spot area.

4. The latitude distribution of sunspots and their associated solar flares.

Behr and Siedentopf (36) found that the distribution of solar flares over the sun's disk closely follows the spot distribution, but no attempt was made to group the spots according to their magnetic classification. This section of the analysis will be concerned with this problem.

The importance and latitude of each flare was tabulated together with the latitude, magnetic classification, and daily corrected areas of the associated spot group. The flare and spot latitudes were grouped into class-intervals of 5^{o} and the frequency of class 1, class 2 and class 3 flares together with the total daily corrected areas for each type of sunspot occurring in each class-interval was determined. The following tables were then constructed:

TABLE 5. For all spots irrespective of magnetic classification.

Hemisphere	Latitude	Total daily Area.	Flares. Class 1	Class 2	Class 3	Total.
NORTH.	>30	16,550	4	4	0	8
	26 - 30	39,984	41	7	2	50
	21 - 25	108,504	132	35	9	176
	16 - 20	150,243	192	42	6	240
	11 - 15	198,949	213	54	5	272
	6 - 10	76,844	166	36	2	204
	1 - 5	33,240	31	5	0	36
Total.		624,314	779	183	24	986
SOUTH.	>30	1,329	13	2	0	15
	26 - 30	69,512	39	7	1	47
	21 - 25	125,760	133	29	3	165
	16 - 20	139,259	203	38	3	244
	11 - 15	226,609	252	53	5	310
	6 - 10	185,779	175	48	5	228
	1 - 5	28,768	41	7	0	48
Total.		777,016	856	184	17	1057

TABLE 6. For βp-spots.

Hemisphere	Latitude	Total daily Area.	Flares. Class 1	Class 2	Class 3	Total.
NORTH.	>30	0	0	0	0	0
	26 - 30	223	11	1	1	13
	21 - 25	55,700	36	13	3	52
	16 - 20	85,201	83	14	1	98
	11 - 15	44,918	78	24	1	103
	6 - 10	42,806	64	11	0	75
	1 - 5	9,951	11	2	0	13
Total.		238,779	283	65	6	354
SOUTH.	>30	1,329	2	0	0	2
	26 - 30	3,662	2	1	0	3
	21 - 25	30,640	47	6	0	53
	16 - 20	79,560	99	7	2	108
	11 - 15	80,806	124	26	1	151
	6 - 10	119,904	85	27	3	115
	1 - 5	15,894	22	4	0	26
Total.		331,795	381	71	6	458

TABLE 7. For β-spots.

Hemisphere	Latitude	Total daily Area.	Flares.			
			Class 1	Class 2	Class 3	Total.
NORTH.	>30	16,550	4	1	0	5
	26 - 30	129	7	0	0	7
	21 - 25	14,851	30	8	0	38
	16 - 20	4,207	28	9	0	37
	11 - 15	48,931	50	9	1	60
	6 - 10	8,274	37	7	1	45
	1 - 5	11,752	11	0	0	11
Total.		104,694	167	34	2	203
SOUTH.	>30	0	0	0	0	0
	26 - 30	8,238	8	0	1	9
	21 - 25	10,124	17	4	1	22
	16 - 20	22,085	40	5	0	45
	11 - 15	42,401	53	8	3	64
	6 - 10	22,413	28	6	1	35
	1 - 5	4,519	11	2	0	13
Total.		109,780	157	25	6	188

TABLE 8. For βf-spots.

Hemisphere	Latitude	Total daily Area.				
			Class 1	Class 2	Class 3	Total.
NORTH.	>30	0	0	0	0	0
	26 - 30	2,229	4	0	0	0
	21 - 25	1,520	12	5	0	17
	16 - 20	11,088	32	7	0	39
	11 - 15	50,387	24	8	1	33
	6 - 10	19,928	16	3	0	19
	1 - 5	0	2	0	0	2
Total.		85,152	90	23	1	114
SOUTH.	>30	0	4	0	0	4
	26 - 30	6,776	5	0	0	5
	21 - 25	1,140	3	1	0	4
	16 - 20	3,857	6	1	0	7
	11 - 15	26,889	10	3	0	13
	6 - 10	1,388	13	6	0	19
	1 - 5	1,545	1	0	0	1
Total.		41,595	42	11	0	53

TABLE 9. For $\alpha\beta$ -spots.

Hemisphere	Latitude	Total daily Area.	Flares.			
			Class 1	Class 2	Class 3	Total.
NORTH.	>30	0	0	0	0	0
	26 - 30	6,772	6	2	0	8
	21 - 25	28,660	24	3	0	27
	16 - 20	32,815	32	4	1	37
	11 - 15	27,627	21	3	0	24
	6 - 10	5,836	20	3	0	23
	1 - 5	11,537	5	2	0	7
Total.		113,247	108	17	1	126
SOUTH.	>30	0	0	0	0	0
	26 - 30	2,558	3	0	0	3
	21 - 25	2,532	4	1	0	5
	16 - 20	1,501	9	2	0	11
	11 - 15	26,780	26	12	1	39
	6 - 10	31,401	44	8	1	53
	1 - 5	1,076	5	0	0	5
Total.		65,878	91	23	2	116

The above tables give, for each type of spot group, the total daily areas and the frequency of solar flares occurring in each class-interval of 5° latitude for both the north and south hemispheres. Table 5 includes those spot groups classified as γ, $\beta\gamma$, $\alpha\gamma$ and α. The spot areas are in millionths of the solar hemisphere.

Throughout this section the latitude distribution of spots and flares are considered separately for the north and south hemispheres. Table 10 shows the mean latitude, the median latitude, the estimated standard deviation and the measure of skewness of each distribution. The latter is given by (Mean - median)/(standard deviation) and its sign gives the

direction of skewness. If a distribution is positively skewed it is skewed towards the lower latitudes. It appears that all the distributions are skewed but that, in general, the flare distributions are less skewed than the spot distributions.

Table 11 shows the frequency of flares and the total daily corrected areas for each type of spot group occurring in the north and south hemispheres. Some points of interest arise from this table. There appaars to be a preponderance of spots in the southern hemisphere when all the spots are grouped together, but when they are subdivided according to their magnetic classification we see that for types βf and αp the preponderance is in the northern hemisphere. The flare frequencies also follow this pattern.

Figures 12, 13, 14, 15 and 16 show the latitude distribution for each type of spot together with the latitude distribution of their associated solar flares. On a visual inspection of these frequency polygons it appears that when all types of spot groups are grouped together the associated flare latitude distribution closely follows the spot latitude distribution, in agreement with Behr and Siedentopf's conclusion. The flare distribution is also similar to the spot distribution for spot types β and αp. However, for spot types βp and βf there appear to be differences in the spot and flare distributions. In the case of βp-spots the flare

TABLE 10.

For spot group latitude distributions.

Type and Hemisphere.	Mean. °	Median. °	St.Deviation °	Skewness.
All types N.H.	16.29	15.60	6.70	+0.103
All types S.H.	15.32	14.33	6.76	+0.147
βp - N.H.	15.81	17.80	5.76	-0.346
βp - S.H.	13.08	12.30	5.76	+0.136
βγ - N.H.	16.28	13.80	9.00	+0.275
βγ - S.H.	14.62	13.80	6.04	+0.135
βγδ - N.H.	13.06	12.70	4.08	+0.088
βγδ - S.H.	15.66	13.80	6.27	+0.296
αp - N.H.	16.61	17.20	6.67	-0.089
αp - S.H.	11.53	10.50	4.95	+0.208

For flare latitude distributions.

Type and Hemisphere.	Mean. °	Median. °	St.Deviation °	Skewness.
All types N.H.	15.52	15.15	6.40	+0.058
All types S.H.	15.14	14.58	6.41	+0.087
βp - N.H.	14.97	14.82	5.89	+0.026
βp - S.H.	13.70	15.29	5.67	-0.281
βγ - N.H.	15.14	14.33	6.84	+0.118
βγ - S.H.	14.46	14.09	6.14	+0.060
βγδ - N.H.	15.72	15.88	5.55	-0.029
βγδ - S.H.	15.36	13.19	8.20	+0.265
αp -qN.H.	16.10	16.70	6.58	-0.091
αp - S.H.	11.58	10.50	5.12	+0.211

TABLE 11. A comparison of spot areas and flare frequencies in the two solar hemispheres.

Type of spot.	South hemisphere.		North hemisphere.	
	Total daily spot area.	Flare frequency.	Total daily spot area.	Flare frequency.
All spots.	777,016	1,057	624,314	986
βp	331,795	458	238,799	354
βγ	109,780	188	104,694	203
βγδ	41,595	53	85,152	114
αp	65,878	116	113,247	126
αγδ	150	2	242	2
βγ	18,057	48	2,857	9
γ	159,714	153	66,550	99
	50,077	39	12,783	79

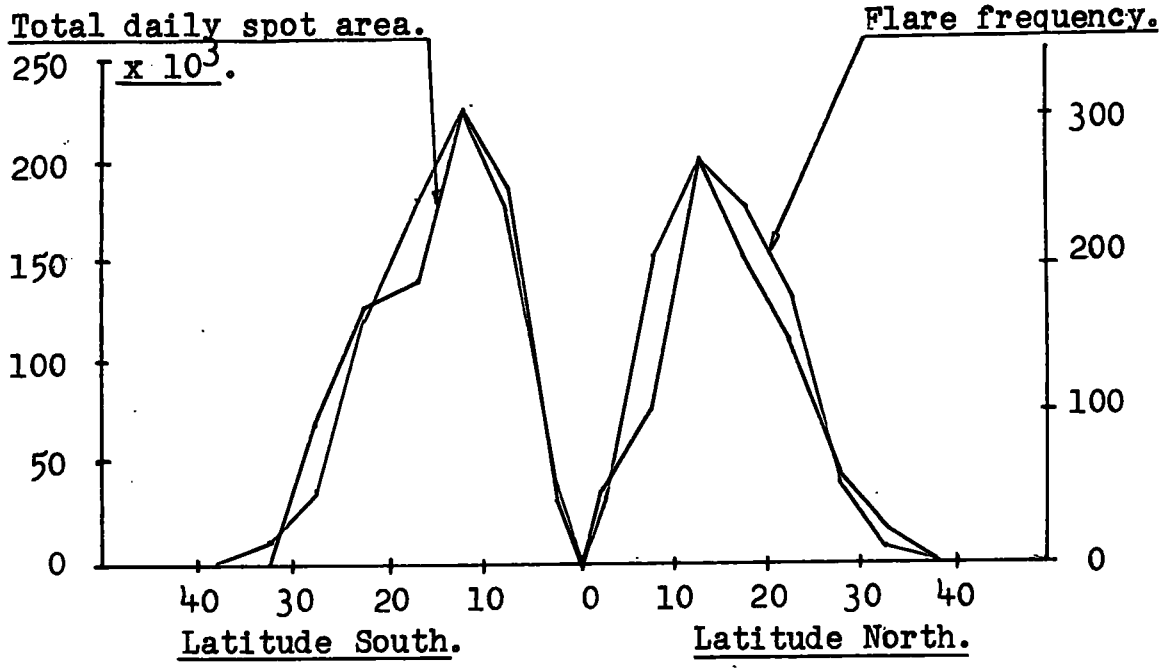

Figure 12. The latitude distribution of spot groups and associated solar flares over the solar disk. It is seen that the modes of each frequency polygon occur at the same latitudes.

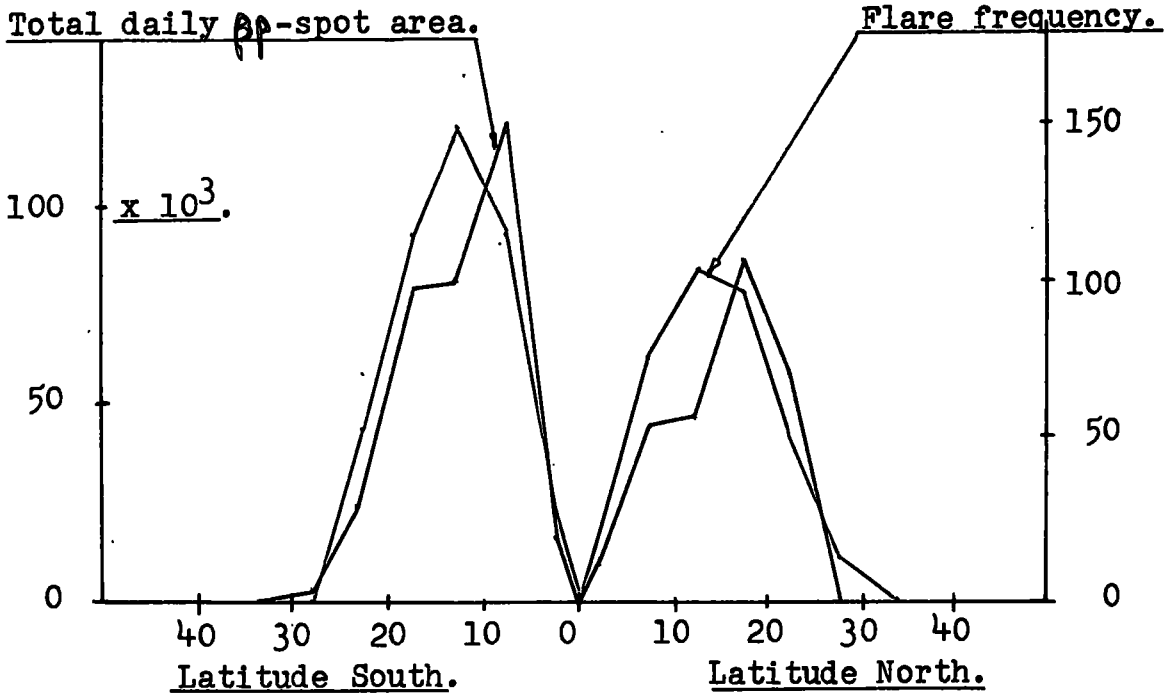

Figure 13. The latitude distribution of βp -spot groups and associated solar flares over the solar disk. The flare frequency modes are displaced to the South of the βp-spot group modes.

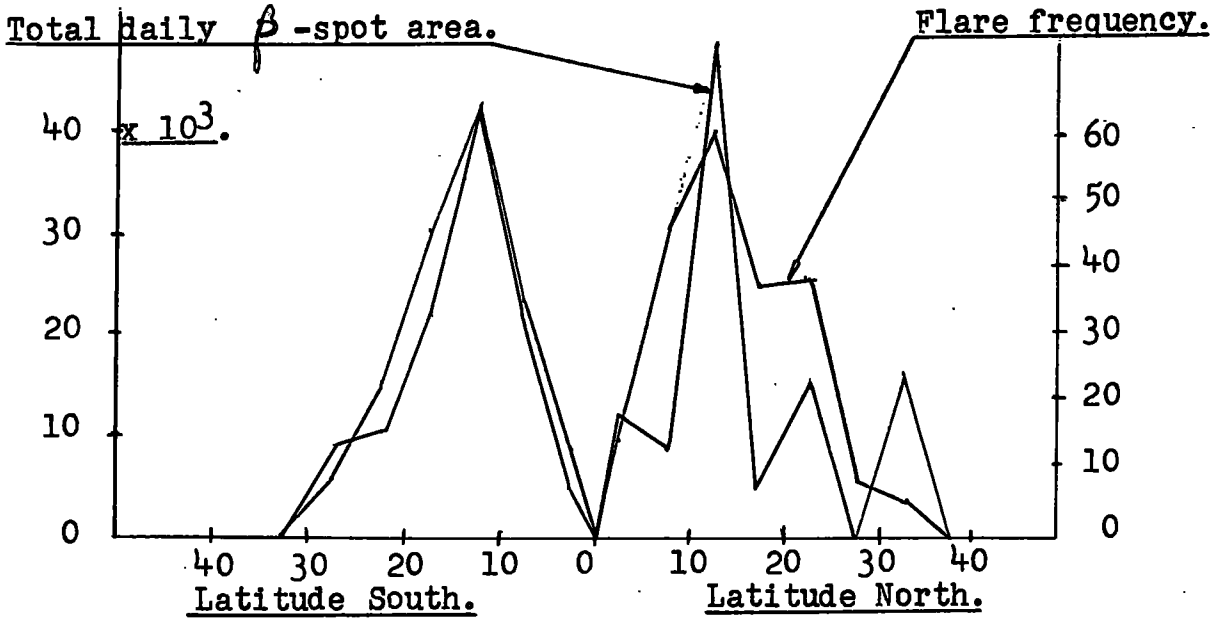

Figure 14. The latitude distribution of β-spot groups and associated solar flares over the solar disk. The flare frequency modes occur at the same latitudes as the β-spot group modes.

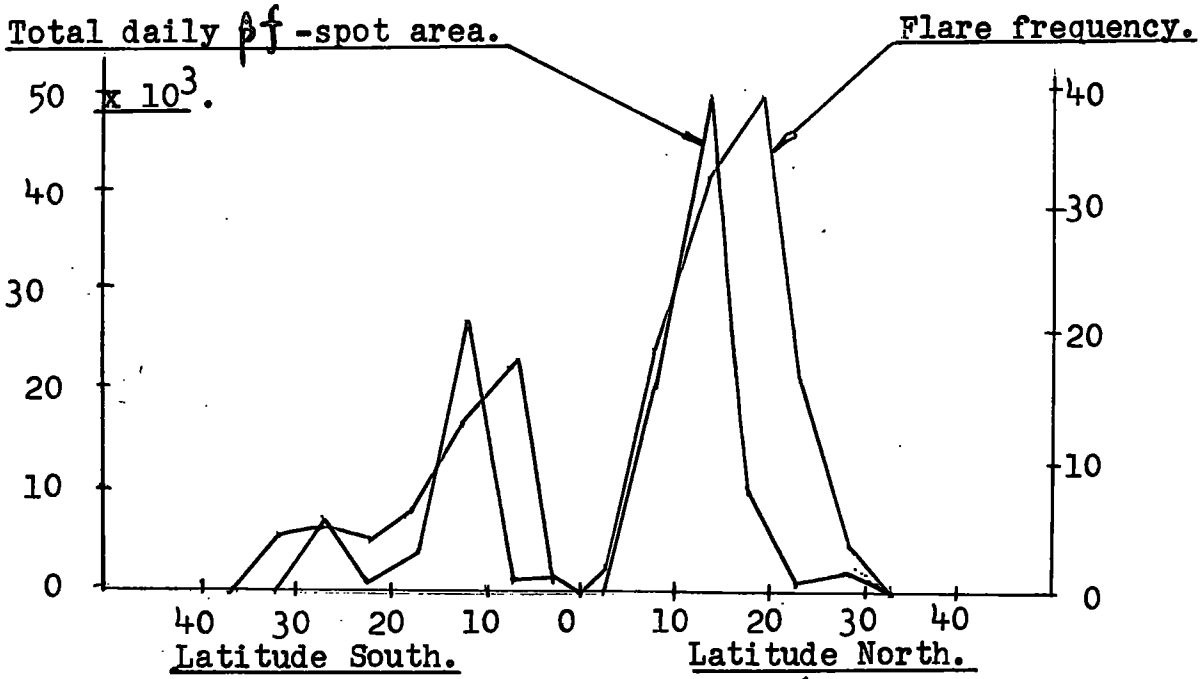

Figure 15. The latitude distribution of βf-spot groups and associated solar flares. The flare frequency modes are displaced to the North of the βf-spot group modes.

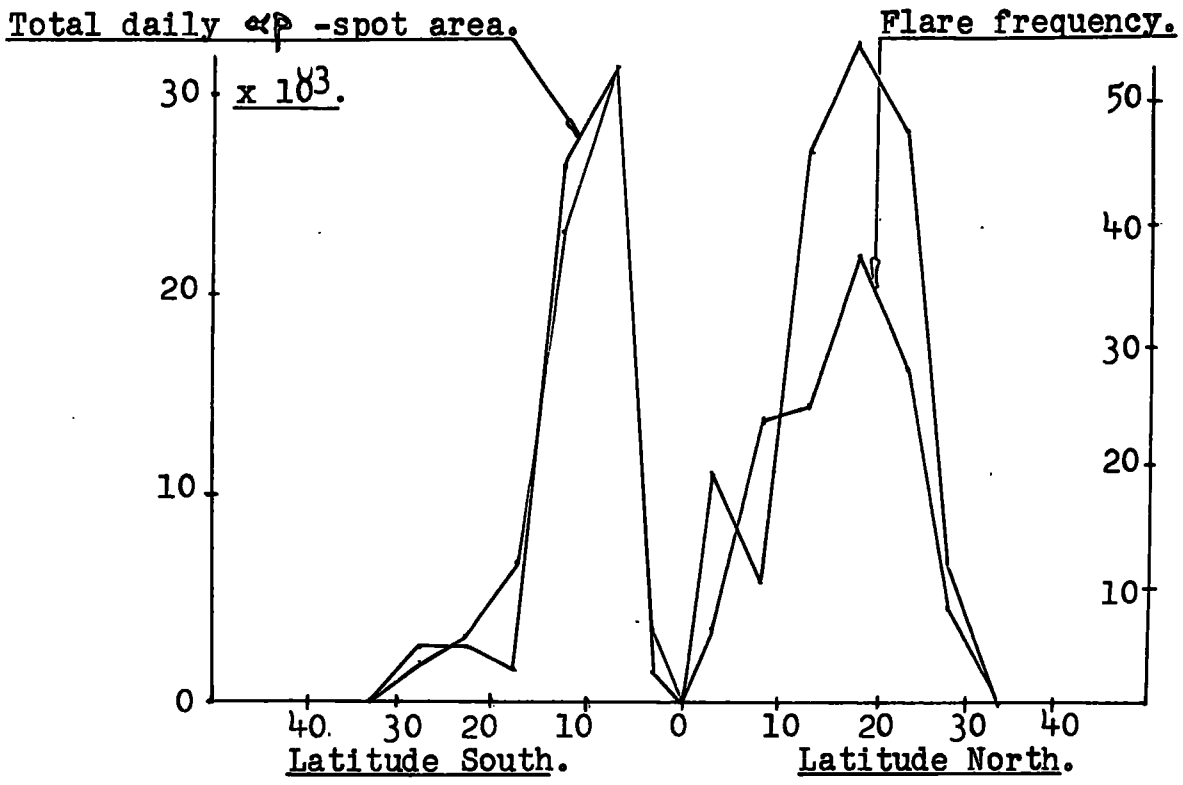

Figure 16. The latitude distribution of ∝p-spot groups and associated solarhflares. The flare and spot group modes are coincident in latitudes.

frequency modes are displaced to the South of the spot group modes, while in the case of the $\beta\gamma$-spots the flare frequency modes are displaced to the North of the spot group modes.

We may now try to answer two questions:

(1). Is there any significant difference between the latitude distribution of a particular type of spot and the latitude distribution of its associated solar flares?

(2). Is there any significant difference between the latitude distribution of the flares of class 1, class 2 and class 3 associated with each type of spot?

In the first instance we consider all spots together irrespective of magnetic classification. We have seen that, in this case, the modes of the spot distribution seem to be approximately coincident with the modes of the associated flare distribution, and we wish to test whether or not this is so. The mode, however, is an insensitive measure of central tendency and the most convenient measure for our purposes is the median. If the spot and flare distributions are the same in each solar hemisphere the median latitudes of the two distributions will coincide. The median latitude for all spots in the northern hemisphere is 15.60° showing that the total daily spot areas in the range of latitudes 15.60° to 0° is equal to the total daily spot areas in the range of latitudes $>15.60^{\circ}$. Thus, if the associated flare distribution does not differ significantly from the spot distribution, the total number of flares occurring in the latitudes on either side of 15.60°

will not be significantly different from each other.

The total number of flares which occurred in the range of latitudes 0^{o} to 15.60^{o} North was 512, and 474 flares occurred in the latitudes $>15.60^{o}$ North. The total number of flares occurring in the northern hemisphere is thus 986, and so, if our hypothesis is correct, these observed values should not differ significantly from 493, which is the expected value for both cases. The hypothesis can now be tested by means of the χ^2-test:

North Hemisphere.	15.60^{o}	15.60^{o}	Total.
Observed value.	512	474	986
Expected value.	493	493	986
$(O - E)^2/E.$	0.73	0.73	1.46

This value of χ^2 has one degree of freedom and is not significant. We conclude, therefore, that the median of the flare distribution is not significantly different from the median of the spot distribution. This answers the first of our two questions.

To answer the second question, the flares must be grouped according to their intensity. Of the 986 flares which occurred in the northern hemisphere 779 were of class 1, 183 of class 2, and 24 of class 3. Of the class 1 flares 410 occurred in the latitude range 0^{o} to 15.60^{o}, and 369 occurred in the latitude range $\geq 15.60^{o}$. Of the more intense flares, 95 class 2 and 7 class 3 occurred in the range 0^{o} to 15.60^{o},

and 88 class 2 and 17 class 3 occurred in the range $\geq 15.60^{\circ}$. In order to test whether the ratios of 410 : 95 : 7 are significantly different to the ratios 369: 88 : 17 we use the χ^2-test. The first table gives the observed values while the second table gives the expected values based on the null hypothesis that the above ratios are not significantly different. The observed values for the class 3 flares are rather low and Yate's correction for continuity has therefore been applied to them. Using the observed and expected values in these two tables we may calculate the contribution of each cell to the value of χ^2. In this case χ^2 will have two degrees of freedom.

Latitude North. Observed.	Flares. Class 1	Class 2	Class 3	Total Observed
$\geq 15.60^{\circ}$	369	88	16.5	473.5
$< 15.60^{\circ}$	410	95	7.5	512.5
Total.	779	183	24	986

Latitude North. Observed.	Flares. Class 1	Class 2.	Class 3	Total. Expected
$\geq 15.60^{\circ}$	375	87	11.5	474
$< 15.60^{\circ}$	404	96	12.5	512
Total.	779	183	24	986

The total value of χ^2 on two degrees of freedom is given by:

$$\chi^2_{(2)} = \frac{6^2}{375} + \frac{1^2}{87} + \frac{5^2}{11.5} + \frac{6^2}{404} + \frac{1^2}{96} + \frac{5^2}{12.5} = \underline{4.38}$$

This value of χ^2 does not quite reach the 10% level and so is not significant. We conclude, therefore, that there is no significant difference between the latitude distributions of class 1 flares, of class 2 flares and of class 3 flares.

For the southern hemisphere the median spot latitude is 14.33° and the χ^2-tests are as follows:

South Hemisphere.	< 14.33	≥ 14.33	Total.
Observed value	505.0	552.0	1,057
Expected value	528.5	528.5	1,057
$(O - E)^2/E$.	1.05	1.05	2.10

and for the observed distributions:

Latitude South. Observed.	Flares. Class 1	Class 2	Class 3	Total. Observed.
$\geq 14.33°$	457	85	9.5	551.5
$< 14.33°$	399	99	7.5	505.5
Total.	856	184	17	1,057

For the expected values:

Latitude South. Expected.	Flares. Class 1	Class 2	Class 3	Total. Expected.
$\geq 14.33°$	447	96	9.0	552
$< 14.33°$	409	88	8.0	505
Total.	856	184	17	1,057

The total value of χ^2 on two degrees of freedom is given by:

$$\chi^2_{(2)} = \frac{10^2}{447} + \frac{11^2}{96} + \frac{0.5^2}{9} + \frac{10^2}{409} + \frac{11^2}{88} + \frac{0.5^2}{8}$$

$$= 3.11 \text{ which is not significant.}$$

Since neither of these two values of χ^2 is significant our conclusions regarding the northern hemisphere become applicable to the southern hemisphere as well.

The spots are now grouped according to their magnetic classification and the same procedure as above is used in each case. Since the frequencies of class 3 flares are so low they have been pooled with the class 2 flares. No analysis has been made of the flares associated with spot types αf, γ, $\beta\gamma$ and α because of the meagre data. The following χ^2-tests were carried out:-

βp-spots - Northern Hemisphere.

Northern Hemisphere.	$<17.8^\circ$	$\geqslant 17.8^\circ$	Total.
Observed value.	220	134	354
Expected value.	177	177	354
$(O - E)^2/E$.	10.5	10.5	21.0

χ^2 is highly significant.

Northern Hemisphere.	Class 1	Class $\geqslant 2$	Total.
$\geqslant 17.8^\circ$	105	29	134
$<17.8^\circ$	178	42	220
Total.	283	71	354

$\chi^2 = 0.336$ and is not significant.

βp-spots - Southern Hemisphere.

Southern Hemisphere.	$< 12.3^{\circ}$	$\geqslant 12.3^{\circ}$	Total.
Observed value.	189	269	458
Expected value.	229	229	458
$(O - E)^2/E.$	7.0	7.0	14.0

χ^2 is highly significant.

Southern Hemisphere	Class 1	Class $\geqslant 2$	Total.
$\geqslant 12.3^{\circ}$	220	49	269
$< 12.3^{\circ}$	161	28	189
Total.	381	77	458

$\chi^2 = 0.930$ and is not significant.

β -spots Northern Hemisphere.

Northern Hemisphere.	$< 13.8^{\circ}$	$\geqslant 13.8^{\circ}$	Total.
Observed value.	90.0	113.0	203
Expected value.	101.5	101.5	203
$(O - E)^2/E.$	1.31	1.31	2.62

χ^2 is not significant.

Northern Hemisphere.	Class 1	Class $\geqslant 2$	Total.
$\geqslant 13.8^{\circ}$	93	20	113
$< 13.8^{\circ}$	74	16	90
Total.	167	36	203

$\chi^2 = 2.13 \times 10^{-4}$ and is not significant.

β spots, Southern Hemisphere.

Southern Hemisphere.	$< 13.8^{o}$	$\geqslant 13.8^{o}$	Total.
Observed value.	84	104	188
Expected value.	94	94	188
$(O - E)^2/E.$	1.06	1.06	2.12

χ^2 is not significant.

Southern Hemisphere.	Class 1	Class $\geqslant 2$	Total.
$\geqslant 13.8^{o}$	88	16	104
$< 13.8^{o}$	69	15	84
Total.	157	31	188

$\chi^2 = 0.215$ and is not significant.

βf-spots Northern Hemisphere.

Northern Hemisphere.	$< 12.7^{o}$	$\geqslant 12.7^{o}$	Total.
Observed value.	34	80	114
Expected value.	57	57	114
$(O - E)^2/E.$	9.3	9.3	18.6

χ^2 is highly significant.

Northern Hemisphere.	Class 1	Class $\geqslant 2$	Total.
$\geqslant 12.7^{o}$	65	15	80
$< 12.7^{o}$	25	9	34
Total.	90	24	114

$\chi^2 = 0.87$ and is not significant.

βf-spots Southern Hemisphere.

Southern Hemisphere.	$< 13.8^{o}$	$\geqslant 13.8^{o}$	Total.
Observed value.	23.0	30.0	53
Expected value.	26.5	26.5	53
$(O - E)^2/E.$	0.46	0.46	0.92

χ^2 is not significant.

Southern Hemisphere.	Class 1	Class ≥2	Total.
≥ 13.8°	26	4	30
< 13.8°	16	7	23
Total.	42	11	53

χ^2 = 2.32 and is not significant.

$\alpha\rho$-spots Northern Hemisphere.

Northern Hemisphere.	< 17.2°	≥ 17.2°	Total.
Observed value.	71	55	126
Expected value.	63	63	126
$(O - E)^2/E$.	1.02	1.02	2.04

χ^2 is not significant.

Northern Hemisphere.	Class 1	Class ≥2	Total.
≥ 17.2°	47	8	55
< 17.2°	61	10	71
Total.	108	18	126

$\chi^2 = 5.36 \times 10^{-3}$ and is not significant.

$\alpha\rho$-spots Southern Hemisphere.

Southern Hemisphere.	< 10.5°	≥ 10.5°	Total.
Observed value.	58	58	116
Expected value.	58	58	116
$(O - E)^2/E$.	0	0	0

χ^2 is obviously not significant.

Southern Hemisphere.	Class 1	Class ≥2	Total.
$\geq 10.5^{o}$	42	16	58
$< 10.5^{o}$	49	9	58
Total.	91	25	116

$\chi^2 = 2.48$ which is not significant.

To summarise these results, we find that in every case the distribution of class 1 flares is not significantly different from the distributions of the more intense flares. The distribution of flares associated with βp-spot groups is significantly differemt from the βp-spot distribution. The medians of the flare distributions are displaced to the south of the medians of the βp-spot distribution.

In the case of flares associated with βf-spots, the median flare latitude in the northern hemisphere is displaced to the north of the corresponding βf-spot median latitude. For flares associated with βf-spots in the southern hemisphere, although the flare mode appears to be displaced to the north of the corresponding βf-spot mode, there is no evidence of a significant difference in the medians of the two distributions. Of course, further observational data may make the difference significant.

Discussion and Conclusions.

The relation between the area and the magnetic field strength of a typical sunspot is given in figure 17 and it appears that the relation is not a close one. However, the magnetic flux going through a sunspot area equals $\int Hds$, where s is a surface element, and it may be concluded from figure 17 that the flux increases rapidly at first, decreases as the area during the period of constant field, and decreases rapidly during the final stages of spot decay. Thus, the magnetic flux changes as the area except in the final stage of spot decay. This final stage represents a small fraction of the total life of the spot. We may, therefore, modify the conclusions derived from the preceding statistical work by substituting the words 'magnetic flux'going through the sunspot' in place of the words 'spot area'. These conclusions may then be briefly summarised as follows:

(a). The intensity of a solar flare appears to be dependent only on the geometry of the associated sunspot magnetic field. The more complex the geometry, the greater the probability of an intense flare occurring.

(b). The frequency of solar flares occurring in a given spot group is dependent on the spot magnetic classification, the magnetic flux going through the spot, and the rate of change of that magnetic flux.

(c). In certain cases, the latitude distribution over the solar disk of flares associated with spot groups of a given magnetic classification is skewed relative to the associated spot distribution. The direction of skewness is dependent on the magnetic classification.

It is interesting to compare the more detailed results obtained from the present analysis with those obtained by R.G.Giovanelli (21) for the maximum of the previous solar cycle. The regression equation of flare frequency on associated spot area for the 18th. solar cycle was

$$F = 6.36 \times 10^{-4} A + 0.36.$$

while the corresponding regression line deduced from Giovanelli's data for the 17th. solar cycle was

$$F = 8.75 \times 10^{-4} A + 0.21.$$

The difference in the gradients of these regression lines would arise by pure chance in less than 5% of all cases and so there appears to be good evidence for saying that the average flare activity per spot group was higher during the 17th. cycle than during the 18th. cycle. The ratio of these gradients is 1.38. Now Behr and Siedentopf (36) found that there is a close statistical relation between the reduced number of flares per solar rotation, N_F, and the corresponding mean spot numbers, R. If the relation is represented in the form $N_F = \underline{a}(R - 10)$, the following mean values for $\underline{a}$ are found

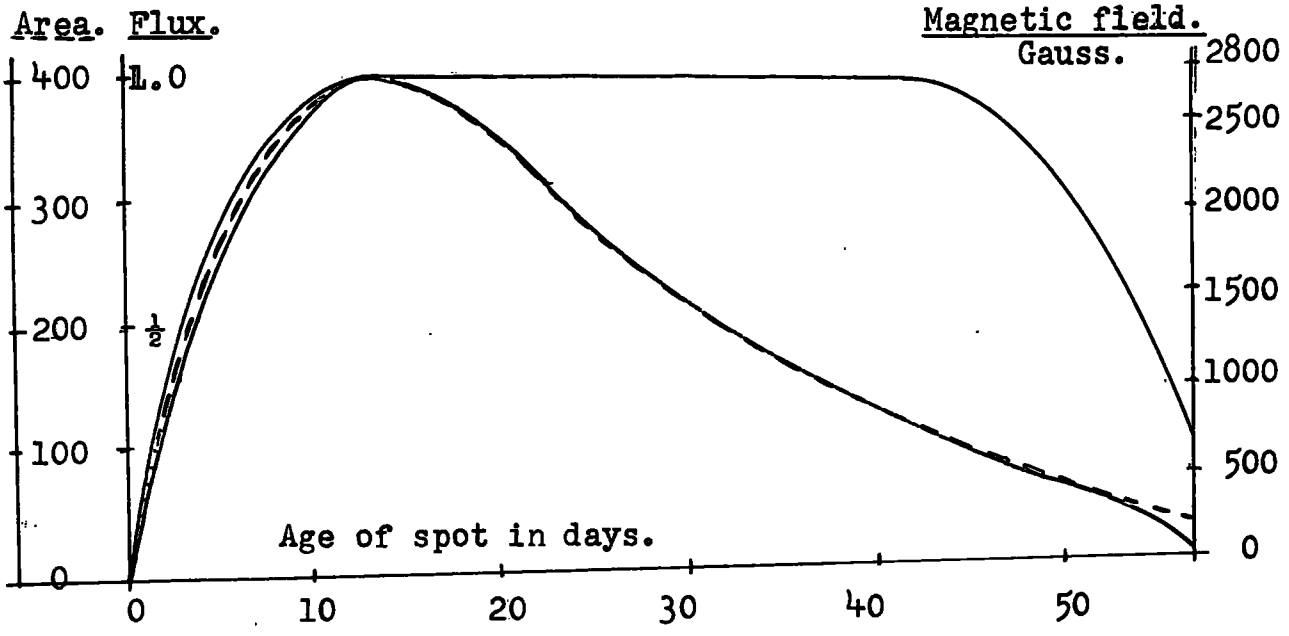

Figure 17. The relation between the magnetic field, the area and the magnetic flux going through the spot. ——— magnetic field; - - - - - - area; ———— magnetic flux. The scales have been adjusted to give the same maximum. Note how the magnetic flux is proportional to the area of the spot except after the 50th. day, when the spot is decaying rapidly.

$\underline{a}$ = 1.98 ± 0.02, (For the 17th.cycle. Maximum 1937).

$\underline{a}$ = 1.47 ± 0.02 (For the 18th.cycle. Maximum 1948).

The ratio of these two values is 1.35±0.03 and might be compared with the ratio of the gradients mentioned above.

The 18th.cycle had more spots than the 17th.cycle, but $\underline{a}$ is smaller and the flares about the same in number. Behr and Siedentopf suggested that flares may in general fluctuate less in number than spots do, and the present analysis appears to support this suggestion.

Giovanelli (21) found that the flare frequency was hardly affected by negative rates of change in spot area and small positive rates of change. This result contrasts strongly with the conclusions derived from the present analysis. However, the data available to Giovanelli concerning negative rates of change of spot area only extended to -500 millionths of the solar hemisphere per day and information regarding larger negative values would quite probably have yielded a less contrasting result. Giovanelli represented the relation between flare frequency and positive rates of change >+75 millionths of the solar hemisphere by the straight line

$$F = 2.5 \times 10^{-3} i + 0.70.$$

while the corresponding straight line obtained here is

$$F = 2.6 \times 10^{-3} i + 0.33.$$

The similarity of the two gradients is very close, and probably indicates that the dependence of flare frequency on

rate of change of spot area does not change with time.

Giovanelli also investigated the influence of the age of the spot group on flare frequency and concluded that there was a possible increase in flare activity during the final stages of spot decay. It was noted earlier that the magnetic flux going through a spot changes as the area except during this final stage where the decrease in flux was greater than the corresponding decrease in area. This appears to justify the substitution of 'magnetic flux' in place of 'area', for then the above increase in activity would be accounted for.

Behr and Siedentopf also found that the distribution of flares over the solar disk closely follows the spot distribution. However, no attempt was made to group the spots according to their magnetic classification. When this is done it is found that there are differences between the distributions of solar flares and certain types of spot groups. For example, the latitude distribution of solar flares associated with βp -spot groups is skewed to the south of the corresponding βp -spot distribution, while the latitude distribution of flares associated with βf -spots is skewed to the north of the corresponding βf -spot distribution. The distributions of flares associated with β -spots and αp-spots follow the distributions of the corresponding spot groups. If all the spots are grouped together, irrespective of magnetic

classification these differences are masked and the overall effect is one of apparent similarity.

The above differences are all consistent with the hypothesis that the sun has a general magnetic field which extends down into the sunspot zones, and the next part of this section will be concerned with this matter.

The General Magnetic Field of the Sun.

Consider a bipolar spot group situated in a general magnetic field. The geometry of the magnetic field around such a spot group is shown in figure 18. The horizontal plane represents the photosphere while the oblique plane contains two spot components L and F and the neutral point N. The points n_1 and n_2 are the traces of the limiting line of force which meets the photosphere at 90^o and passes through the neutral point N. For purposes of this discussion the topology represented in figure 18 can more conveniently be represented by the limiting lines of force passing through the points N, n_1 and n_2, as shown in figure 19. This topology can be divided up into four distinct zones. Zone A containing lines of force belonging to the general field only; zone B containing lines of force belonging to the spot group only; zone C containing lines of force entering the spot component F from the general field and zone D containing lines of force emerging from the spot component L and joinigg up with the general field.

Figure 18. The topology of the magnetic field around a bipolar spot group.

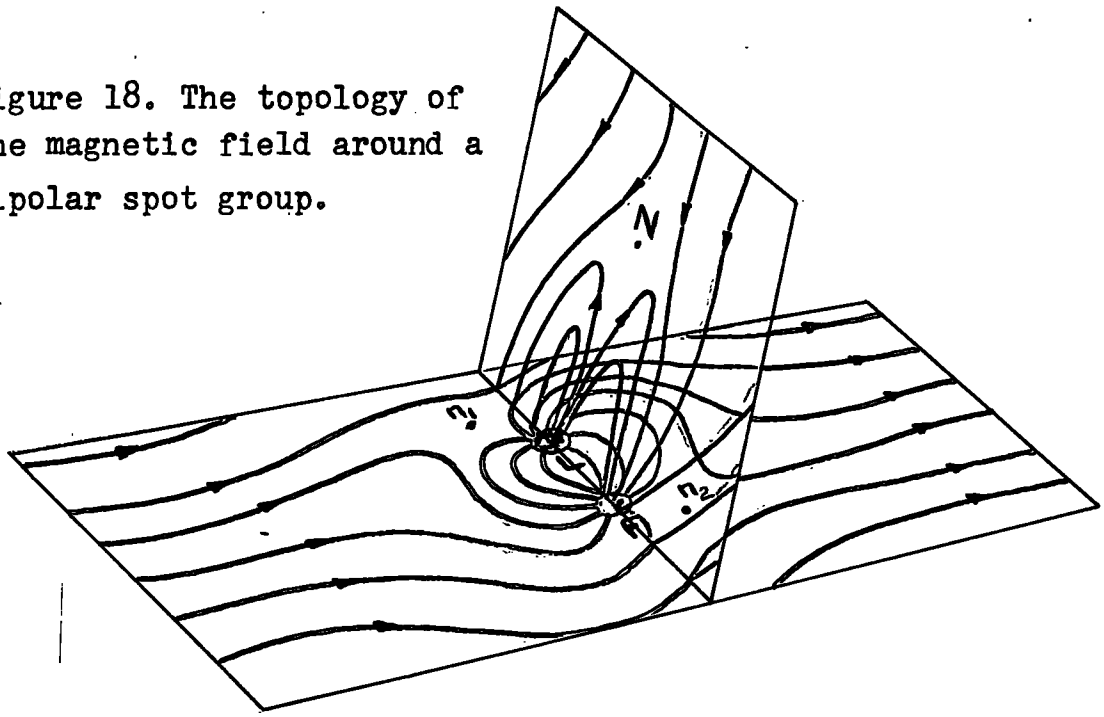

Figure 19. The topology of the magnetic field around a bipolar spot group.

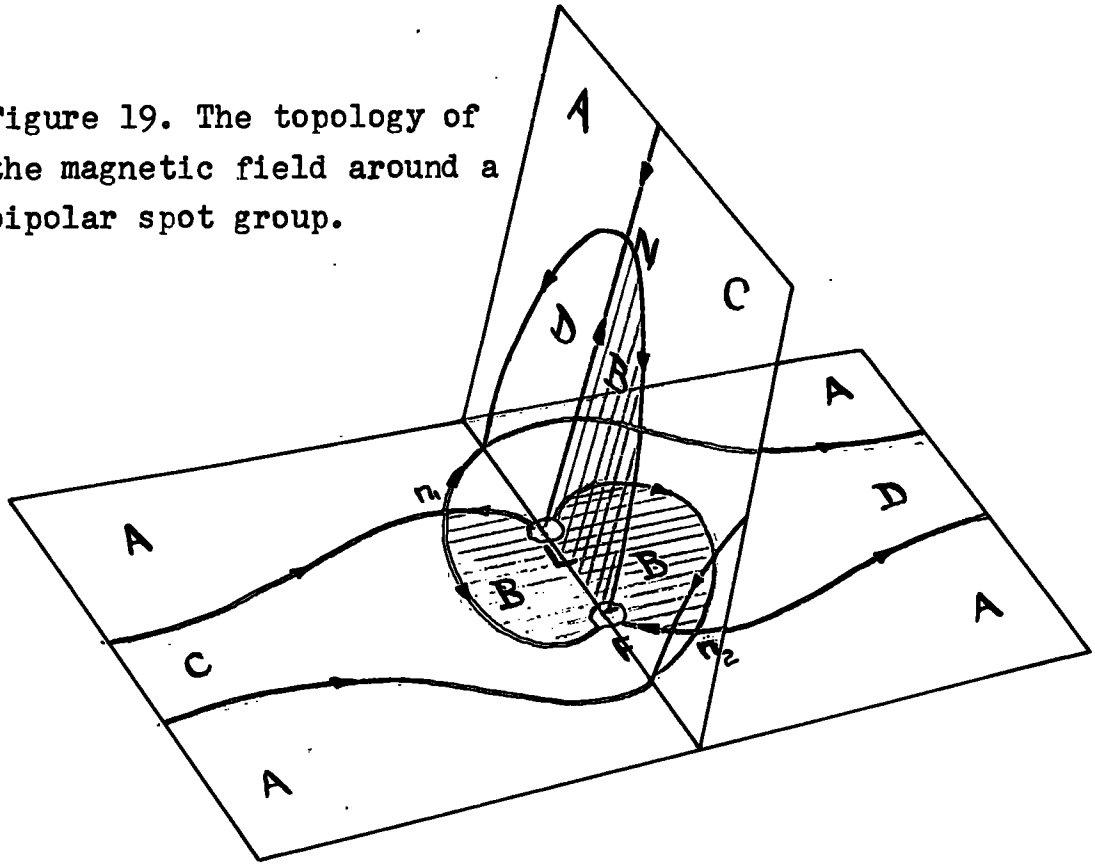

In the absence of a general field the points N, n_1 and n_2 will all be at infinity and only zone B will exist.

These four zones may be considered as tubes of force containing certain quantities of magnetic flux. The majority of bipolar spot groups are asymmetric in character and the magnetic field of one of the components usually exceeds the magnetic field of the other component. If the field strength in component L is increased then there will be an increase in the quantity of magneticflux emerging from L. All this flux must be distributed between the two zones B and D. Although the interzone boundary will be shifted the quantity of flux in zones A and C will remain unchanged. If the spot group is symmetric then the quantities of flux in zones C and D will be equal. Since an increase in the field strength of component L is accompanied by a corresponding increase in the quantity of flux in zone D, there will be more flux leaving the spot group via component L than there is entering the spot group via component F. If the field strength in component L is greater than the field strength in component F the spot group will lose more flux to the general field than it gains from the general field.

In a similar manner if component F has an increase in field strength then the corresponding increase in flux must be distributed between zones B and C. There will now be more flux entering the spot group via component F than there is leaving the group via component L and consequently the group

will have a gain in magnetic flux from the general field.

The present statistical analysis has shown that the probability of a flare occurring in a given spot group is proportional to the total magnetic flux threading the spot group. For a spot group in the presence of a general field, any relative changes in the field strengths of the spot components will be accompanied by a gain or loss of flux to the general field. Under these conditions the flux threading the two spot components will not be quite proportional to the area of the spot group. In consequence, the probability of a flare occurring in a given spot group will be either reduced or increased in proportion to the flux lost or gained to the general field.

During the 18th.solar cycle (maximum 1948) the leaders of bipolar spot groups in the northern hemisphere of the sun were of south polarity, while in the southern hemisphere they were of north polarity. The measurements of Babcock,H.W. and Babcock,H.D. (37) indicated that the polarity of the general field in the northern hemisphere was north seeking (opposite to that of the Earth). Thus, in the northern hemisphere all the leaders would lose flux to the general field and all the followers would gain flux. In the southern hemisphere the situation would be reversed. From the above arguments it is clear that βp-spot groups in the northern hemisphere will lose more flux than they gain,

while $\beta\gamma$-groups will gain more flux than they lose. In the southern hemisphere the situation would be reversed. For β-spot groups the fluxes gained and lost are equal.

Figure 20 shows the various types of spot groups in the two solar hemispheres together with their respective gains and losses of magnetic flux. If a spot group has a gain in flux from the general field its associated flare frequency will be increased. If a spot group loses flux to the general field its associated flare frequency will be decreased.

Assuming that the solar general magnetic field is strongest in the polar regions and weakest at the equator (as with the Earth) then, for a spot group in high solar latitudes the quantities of flux in zones C and D will be greater than for a similar spot group in lower latitudes nearer the equator. Thus, for a given change in field strength of one of the spot components relative to the other component, the resulting differences in the flux gained from and lost to the general field will be greater for the spot group in the high latitudes than for the group in the low latitudes. Consequently the flare frequency associated with a given spot group will be affected by the general field, and the magnitude of this effect will increase with increasing latitude. This effect will be reflected in the latitude distributions of βp-spot groups in the northern hemisphere and their associated solar flares, in that the flare distribution will be skewed

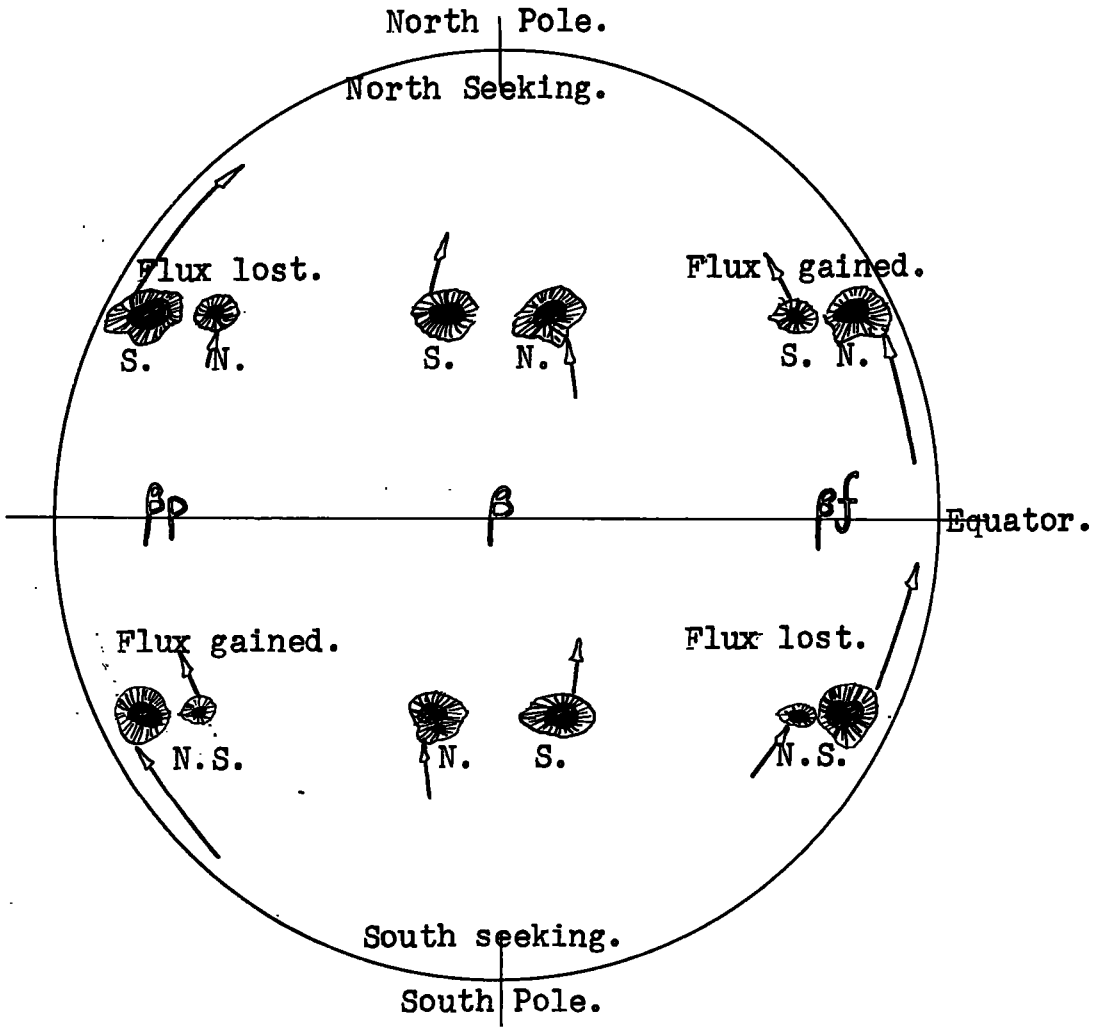

Figure 20. A diagrammatic representation of the various types of spot groups showing the quantities of magnetic flux gained and lost. (Red arrows).

toward the equator relative to the βp-spot distribution. For βf-spot groups in the northern hemisphere the flare distribution will be skewed ~~toward~~ toward the pole since the flare frequency for βf groups is increased toward the pole. The situations for βp and βf spot groups in the southern hemisphere can be predicted in a similar manner. For β -spot groups the magnetic flux threading the spot components remains unchanged with respect to the area of the spot group and so we should expect the flare latitude distribution to follow closely the corresponding β -spot latitude distribution. For unipolar spots there will also be no change in the flux entering or leaving the spot with respect to the spot area and so we should again expect the flare latitude distribution to follow closely the corresponding spot latitude distribution. This is again in accord with the results obtained for the flares associated with αp -spots.

The work of the Babcocks (37) on the measurements of magnetic fields of the sun has revealed a weak general field of about 2 gauss (component in the line of sight). The predominant magnetic polarity near the north and south poles of the sun is opposite. Their equipment utilises a large plane grating having a resolving power of 600,000 in the fifth order green and a dispersion of 11 mm./A.; a photoelectric device having two slits placed symmetrically on the wings of the chosen line where the profile is steepest. Two photomultipliers

connected to a difference amplifier are used and provision is made for scanning the solar disk and mapping the solar disk with a cathode ray tube and camera the intensity and polarity of the magnetic fields on the surface. A check on systematic errors and on the noise level of the apparatus can be made by using the magnetically unaffected line Fe λ5123.730. The root-mean-square noise level in the signal trace is of the order of one gauss.

The field seen on the above 'magnetograph' appears to be confined to latitudes greater than 55° North and South. These latitudes are well outside the spot zones where all flares occur. If the general field were, in fact, confined to these latitudes then it could have no influence on flare activity. It is quite possible that a weak general field extends down into the spot zones and is not detectable on the magnetograph because it is masked by the noise level. A statistical analysis of the type presented here may be far more sensitive to such weak fields.

The topology of the magnetic field around a bipolar spot group, as shown in figure 18, is similar to that expected for a vacuum as medium. Since the solar atmosphere is highly conducting this topology may well be questioned. How do material motions affect the topology and do the spot magnetic fields penetrate to that height where solar flares most frequently occur?

The field shown in figure 18 is the resultant of the bipolar spot field and the general field of the sun. The variation of field with height can be estimated in several ways. Using the divergence of the lines of force observed by Hale and Nicholson (38) a value of 0.5 gauss/km. is found. If one uses the differences in the Zeeman effect observed on strong and weak Fraunhofer lines the resulting gradient is 2.5 gauss/km. These estimated gradients roughly agree and indicate that the field structure is approximately that expected for a vacuum. The upper chromosphere and lower corona seems to have little influence on the field distribution overlying a sunspot. This result is confirmed by the behaviour of prominences in the neighbourhood of sunspots. The magnetic field of a spot can be propagated into the chromosphere quite rapidly provided $H^2/8\pi > \frac{1}{2}\rho v^2$ which is satisfied at all points in the solar at atmosphere in the vicinity of a spot group. Thus the solar atmosphere around a spot group is anchored in the magnetic field and keeps step with its variations. Sudden variations of the field, the occurrence of which can be concluded from prominences and flares, have to be accompanied by rapid motions in the solar atmosphere. Observation indicates that the distribution of the angles of the lines of force from a spot is roughly $\theta = 90r/b$, where r is the distance from the spot centre and b is the radius of the penumbra outer edge, and

θ is the tilt to the vertical. The magnetic field in the solar atmosphere penetrates to heights of $\sim 8 \times 10^3$ km. If we assume a field gradient of 0.5 gauss/km. then, for a 2×10^3 gauss spot the field intensity at a height of 4×10^3 km. will be of the same order as the expected intensity of the general magmetic field. Flares are most frequent in the height range $\gtrsim 4 \times 10^3$ km. With the exception of the recent theory of solar flares of Hoyle,F, and Gold,T (39) all electromagnetic theories are based on the importance of neutral points and neutral lines of the resultant magnetic field formed from the spot field and the general field. It would therefore seem to be permissable to invoke a field of about 2 gauss to explain the observed differences between the spot and flare latitude distributions since flares occur in regions of relatively weak magnetic field. Recent observational work by A.B.Severny (40) gives evidence that flares first appear at neutral points in the chromospheric magnetic field.

Concerning the asymmetric character of most spot groups, Grotrian and Kunzel (41) found that for the spot groups of the years 1918 to 1924 the mean flux through the p spots is about three times as large as that through the f spots. The average flux through a spot of average dimensions is roughly 10^{21} gauss cm^2. For asymmetric spot groups the flux from the p spots must extend over a wider region. The work of Richardson at Mt.Wilson; H.von Kluber; and the Babcocks

find evidence of outlying weak magnetic fields of about 1% of the central spot field intensity and opposite in polarity. These weak fields can be detected to about 5 or 6 spot diameters from the spot group centre. The arrangement of chromospheric elements in the vicinity of a spot group closely resembles that of iron filings near the poles of a magnet. Richardson (42) found that this arrangement could not be understood on the basis of the coriolis force. The structure must be due to the magnetic character of the group.

H.D.Babcock (43) found that the geheral magnetic field of the sun reversed polarity between 1956 and 1958. His results show that at the time of sunspot maximum the polar field was zero. It has tacitly been assumed, on the basis of these observations, that the solar general field will reverse polarity at every sunspot maximum. The very fact that the field reversed in such a short time provides good support for this assumption, for Cowling (44) has shown that the life of a dipolar solar general field should be of the order of 10^{10} years. This forces the conclusion that the structure of the field is not strictly dipolar in the sense that it penetrates through the deep interior of the sun, the field must exist only in the surface layers for otherwise a rapid reversal of polarity is impossible. Nevertheless, the structure of the field above the sun's surface has the character of an approximately dipolar field with its axis probably parallel to the sun's rotational axis. C.W.Allen (45) has proposed that the general field might

be closely associated with the fields of sunspots, its character being dictated by the pattern of the sunspot cycle. The model adopted by Allen is a modification of the hydrodynamical circulatory system of V.Bjerknes (46), with the vortices replaced by toroidal magnetic strands. These strands lie below the solar surface, but occasionally are forced up here and there and break through the surface to form bipolar spot groups. (See figure 21).

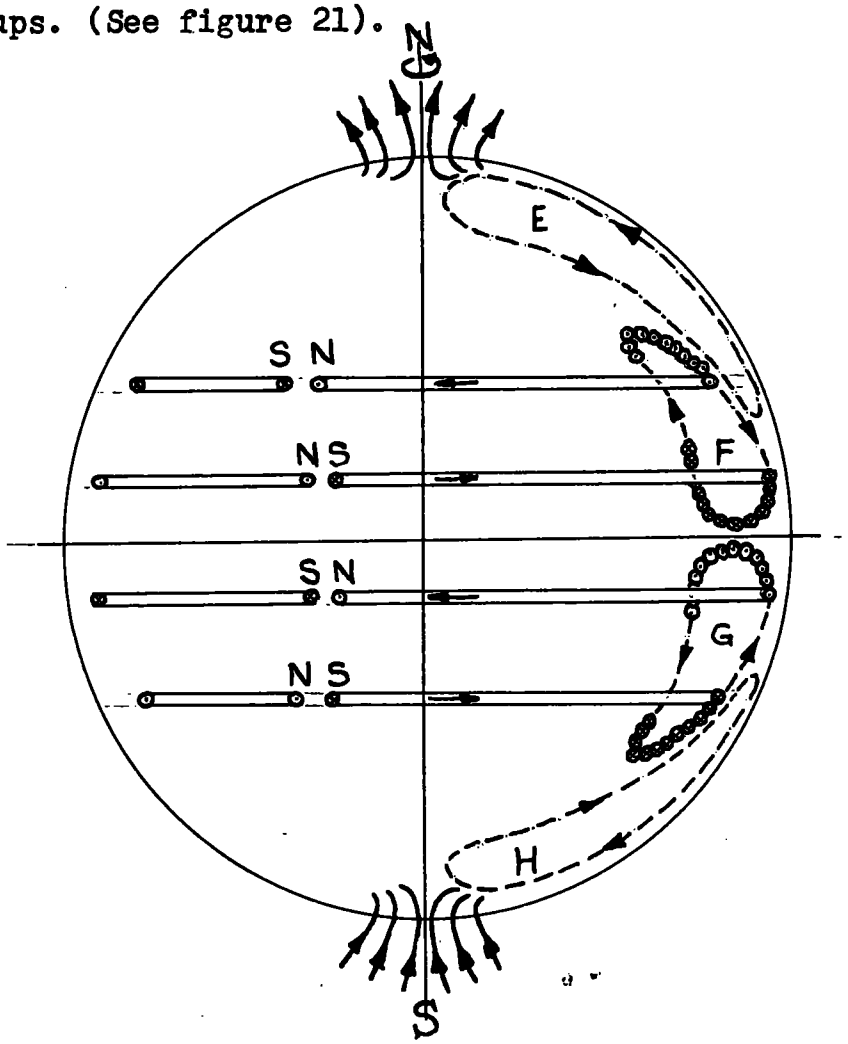

Figure 21. Circulation and magnetic fields during 1954. Movements are represented by broken lines and magnetic fields by continuous lines. The strands extending to the left are near the surface.

Following M.Waldmeier (47), Allen includes a circulation in the opposite direction in the higher latitudes. It has been noticed that towards sunspot maximum there is some latitudinal segregation of the magnetic polarity in the sunspot zones in the sense that the polarity of leading spots is usually nearer the equator. Allen proposes that, under these conditions, the high latitude circulation will tend to carry an excess of surface from the following spots bearing their polarity. This indicates that the 'general field' in the latitudes immediately higher than the spot zones will have the same polarity as the following spots in that hemisphere. At some latitude between the spot zone and the pole the field will be zero due to the neutralisation of the 'general field' set up by the previous sunspot cycle. As the sunspot activity increases this latitude of neutralisation advances towards the pole, until, at the period of maximum activity the actual polar field becomes zero. During the subsequent decline in activity the new 'general field' begins to build up.

The point at issue here is that there will be a magnetic interaction between the spot fields and the 'general field' prevalent in the latitudes immediately higher than the spot zones. The polarity of this 'general field' will be the same as that of the following spots of the bipolar groups in that hemisphere. The interaction will be strongest for those spots which appear in the highest latitudes.

The period covered by the data used in this

analysis included the period of maximum activity in 1947 during which there was probably a reversal of the general field. However, if the model of C.W.Allen is correct the polarity in the latitudes immediately higher than the spot zones would always be the same as the following spots in that hemisphere. During the period considered the polarity of the following spots in the northern hemisphere was north and so the general field in the latitudes above the northern spot zone would also be of north polarity. In the southern hemisphere the situation would be reversed. This pattern of polarities is still in accord with that used in the explanation of the latitude displacements given earlier, and even if a reversal of the polar field did take place that explanation would still be valid.

So far, no explanation has been given for the sudden drop in flare frequency associated with a rate of change of spot area of about 750 millionths of the solar hemisphere per day. (See figures 7, 8, 9 and 10). Obviously, the visible flare must be due to the excitation of hydrogen atoms by electrons which have been accelerated in the chromosphere overlying a spot group. Observational evidence (48) shows that flares tend to occur repeatedly in the same locations relative to a spot group. This indicates that flares occur repeatedly along the same paths in the magnetic field. The flare frequency is proportional to the rate of change

of spot area or magnetic flux, but eventually a stage will be reached when the flares are so frequent and the induced electric fields so great that all the hydrogen atoms lying along the f favourable flare paths will be in an ionised state. When this condition is reached no visible flare can occur. However, there will be an outburst at radio frequencies and this may account for some of the radio outbursts which have no visible counterpart.

Flare Theories.

Of the phenomena that occur in the solar atmosphere, flares are perhaps the most complex. They are connected with the greatest amounts of energy and with the greatest range of associated observable effects. The physical conditions existing in that part of the solar atmosphere where flares are known to occur are practically incognito. We cannot, therefore, expect any theoretical interpretation of the flare phenomenon to yield a good explanation of all the events which are usually associated with flares. However, any acceptable theory must account for the enormous energy storage in the solar atmosphere preceding the flare and the suddenness with which this energy is released during the flare. All flares are associated with sunspots and all sunspots are accompanied by strong magnetic fields. An electromagnetic interpretation of flares immediately suggests itself. Such an interpretation is made more attractive since there is no visible material motions into the flare region, all evidence suggests that flares suddenly appear without any warning. Recent theoretical and observational

work by A.B. Severny (40) has gone far towards demonstrating the correctness of such an interpretation. The preceding analysis also adds support to this suggestion.

It is obviously important that any theory should not be inconsistent with observation. The conclusions derived in the statistical analysis were obtained directly from observational data and will therefore play an important role in deciding which theories are the most acceptable. The possibility of electric discharges in the solar atmosphere has been considered by R.G.Giovanelli (49), F.Hoyle (35), C.E.R.Bruce (50), F.Hoyle and T.Gold (39), and others.

Giovanelli's explanation of a solar flare is, briefly, as follows. A fast electron will lose relatively little of its excess energy in an elastic collision with an ion. This is because of the relatively small mass of the electron. When electrons move in an electric field they will gain extra energy from this field between collisions. If the electrons gain energy from the electric field faster than they lose it in collisions, they may easily acqire energies very much greater than the thermal energies of the ions.

We have seen that the electron-proton collision frequency, ν , is given by $\nu = 15 n_e T^{-3/2}$ and so ν decreases with increasing temperature..The temperature to be considered here is the electron temperature. Thus, the electric field produces increased electron energies and this leads to a decrease

in the electron-proton collision frequency and hence to a decrease in the rate of loss of energy at collisions. If the electric field is big enough, the electron energies may increase without limit, and the resulting enhanced conductivity leads to something like an electric discharge. Giovanelli found that the condition for 'runaway electron energies' can be represented by

$$\frac{m_i e^2 E^2}{2m_e^2 a^2 n_i^2} > \frac{4}{27 W_i^2}.$$

where m_i, m_e are the masses of hydrogen ions and electrons respectively, W_i is the mean thermal energy of the ions, e is the electronic charge in e.m.u., E is the electric field due to the changing magnetic flux of the sunspot, n_i is the ion density per c.c., and

$$a = \gamma W_e^{3/2}/n_i.$$

where W_e is the mean energy of the electrons. If the hydrogen ions are at thermal energies corresponding to 5750°K, this condition gives $E > 1.5 \times 10^{-6} n_i$ e.m.u. If n_i is taken as $\sim 10^{11}$ then $E > 1.5 \times 10^{5}$ e.m.u.

According to this theory electrons cannot acquire 'runaway' energies unless the electric field exceeds a certain critical value. The electric field is governed by the changing magnetic flux of the spot group. The flux is proportional to the area of the spot group. Figures 7, 8, 9, and 10 show no indication of any such critical stage.

The electrons gain energy from the electric field and, when a state of quasi-stability is reached, the rate of

emission by the whole flare must equal the rate at which the electrons gain energy from the electric field. Thus the intensity of the flare will be governed by the magnitude of the electric field. Accordingly we should expect the flare intensity to increase with increasing rate of change of spot area, but no evidence of this could be found in the preceding statistical an analysis.

F.Hoylé's theory of the origin of solar flares is a modification of Giovanelli's theory and will suffer from the same objections. The most favourable place for the electrons to acquire 'runaway' energies is near to the neutral points in the magnetic field where the electric field will be largest. This region can therefore be designated as the accelerating region. Hoyle takes the characteristic dimension, b, of this region as 100 km. and arrives at the following expression for the average emission from the flare:

$$(n_e e^{3/2} b^{7/2} |E|)/m_e^{\frac{1}{2}} . A \quad \text{ergs.cm.}^{-2}.\text{sec.}^{-1}.$$

where A is the area of the flare. Unfortunately this formula is incorrect, as can be seen from the following simple argument:

Consider an electron situated at the edge of the accelerating region. The electric field E will cause this electron to be accelerated at a rate eE/m_e and the time taken for it to cross the accelerating region will be $(2bm_e/eE)^{\frac{1}{2}}$ secs.

Thus the rate at which the electric field does work on the electron is $eEb(eE/2bm_e)^{\frac{1}{2}}$. The total number of electrons in the accelerating region is $n_e b^3$, and so the rate at which the electric field E does work is $n_e eEb^4(eE/2bm_e)^{\frac{1}{2}}$ or $(n_e e^{3/2} b^{7/2} |E|^{3/2})/(2m_e)^{\frac{1}{2}}$ ergs./sec.

If A is the area of the flare the average emission will be $(n_e e^{3/2} b^{7/2} |E|^{3/2})/A(2m_e)^{\frac{1}{2}}$ ergs./cm^2./sec. . . . (i).

This formula differs from Hoyle's by a factor of $(E/2)^{\frac{1}{2}}$, and, furthermore, Hoyle's formula does not appear to be dimensionally correct.

If A is about 1% of the solar disk ($\sim 10^{20}$ cm^2) formula (i) gives an emission of 4.7×10^5 ergs./cm^2./sec. which would yield a total emission in 10^3 secs of 4.7×10^{28} ergs. Since the energy liberated by a normal flare is $>10^{30}$ergs it would seem that this value is far too low. In any case, the flare intensity is proportional to $|E|^{3/2}$ and so should increase as the rate of change of spot area increases. This is contradictory to the conclusions derived from the statistical analysis.

C.E.R.Bruce considered the flare phenomenon as analogous to terrestrial lightening. The short-lived broadening of the Balmer emission lines would then arise through the Zeeman effect. Bruce, making extrapolations for the

parameters involved from those observed in laboratory discharges, determined the current carried by the flare discharge as being of the order of 10^{14} amps, giving rise to magnetic fields of about 10^5 gauss. These fields are of the required order of magnitude to explain the splitting of the Hα line on the basis of the Zeeman effect. However, no comparable broadening has been observed in the emmission lines of iron, calcium and silicon, and there appears to be no other observational evidence of fields greater than about 10^3 gauss in flare regions.(51). Again, the terrestrial atmosphere where lightening discharges occur is non-conducting, allowing the accumulation and separation of charge. The solar atmosphere, on the other hand, is highly conducting making any charge separation impossible.

Recently, F.Hoyle and T.Gold have introduced a new theory for the origin of solar flares. According to this theory high concentrations of energy can gradually be built up in the chromosphere overlying sunspots. The energy storage can be accounted for by a particular class of magnetic fields whose lines of force have the general shape of twisted loops protruding above the photosphere. In a highly conducting atmosphere like the chromosphere and lower corona the motions of the material are such that at each moment a force-free field is obtained compatible with the magnetic boundary conditions at the photosphere and, with the past history of

the motion. Thus, in regions with strong magnetic fields, the chromospheric motions are probably entirely dictated by the flow of the much more massive photospheric material. Magnetic energy is gradually fed into the chromosphere as a consequence of events that take place at and below the photosphere. A sudden release of the energy in such a system can result only in a case where the magnetic forces act so as to drive the system away from its force-free configuration. The stored magnetic energy can then be dissipated into motion and heat. This will occur when twisted magnetic loops of opposite sense and twist meet. Such loops attract each other, and the annihilation of the longitudinal component of the field where they meet leads to a sudden constriction of the current and through this to a dissipation of the energy associated with that current. This condition will occur quite rarely limiting flares to their observed rate of occurrence. Normally the energy storage process can proceed without hindrance. The intensity of the flare will be dependent on the time that the energy storage has been allowed to proceed.

The frequency of flares associated with a particular spot group will depend on the number and movement of the magnetic loops postulated above. The larger the spot group the more magnetic loops, and hence the greater the probability of

a flare occurring in that spot group. If the area of a spot group is changing these magnetic loops will be moving relative to each other within the confines of the spot group, and the above conditions will occur more frequently. It might be argued that if flares become more frequent within a spot group the time allowed for the energy storage must be reduced and intense flares must become more rare. However, although flare frequency is proportional to spot area the number of flares of any class occurring per unit area of spot remains constant. The frequency of flares occurring per unit of spot area alters only if the area of the spot group as a whole alters. If the area of the spot changes rapidly the frequency of solar flares associated with that group is large, but, although the time allowed for the energy storage is reduced the amount of movement and other activity taking place at and below the photosphere must be necessarily greater and larger quantities of energy will be fed into the chromosphere. The two effects merely cancel each other out.

Thus, the theory of Hoyle and Gold seems to be much more in accord with the results of the statistical analysis than are the other electromagnetic theories.

The above criticisms of the theories of solar flares are not exhaustive; this work is not meant to be a critical study but to create more implements of criticism built up from observational rather than theoretical evidence.

The principal feature of this work is the statistical analysis and the results that have been obtained directly from it. An attempt has been made to translate these results into a more suitable 'electromagnetic' form. The conclusion that the intensity of a solar flare is independent of its position on the solar disk, the quantity of magnetic flux associated with the spot group, and also the rate of change of that flux, should prove a powerful tool for criticism and may hold a vital clue for the correct interpretation of the flare phenomenon.

The interpretation of the relative displacements of the various spot and flare latitude distributions in terms of a magnetic interaction between the flare, the spot magnetic field, and the 'general field', appears to be very attractive. If this interpretation is correct, similar statistical analyses carried out for different periods of sunspot activity should prove of great value. Firstly, they will yield more information on the behaviour of the general field especially as regards the pattern of the reversal in polarity; and secondly, they will tell us how the relations between flares, spots, and the general field change with time. To this end the analysis has been carried out so that detailed statistical comparisons may be made whenever any future, similar, work is carried out on data covering a different period.

Acknowledgment.

I am grateful to Dr.W.A.Prowse of the Physics Department, University of Durham, for his advice and encouragement in the course of this work.

Note.

P.A.Sweet (Nuovo Cimento, Supp.8.,Ser.10, 188, 1958) has also suggested a mechanism for the origin of solar flares very similar to that given by F.Hoyle and T.Gold, but with the emphasis on the production of high energy particles. Sweet's interpretation of the flare phenomenon is a modification of the neutral point theories of Hoyle and Giovanelli. He considers an isolated sunspot group having four components arising from flux tubes protruding through the photosphere. In this system two neutral points must occur. When the flux tubes are in relative motion a voltage drop occurs down the limiting line of force connecting the two neutral points. This voltage drop is sufficient to produce cosmic ray particles of 10^{10}e.V. if the relative velocities of the flux tubes are of the order of 10 Km./sec. Such high velocities might well arise from hydromagnetic waves travelling from below the photosphere upwards along the flux tubes and into the chromosphere. Further papers on the above mechanism are being published by Sweet.

REFERENCES.

For convenience, two lists of references have been compiled. The first list gives the references in the same order as they appear in the text, while the second list has been arranged alphabetically according to author.

List 1.

1. Ellison,M.A. 1949. M.N.R.A.S., 109, 3.
2. Dodson,H.W. 1953. The Sun, Ed.Kuiper,G.P., Chicago Univ.Press. p.698.
3. Giovanelli,R.G. & McCabe,M.K. 1958. J.Austr.Phys., Vol.II.,No.2., 191.
4. Newton,H.W. 1942. M.N.R.A.S., 102, 22.
5. Bracewell,R.N. & Straker,T.W. 1949. M.N.R.A.S., 109, 28.
6. Chubb,T.A. et al. 1957. J.Geophys.Res.,Vol.62, No.3, 389.
7. Newton,H.W. & Jackson,W. 1951. 7th.Report of the Commission for the study of Solar-terrestrial relations. (Paris: Hemmerle, Petit & Co.) p.107.
8. Brunt,Sir D., 1960. Proc.I.E.E.,Vol.106. Part B,No.29, 437.
9. Gartlein,W. 1950. Internat.Union of Geodesy and Geophys. Trans.Oslo Meeting IATME Bull. No.13 Washington p.491.
10. Meinel,A.B. 1950. Ap.J.,111, 555.
11. Forbush,S.E. 1946. Phys.Rev.,70, 771.
12. Lord,J.J. et al. 1950. Phys.Rev.,79, 540.
13. Payne-Scott,R; Yabsley,D.E. & Bolton,J.G. 1947. Nature, 160, 256.

14. Wild,J.P., Murray,J.D.,& Rowe,W.C. 1953. Nature, 172, 533.

15. Wild,J.P. Vistas in Astronomy, Vol.1.,p.573.

16. Davies,R.D. 1954. M.N.R.A.S., 114, 74.

17. Ellison,M.A. 1949.. M.N.R.A.S., 109, 3.

18. Hunter,A., 1943. Repts.on the Progress in Phys, Vol.IX.

19. Giovanelli,R.G. 1948. M.N.R.A.S., 108, 163.

20. Kiepenheuer,K.O.1953. The Sun, Ed.G.P.Kuiper, p.376, Chicago Univ.Press.

21. Giovanelli,R.G. 1939. Ap.J., 89, 555.

22. Allen,C.W. 1940. M.N.R.A.S., 100, 635.

23. Ellison,M.A.& Conway,M. 1950. Observatory, 70, 77.

24. Bruck,H.A. & Ruttlant,F. 1946. M.N.R.A.S., 106, 130.

25. Richardson,R.S. & Minkowski,R. 1939. Ap.J., 89, 347.

26. Akabane,K & Atanaka,T. 1957. Nature, 180, 1062 - 3.

27. Gartlein,W. 1950. Internat.Union of Geodesy and Geophys. Trans.Oslo Meeting IATME Bull.No.13 Washington p.491.

28. Meinel,A.B. & Fan,C.Y. 1952. Ap.J., 115, 330. and 1953. Ap.J., 118, 205.

29. Harang,L. 1951. The Aurora, New York: John Wiley & Sons Inc.

30. Warwick,C.S. 1955. Ap.J., 121, 385.

31. Nonweiler,T. 1958. Nature, 182, 468.

32. Van de Hulst,H. 1953. The Sun, Ed.G.P.Kuiper, p.223, Chicago Univ.Press.

33. Cowling,T.G. 1945. Proc.Roy.Soc.,183A, 453.

34. Dungey,J.W. 1958. Cosmic Electrodynamics. (Cambridge).

35. Hoyle,F. 1949. Some Recent Researches in Solar Physics, (Cambridge).

36. Behr,A & Siedentopf,H. 1952. Zs. f. Ap., 30, 177.

37. Babcock,H.W. & Babcock,H.D. 1955. Ap.J., 121, 349.

38. Hale,G.E. & Nicholson,S.B. 1938. Magnetic Observations of Sunspots, 1917 to 1924. (Washington: Carnegie Institution), Part I, p.56.

39. Hoyle,F & Gold,T. 1960. M.N.R.A.S., 120, 89.

40. Severny,A.B. 1958. Pub. Crimean Astr. Obs., 20, 22.

41. Grotrian,W. & Kunzel,H. 1950. Zs. f. Ap., 28, 28.

42. Richardson,R.S. 1940. Pub.A.S.P., 52, 282.

43. Babcock,H.D. 1959. Ap.J., 130, 364.

44. Cowling,T.G. 1953. The Sun, Ed.G.P.Kuiper, p.545, (Chicago Univ.Press).

45. Allen,C.W. 1960. Observatory, 80, 94.

46. Bjerknes,V. 1926. Ap.J., 64, 93.

47. Waldmeier,M. 1955. Ergebnisse und Probleme der Sonnenforschung, 2nd.Ed., p.198.

48. Dodson,H.W. 1949. Ap.J., 110, 382.

49. Giovanelli,R.G. 1947. M.N.R.A.S., 107, 338.
1948. M.N.R.A.S., 108, 163.
1949. Phil.Mag.,40, 206.

50. Bruce,C.E.R. 1948. Brit.Elec.& Allied Ind.Res.Assn., Report Ref. L/T204. The Origin of Solar Noise.

51. Von Kluber,H. 1947. Zs. f. Astroph., 24, 1.

List 2.

Allen,C.W. 1940. M.N.R.A.S., 100, 635.
1960. Observatory, 80, 94.

Akabane,K.,& Atanaka,T. 1957, Nature, 180, 1062 - 3.

Babcock,H.D. 1959, Ap.J., 130, 364.

Babcock,H.W. and Babcock,H.D. 1955, Ap.J., 121, 349½

Behr,A. and Siedentopf,H. 1952, Zs. f. Ap., 30, 177.

Bjerknes,V. 1926, Ap.J., 64, 93.

Bracewell,R.N. and Straker,T.W. 1949, M.N.R.A.S., 109, 28.

Bruce,C.E.R., 1948, Brit.Elec. & Allied Ind.Res.Ass., Report Ref. L/T204. The Origin of Solar Noise.

Bruck,H.A. and Ruttlant,F. 1946, M.N.R.A.S., 106, 130.

Brunt, Sir D. 1960. Proc.I.E.E., Vol.106. part B. No.29. p.437.

Chubb,T.A. et al. 1957,+ J.Geophys.Res., Vol.62, No.3. 389.

Cowling,T.G. 1945, Proc.Roy.Soc., 183A, 453.
1953, The Sun, Ed.G.P.Kuiper. p.545. (Chicago).

Davies,R.D. 1954, M.N.R.A.S., 114, 74.

Dodson,H.W. 1953, The Sun, Ed.G.P.Kuiper. p.698. (Chicago).
1949, Ap.J., 110, 382.

Dungey,J.W. 1958, Cosmic Electrodynamics. (Cambridge).

EllisonM.A. 1949, M.N.R.A.S., 109, 3.

Forbush,S.E. 1946, Phys.Rev., 70, 771.

Gartlein,W. 1950, Internat. Union of Geodesy and Geophys. Trans. Oslo Meeting IATME Bull. No.13. Washington.p.491

Giovanelli,R.G. 1939, Ap.J., 89, 555.
1947, M.N.R.A.S., 107, 338.
1948, M.N.R.A.S., 108, 163.
1949, Phil.Mag., 40, 206.

Giovanelli,R.G. and McCabe,M.K. 1958, J.Austr.Phys., Vol.II, No.2., 191.

Grotrian,W. and Kunzel,H. 1950, Zs. f. Ap., 28, 28.

Hale,G.E. and Nicholson,S.B. 1938, Magnetic Observations of sunspots, 1917 to 1924. Washington: Carnegie Inst. Part 1, p.56.

Harang,L. 1951, The Aurora, New York: John Wiley & Sons Inc.

Hoyle,F. 1949, Some Recent Researches in Solar Physics, Cambridge.

Hoyle,F. and Gold,T. 1960, M.N.R.A.S., 120, 89.

Hunter,A., 1943, Repts. on the Progress in Physics, Vol.IX.

Kiepenheuer,K.O., 1953, The Sun, Ed.G.P.Kuiper. p.376. Chicago.

Lord,J.J. et al., 1950, Phys.Rev., 79, 540.

Meinel,A.B. 1950, Ap.J., 111, 555.

Meinel,A.B. and Fan,C.Y. 1952, Ap.J., 115, 330.
1953, Ap.J., 118, 205.

Newton,H.W. 1942, M.N.R.A.S., 102, 2.

Newton,H.W. and Jackson,W. 7th. Report of the Commission for the study of Solar-terrestrial relationships p.107. (Paris: Hemmerle, Petit & Co.)

Nonweiler,T. 1958, Nature, 182, 468.

Payne-Scott,R., Yabsley,D.E. and Bolton,J.G. 1947, Nature,160,256.

Richardson,R.S. 1940, Pub.A.S.P., 52, 282.

Richardson,R.S. and Minkowski,R. 1939, Ap.J., 89, 347.

Severny,A.B., 1958, Pub.Crimean Ast.Obs., 20, 22.

Van de Hulst,H.C., 1953, The Sun, Ed.G.P.Kuiper, p.223, Chicago.

Von Kluber,H. 1947, Zs. f. Asp., 24, 1.

Warwick,C.S. 1955, Ap.J., 121, 385.

Waldmeier,M., 1955, Ergebnisse und Probleme der Sonnenforschung. 2nd Ed., p.198.

Wild,J.P., Vistas in Astronomy, Vol.1., p.573.

Wild,J.P., Murray,J.D. and Rowe,W.C. 1953, Nature, 172, 533.

- - - o 0 o - - -

The data for the statistical analysis was obtained from the following:-

1. Quarterly Bulletin on Solar Activity (I.A.U.), published by the Eidgenossische Sternwarte Zurich.

2. Greenwich Photoheliographic Results, published by the Royal Observatory, Greenwich.

3. Publications of the Astronomical Society of the Pacific,

- - - o 0 o - - -

29.12.60.